

**UNIVERSITA' DELLA CALABRIA**

**Dipartimento di Chimica**

**DOTTORATO DI RICERCA IN  
"METODOLOGIE PER LO SVILUPPO DI MOLECOLE DI INTERESSE  
FARMACOLOGICO"**

**QUALITY AND SAFETY IN THE AGRIFOOD INDUSTRY. A MASS  
SPECTROMETRIC APPROACH FOR THE IDENTIFICATION AND  
ASSAY OF ACTIVE PRINCIPLES AND ADDITIVES.**

Supervisore  
Prof. Giovanni Sindona

Candidato  
Raffaele Salerno

Coordinatore  
Prof. Bartolo Gabriele

**CICLO XX, 2005/2007**



*A Prezzemolo,*  
il clown che vive dentro di me.



# Contents

## Chapter 1

### *Liquid chromatographic separations and mass spectrometry*

1.1	Liquid chromatography	9
1.1.1	HPLC general features	10
1.1.2	Analytical and preparative chromatography	14
1.1.3	Detectors	16
1.2	Mass spectrometry	17
1.2.1	Electrospray Ionization (ESI) and atmospheric pressure chemical ionization (APCI)	19
1.2.2	Commonly Mass analyzers: quadrupole and TOF	22
1.2.3	Hybrid mass analyzers: triple quadrupole and QqTOF	25
1.3	Liquid chromatography-Mass spectrometry	27

## Chapter 2

### *LC/MS applications on food chemistry.*

2.1	Flavonoids	25
2.1.1	Flavonoids in food	26
2.1.2	Citrus and leek flavonoids	27
2.1.3	Liquid chromatography/mass spectrometry for separation and structural determination.	29
2.2	Secoiridoids	30
2.3	SudanI-IV and Para-red	33
	Scope of the thesis	35

## Chapter 3

### *Results and discussion*

3.1	New microcomponents detected in drupes and leaves of <i>Olea europaea</i> L. by ESI/high-resolution MS/MS and statistical analysis of leaves for cultivar discrimination.	41
-----	---	----

3.2	Characterization of new flavonoids in bergamot and pummelo juice.	57
3.3	Determination of new flavonoidic compounds by high-resolution ESI-MS/MS in Allium Porrum.	70
3.4.	Gas-phase chemistry of all set of Sudan Azo dyes (I, II, III, IV and Para-red) and relative investigation in foodstuff by LC/MS-MS and Isotope dilution methodology.	75

## **Chapter 4**

### *Experimental.*

4.1	Materials	116
4.2	Samples preparation	116
4.3	HPLC conditions	118
4.4	Chemical hydrolysis	120
4.5	Mass spectrometry	120

# **Chapter 1**

*Liquid chromatographic separations and mass spectrometry*





Mass spectrometry is an important tool virtually in all the application of atomic and molecular sciences. In some fields, the practice of mass spectrometry can be described as mature. In others, both the technology and the basic science associated with the application of mass spectrometry are rapidly evolving. The combination of chromatography and mass spectrometry is a subject that has attracted much interest over the last forty years or so because has had a tremendous impact on mass spectrometry with significant time and effort being expended on improving the mating of the two techniques.<sup>1</sup> Similarly, developments in mass spectrometry have also had a dramatic effect in the separation sciences. One of the most important field in which this combination has had a strong improvement is certainly the agricultural sciences.<sup>2</sup> Tandem mass spectrometry has, in addition to single-stage mass spectrometry, become a particularly important analytical methodology in many application areas like a food safety or in the structure elucidation of unknown compounds from biological samples.<sup>3-4</sup> Thus, mass spectrometry provides a perspective on the significant changes in strategies to solve specific problems in the life sciences.

## **1.1 Liquid chromatography**

Liquid chromatography (LC), the generic name used to describe any chromatographic procedure in which the mobile phase is a liquid, is used for analysis of complex mixtures of unvolatile samples. Modern high resolution LC (HPLC), has now become firmly established at the forefront of chromatographic techniques. HPLC is used for a wide range of applications and offers significant advantages in the analysis of pharmaceutical formulations, biological fluids, environmental residues and trace element contaminants.<sup>5</sup> Volatility or thermal stability of the analytes is no longer a limit, as in the Gas Chromatographic (GC) applications, thus making LC the method of choice for polymers, polar, ionic and thermally unstable materials. Moreover, sample detection and quantitation can be achieved by means of continuous flow detectors; thus improving accuracy and precision of analysis.

### 1.1.1 HPLC general features

In HPLC, a liquid sample, or a solid sample dissolved in a suitable solvent, is carried through a chromatographic column by a liquid mobile phase. Separation is determined by solute/stationary-phase interactions.

Different types of columns are available for various types of separation techniques referred as, normal phase, reverse phase, size exclusion, Ion exchange and affinity chromatography. In each case, however, the basic instrumentation is essentially the same (fig 1.1.1).

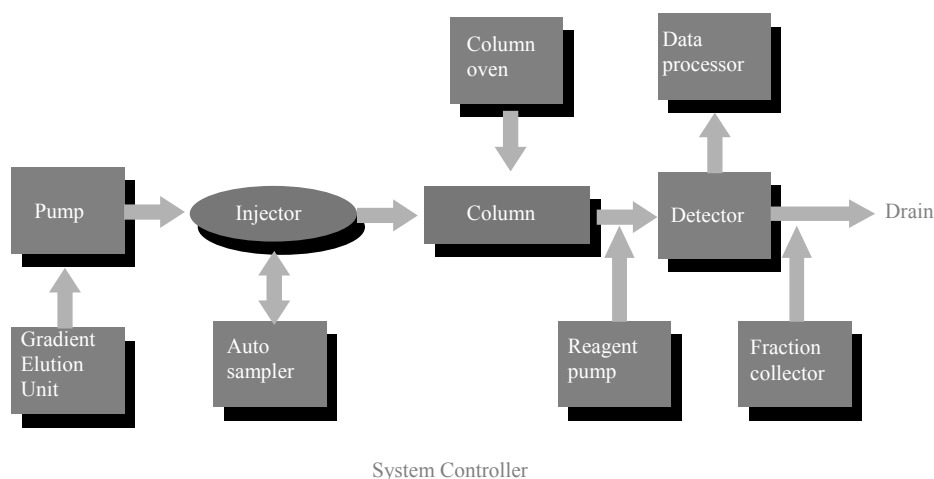


**Figure 1.1.1** Schematic diagram of HPLC system.

In the normal phase mode, the retention is governed by the interaction of the polar parts of the stationary phase and solute. Retention occurs when the packing is more polar than the mobile phase with respect to the sample.

In the reverse phase approach, the packing material is relatively unpolar while the solvent is polar with respect to the sample. Retention is the result of interaction of the unpolar components of the solutes and the unpolar stationary phase. In the ion exchange column type, the mixture components are separated on the basis of attractive ionic forces between molecules carrying charged group of opposite charge on the stationary phase. Finally, affinity chromatography requires that an immobilized ligand, covalently coupled to the column's stationary phase, interacts specifically and reversibly with the

solute of interest. The table 1.1.1, summarizes the different HPLC performances and reports the most commonly used packing materials.

LC mode	Packing materials	Mobile phase	Interaction
Normal phase	Silica gel	n-Hexane/IPE	Adsorbition
Reversed phase	Silica C-18	MeOH/Water	Hydrofobic
Size exclusion	Porous polymer	THF	Gel permeation
Ion exchange	Ion excange gel	Buffer sol.	Ion excange
Affinity	Packings with ligand	Buffer sol.	Affinity

**Table 1.1.1.** Common LC column characteristics.

Reversed phase separation<sup>6-7</sup> are about the most used HPLC method in food analysis and high-performance columns that provide minimum broadening of the separated bands are the heart of the modern LC system. Besides the nature of the packing material, an important role is played by the way how the columns are packed. They need also to be appropriately designed in order to minimize the dispersion and to allow the individual solutes to reach the detector, after they have been moved apart and separated. After injection into an HPLC column, any sample components that do not interact with the stationary phase would be eluted in the void volume ( $v_0$ ) which is characteristic for that column. This void volume represents both the interstitial volume between the particles of the bonded phase and the available volume within the particle pores themselves. The retention times,  $t_r(A)$  and  $t_r(B)$ , for the two sample components shown in Figure 1.1.2 are the times elapsed from injection to the times of maximum concentration in the eluted peaks. Similarly, the retention volumes are the amounts of solvent required for their elution. The basic principle of this separation techniques derive from various parameters that are summarized here:

- Theoretical plates
- HETP (height equivalent to a theoretical plate)
- Retention factor
- Selectivity
- Resolution

The number of theoretical plates ( $N$ ) has traditionally been used as a measure of column efficiency.

$$N = 16(tr/W)^2 \quad (\text{eq. 1})$$

where  $tr$  is the retention time and  $W$  is the peak width at baseline (equation 1).

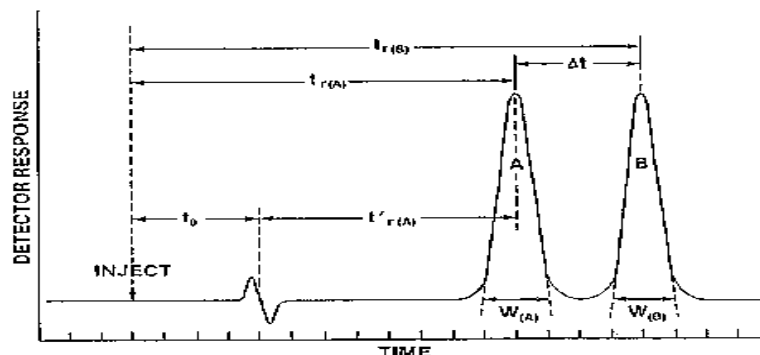


Figure 1.1.2. Important chromatographic parameters.

Generally, the measurement of peak width at half height has been found to be most useful, since it can be applied to peaks not completely resolved, that exhibit tailing, or that are otherwise asymmetrical in shape.

$$N = 5.54(tr/w_{1/2})^2 \quad (\text{eq. 2})$$

where  $w_{1/2}$  is peak width at half height (equation 2).

The value of  $N$  is a useful measure of the performance of a chromatographic column, and in general the more the theoretical plates, the better are the column performances. The number of theoretical plates can be calculated for any peak in a given separation, with each calculation resulting in a slightly different value. The value for  $N$  is to a first approximation, independent of retention time; however, it is proportional to column length. Therefore, height equivalent to a theoretical plate (HETP) is the better measure of column efficiency since it allows for a comparison between columns of different lengths (equation 3):

$$H = \text{HETP} = L/N \quad (\text{eq 3})$$

where  $L$  is the length of the column, usually in mm.

The retention factor ( $k'$ ) is a measure of the degree of retention and can be calculated by the following equation:

$$k' = (V_r - V_o)/V_o = (tr - t_o)/t_o \quad (\text{eq 4})$$

where  $k'$  is the number of column volumes required to elute a particular solute  $V_0$  and to represent the void volume and void time, respectively.

A related concept is that of selectivity ( $\alpha$ ), which can be defined as the relative separation between adjacent resolved peaks. This value is the ratio of the retention factors for the two peaks (equation 5):

$$\alpha = k'_1/k'_2 \quad (\text{eq 5})$$

Resolution is defined as the extent between separation of two chromatographic peaks.

It can be described as a measure of how well a given HPLC column separates the two components (equation 6).

$$R_s = 2(\text{tr}(B) - \text{tr}(A)) / (W_A + W_B) \quad (\text{eq 6})$$

Resolution can also be described in terms of an equation which includes three factors: the selectivity factor  $\alpha$ , the capacity factor  $k'$ , and the plate number,  $N$  (equation 6).

Thus:

$$R_s = \alpha k' N \quad (\text{eq 7})$$

The characteristics of column are:

- *Column dimension* (length and internal diameter of packing bed)
- *Particle shape* (spherical or irregular)
- *Particle size* (average particle diameter, typically 3-20 $\mu\text{m}$ )
- *Surface Area* (sum of particle outer surface and interior pore surface, in  $\text{m}^2/\text{gram}$ )
- *Pore size* (average size of pores or cavities in particles, ranging from 60-10.000  $\text{\AA}$ )
- *Bonding type* (monomeric: single-point attachment of bonded phase molecule; polymeric: multi-point attachment of bonded phase molecule.)
- *Carbon load* (amount of bonded phase attached to base material, expressed as % C)
- *Endcapping* (capping of exposed silanols with short hydrocarbon chains after the primary bonding step).

Column dimensions should be carefully chosen.<sup>8,9</sup> The *short* columns (30-50 mm length) offer short run times, fast equilibration, low backpressure and high sensitivity. *Long* columns (250-300 mm length) provide higher resolving power, but create more

backpressure, lengthen analysis times and use more solvent. *Narrow* column (2.1 mm and smaller) beds inhibit sample diffusion and produce narrower, taller peaks and a lower limit of detection.

They may require instrument modification to minimize distortion of the chromatography. *Wider* columns (10-22 mm) offer the ability to load more sample.

The table 1.1.2 shows the relationship between column internal diameter and flow, mass load and volume injection parameters

ID (mm)	Flow (ml/min)	Mass load (mg)	Injection vol ( $\mu$ l)
0,3-0,5	5-10 $\mu$ l/min	0,00005-0,01	0,01-0,5
1	25-75 $\mu$ l/min	0,005-0,05	0,2-5
2	0,15-0,25	0,002-0,3	1-20
3	0,3-0,6	0,1-1	2-40
4,6	0,5-1,5	0,2-5	5-100
10	2,5-10	1-40	20-50
21,2	15-40	5-200	100-2000
50	50-100	25-1000	600-10000
100	200-500	125-5000	2300-50000

**Table 1.1.2.** Setting of different parameters in HPLC.

### 1.1.2 Analytical and preparative chromatography

The difference between analytical and preparative HPLC concerns the aim of the separation. In analytical HPLC the aim is to separate all individual components of a mixture as completely as possible with subsequent identification of the peaks. In general, sample sizes are small. For 4 mm ID, typical sample sizes are 1 – 100  $\mu$ g analyte per g adsorbent in normal phase columns and 10 – 1000  $\mu$ g analyte per g adsorbent in RP columns. For columns with smaller inner diameters correspondingly smaller samples are applied. Thus analytical HPLC often requires maximum separation efficiency of a column. Due to the small inner diameter, expenses for solvents and packing are low, with the result that in analytical HPLC costs for separation time

(solvent consumption) and packing material can be almost neglected for method development.

On the contrary, in preparative HPLC development of a separation often involves detailed economical-chemical optimization calculations.

Due to the column dimensions, costs for solvents and packing or prepacked columns become more and more important with increasing column diameters. The aim of HPLC now is isolation of the desired product with defined purity, in maximum amounts and with minimum time. The important parameters are called production rate and throughput. Definition of the production rate includes information about the required purity of the isolated product.

When speaking about the production rate of a preparative separation, the term loadability<sup>10-12</sup> of the column should be considered, too. According to general understanding, this is the maximum sample size (with defined sample mass and volume) under which a column still provides optimum selectivity.

The parameters which are important for the optimization of the mass loadability of a column can be described by the formula:

$$M = C_1 \pi r^2 l k d A_S [C_2 (d_p^2/l)]^2$$

M = maximum sample mass

$C_1, C_2$  = constants

r = column radius

l = column length

k = partition coefficient

d = packing density

$A_S$  = adsorbent surface

$d_p$  = particle diameter.

It is important to note how the mass loadability of the column decreases with increasing plate number ( $l/d_p^2$  proportional to the plate number N).

If an increased loadability is required for a given separation efficiency, it is recommended to increase particle size and column length, the increase in column length being the square of the increase in particle diameter. Volume loadability can be related to the dead volume ( $V_0$ ), the maximum overload volume ( $V_L$ ), the relative retention ( $\alpha$ ), the plate number (N) and the capacity factors ( $k_A', k_B'$ ) by equation 8, hence it depends

on the  $k'$  values of the components to be separated and on the separation efficiency of the column.

$$V_L = V_0 [(\alpha-1) k_A' - 2/N^{1/2} (2 + k_A' + k_B')] \quad (\text{eq. 8})$$

The production rate is directly proportional to the column diameter, the linear flow velocity of the mobile phase, the concentration of the component to be isolated (unless under mass overload conditions) and the term  $[1/N-H_0/l]^{1/2}$ , where  $H_0$  is the plate height of the column under ideal conditions,  $l$  is the column length, and  $N$  is the plate number required for separation of the desired product with the purity required.<sup>13</sup>

### 1.1.3 Detectors

Although over the years a large number of LC detectors have been developed and described, the vast majority of all contemporary LC analyses are carried out mainly using four detectors.

The UV, in one of its different forms, the electrical conductivity, the fluorescence and the refractive index.

The widespread use of the UV spectrophotometer approach deserves a detailed description of the method. The coupling with mass analyzers will be treated in a different paragraph. UV absorption detectors respond to those substances that absorb light in the range 180 to 350 nm. Many (but not all) substances absorb light in this wavelength range, including those having one or more double bonds ( $\pi$  electrons) and unshared (unbonded) electrons, *e.g.* olefin and aromatic compounds and species containing C=O, C=S and -N=N- groups.

The sensor of a UV detector consists of a short cylindrical cell having a capacity between 1 and 10 ml through which passes the column eluant. UV light is arranged to pass through the cell and fall on a photo-electric cell (or array). The signal from the photocell is transmitted to a modifying amplifier and then to a recorder or data acquisition system.

The relationship between the intensity of UV light transmitted through a cell ( $I_T$ ) and the concentration of solute contained by it ( $c$ ) is given by Beer's Law (equation 9).

$$I_T = I_0 e^{-kcl}$$

or  $\ln(I_T) = \ln(I_0) - kcl$  (eq 9)



where ( $I_0$ ) is the intensity of the light entering the cell, ( $l$ ) is the path length of the cell, and ( $k$ ) is the molar extinction coefficient of the solute for the specific wavelength of the UV light.

UV detectors can be used with elution gradients, providing the solvents do not absorb significantly in the wavelength range used for the detection. The solvents usually employed in reversed phase chromatography are water, methanol, acetonitrile and tetrahydrofuran (THF), all of which are transparent to UV light over the total wavelength range normally used by UV detectors. In normal phase operation more care is necessary in eluant selection since many solvents that might be appropriate for a given chromatographic phase strongly absorb at the wavelengths used by the detector. The *n*-paraffin, methylene dichloride, aliphatic alcohols and THF are useful solvents that are transparent in the UV and can be used with a polar stationary phase such as silica gel.

## 1.2 Mass spectrometry

Mass spectrometry is essentially a technique for "weighing" molecules. Obviously, this is not done with a conventional balance. Instead, mass spectrometry is based upon the motion of a charged particle, called ion. Figure 1.2.1 is a block diagram that shows the basic parts of a mass spectrometer. The inlet transfers the sample into the vacuum of the mass spectrometer. In the source region, neutral sample molecules are ionized and then accelerated into the mass analyzer.

The mass analyzer is the heart of the mass spectrometer. This section separates ions, either in space or in time, according to their mass to charge ratio. After the ions are separated, they are detected and the signal is transferred to a data system for analysis. All mass spectrometers also have a vacuum system to maintain the low pressure, which is also called high vacuum, required for operation. A variety of ionization techniques are used for mass spectrometry.

Most ionization techniques excite the neutral analyte molecule which then ejects an electron to form a radical cation ( $M^+$ ). Other ionization techniques involve ion molecule reactions that produce adduct ions ( $MH^+$ ). High vacuum minimizes ion-molecule reactions, scattering, and neutralization of the ions.

The most important considerations are the physical state of the analyte and the ionization energy. Electron ionization and chemical ionization are only suitable for gas phase ionization. Electrospray ionisation (ESI)<sup>14-15</sup>, and matrix assisted laser desorption (MALDI)<sup>16</sup> are used to ionize condensed phase samples.

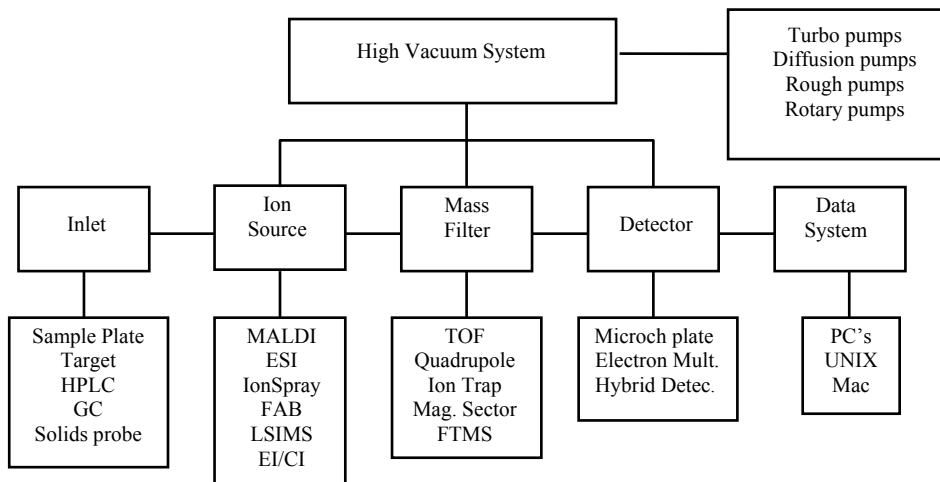


**Figure 1.2.1.** Mass spectrometry block diagram.

The ionization energy is significant because it controls the amount of fragmentation observed in the mass spectrum.

Although this fragmentation complicates the mass spectrum, it provides structural information for the identification of unknown compounds. Some ionization techniques are very soft and only produce molecular ions, other techniques are very energetic and cause ions to undergo extensive fragmentation. Currently, API (ESI and APCI) and MALDI are the most commonly employed ionization methods and they opened doors to the widespread biological and biomedical application of mass spectrometry. These techniques are used to ionize thermally labile samples such as flavonoids, peptides, proteins and polymers directly from the condensed phase. Otherwise, the selection of a mass analyzer is very important and depends upon the resolution, mass range, scan rate and detection limits required for an application.<sup>17</sup> Each analyzer has very different operating characteristics and the selection of an instrument involves important tradeoffs. Analyzers are typically described as either continuous or pulsed.

Continuous analyzers include quadrupole filters and magnetic sectors while pulsed analyzers include time-of-flight, ion cyclotron resonance, and quadrupole ion trap mass spectrometers. There are also different hybrid analyzers; two popular of these are triple quadrupole and Qq-TOF. The former is utilized for quantitative analysis in tandem mass spectrometry, the latter is applied in high resolution analysis.<sup>18-19</sup>

### 1.2.1 Electrospray Ionization (ESI) and atmospheric pressure chemical ionization (APCI)

The electrospray process involves the creation of a fine aerosol of highly charged micro droplets in a strong electric field. Electrospray as an ionization technique for mass spectrometry was developed by Dole and co-workers in the late 1960s<sup>14</sup> and considerably improved upon by Yamashita and Fenn who in 1984 coupled an electrospray source to a quadrupole mass analyser<sup>15</sup>. A continuous flow of solution containing the analyte from a highly charged (2–5 kV) capillary generates an electrospray. The solution elutes from the capillary into a chamber at atmospheric pressure, producing a fine spray of highly charged droplets due to the presence of the electric field (figure 1.2.2), a process called nebulisation. A combination of thermal and pneumatic means is used to desolvate the ions as they enter the ion source.

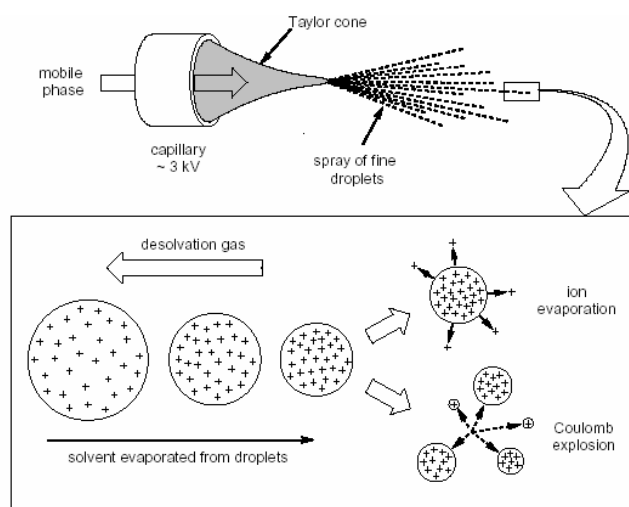


**Figure 1.2.2.** The desolvation process.

The solvent contained in the droplets is evaporated by a warm counter-flow of nitrogen gas until the charge density increases to a point at which the repulsion becomes of the same order as the surface tension. The droplet then may fragment in what is termed a ‘Coulomb explosion’, producing many daughter droplets that undergo the same process, ultimately resulting in bare analyte ions.

An alternative picture is one in which the ions ‘evaporate’ from the surface of the droplet. Whatever the exact mechanism, ESI is a very ‘soft’ means of ionization that causes little or no fragmentation of the sample.<sup>20-21</sup> The electrospray ion source is at very high pressure (atmospheric) with respect to the very low pressure that is required for ion separation by a mass analyzer, so the interface between the two involve a series of skimmer cones (acting as small orifices) between the various differentially pumped regions (figure 1.2.3). Early designs had the capillary exit pointing directly into the mass analyzer but to limit contamination practically all modern designs have an orthogonal (or at least off-axis) spray direction.

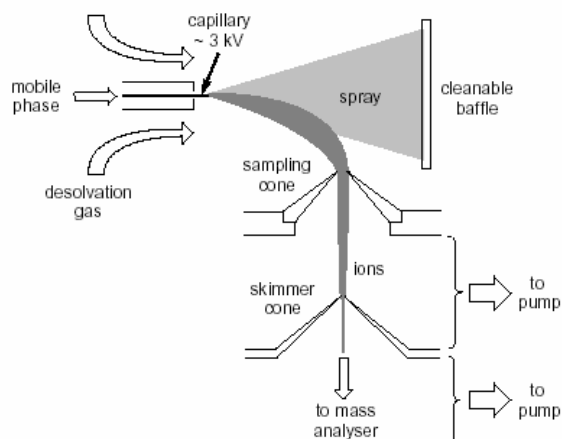


**Figure 1.2.3.** An electrospray source.

The ions are drawn into the spectrometer proper through the skimmer cones. A voltage can be applied (the cone voltage), which will accelerate the ions relative to the neutral gas molecules. This leads to energetic ion-neutral collisions and fragmentation due to what is termed collision induced dissociation (CID)<sup>22</sup>. The remaining bath gas is pumped away in stages (in order to attain the high vacuum necessary for separation of the ions) and the ions are focused through a lensing system into the mass analyzers.

The appearance of multiply charged species enables ESI to characterize compounds whose molecular weight would otherwise be far in excess of that accessible to most mass analysers<sup>23-24</sup>. Biological macromolecules tend to accumulate one unit of charge for every 1 – 2000 Da, so nearly all proteins, for example, produce signals in the region of 1 – 2000 m/z, regardless of their actual molecular weight. Ionization of a neutral analyte often occurs by protonation, or alternatively cationisation, with an adventitious cation present in the solvent used, such as  $\text{Na}^+$ ,  $\text{K}^+$  or  $\text{NH}_4^+$ . In some cases, adduct ions with several cations can occur, giving  $[\text{M} + \text{H}]^+$ ,  $[\text{M} + \text{NH}_4]^+$ ,  $[\text{M} + \text{Na}]^+$  and  $[\text{M} + \text{K}]^+$  ions. Atmospheric-pressure chemical ionization (APCI)<sup>25-26</sup> is another of the techniques in which the stream of liquid emerging from an HPLC column is dispersed into small droplets, in this case by the combination of heat and a nebulizing gas. In this case the liquid flow is passed through a pneumatic nebulizer where the droplets are both generated and desolvated. The successive neutral dried spray, obtained by a heated region, passed through a corona discharge where the analyte are ionized. The mechanism is a chemical ionization but an atmospheric pressure were is necessary, for initial gas ionization, utilized a corona discharge (fig. 1.2.4).

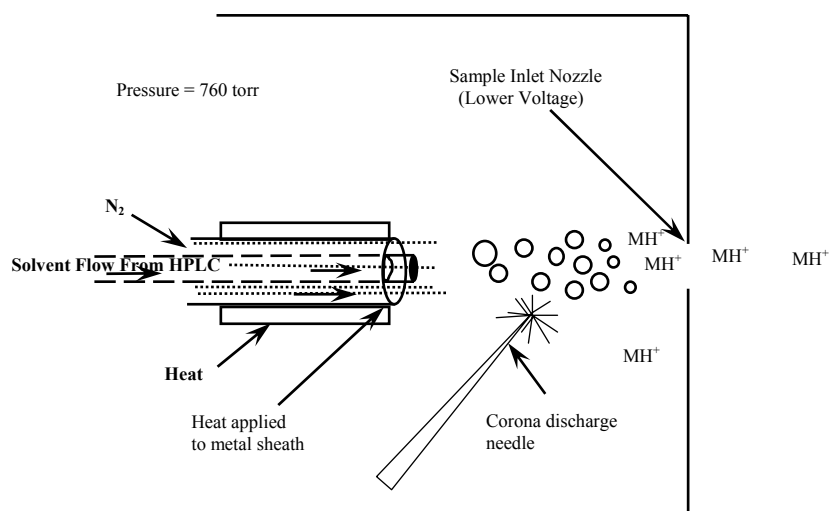


**Figure 1.2.4.** APCI source.

Then, the ions produced by the interaction of the electrons with the surrounding gas, undergo a number of reactions leading to the generation of reactive ions which interact with the analyte molecules present.

The reagent species in the positive-ion mode may be considered to be protonated solvent ions, and in the negative ion mode  $O_2^-$ , its hydrates and clusters. It is also possible the formation of cluster involving solvent molecules which can be removed with use of a “curtain gas”. Finally, this technique can be applied to both volatile and thermally stable and moderate polar compounds but the ionization regime is much more harsh than ESI and this precludes its use for the study of large biomolecules, with the mass limit for APCI being generally considered as below 2000 Da.

### 1.2.2 Common Mass analyzers: quadrupole and TOF

Quadrupole mass analyzers consist of four parallel rods arranged as in Figure 1.2.5. Applied between each pair of opposite and electrically connected rods are a DC voltage and a superimposed radio-frequency potential.

A positive ion entering the quadrupole will be drawn towards a negatively charged rod but if the field changes polarity before the ion reaches it, it will change direction. Under the influence of the combination of fields the ions undergo complex trajectories<sup>27-29</sup>. Within certain limits these trajectories are stable and so ions of a certain  $m/z$  are transmitted by the device, whereas ions with different  $m/z$  values will have an unstable trajectory and be lost by collision with the rods.

The operation of a quadrupole mass analyzer is usually treated in terms of a stability diagram that relates the applied DC potential ( $U$ ), the applied rf potential ( $V$ ) and the radio frequency ( $\omega$ ) to a stable vs unstable ion trajectory through the quadrupole rods.

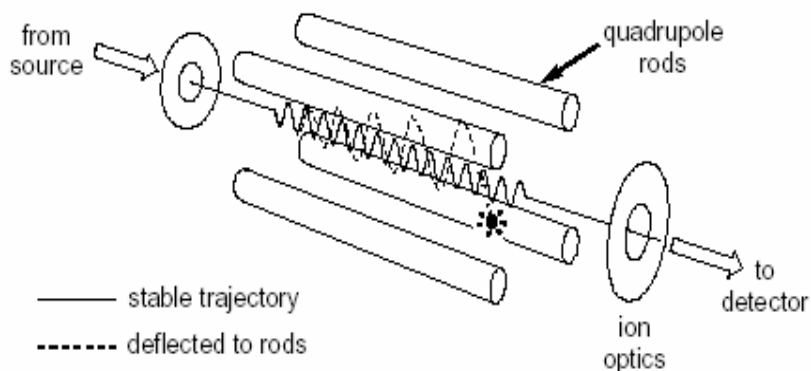


Figure 1.2.5. Diagram of a quadrupole mass analyzer.

A qualitative representation of a stability diagram for a given mass  $m$  is shown in figure 1.2.6;  $a$  and  $q$  are parameters that are proportional to  $U/m$  and  $V/m$  respectively: changing the slope of the scan line will change the resolution. Quadrupoles have other functions besides their use as a mass filter.

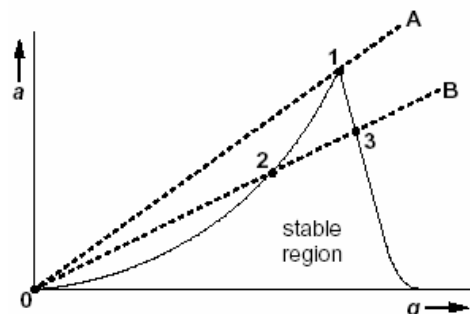


Figure 1.2.6. Stability diagram.

An rf-only quadrupole will act as an ion guide for ions within a broad mass range. In such applications, hexapoles or even octapoles are often employed.

The time-of-flight (TOF)<sup>29-30</sup> mass analyzer separates ions in time as they travel down a flight tube. These instruments have high transmission efficiency, no upper  $m/z$  limit, very low detection limits, and fast scan rates. In the source of a TOF analyzer, a packet of ions is formed by a very fast (ns) ionization pulse. These ions are accelerated into the flight tube by an electric field (typically 2-25 kV) applied between the backing plate and the acceleration grid. Since all the ions are accelerated across the same distance by the same force, they have the same kinetic energy. Because velocity ( $v$ ) is dependent upon the kinetic energy ( $E$ ) and mass ( $m$ ) lighter ions will travel faster.

The velocity of an ion ( $v$ ) is determinate as a function of acceleration voltage and  $m/z$  value (equation 10):

$$v = \sqrt{\frac{2zeV}{m}} \quad (\text{eq 10})$$

After the ions accelerate, they enter a 1 to 2 meter flight tube (fig. 1.2.7). The ions drift through this field free region at the velocity reached during acceleration. At the end of the flight tube they strike a detector. The time delay ( $t$ ) from the formation of the ions to

the time they reach the detector depends upon the length of the drift region ( $L$ ), the mass to charge ratio of the ion, and the acceleration voltage in the source (equation 11):

$$t = \sqrt{\frac{mD}{2zeV}} \quad (\text{eq 11})$$

This second equation shows that low  $m/z$  ions will reach the detector first. The mass spectrum is obtained by measuring the detector signal as a function of time for each pulse of ions produced in the source region. Because all the ions are detected, TOF instruments have very high transmission efficiency which increases the S/N level.

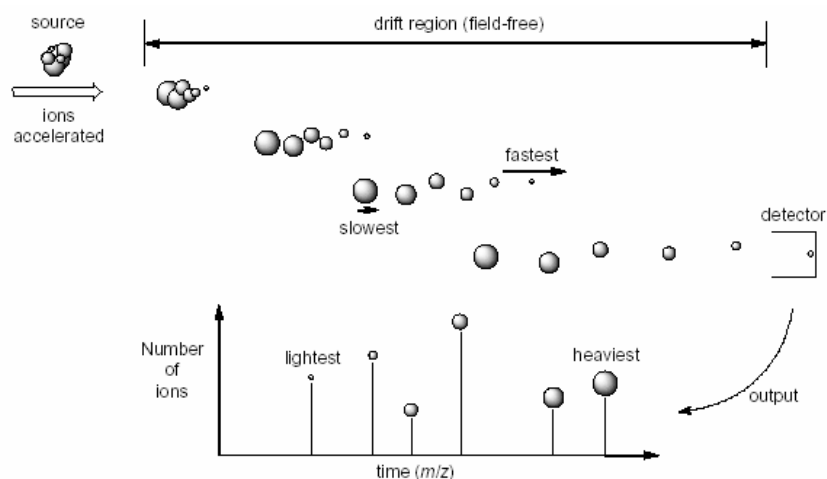


**Figure 1.2.7.** The essential of TOF optics.

The ions leaving the ion source of a time-of-flight mass spectrometer have neither exactly the same starting times nor exactly the same kinetic energies. Improvements in time of-flight mass spectrometer design have been introduced to compensate for these differences, and the most dramatic improvements in performance come with the use of a reflectron.<sup>31</sup>

This is an ion optic device in which ions in a time-of-flight mass spectrometer interact with an electronic ion mirror and their flight is reversed. Ions with greater kinetic energies penetrate deeper into the reflectron than ions with smaller kinetic energies. The reflectron will decrease the spread in the ion flight times, and therefore improve the resolution of the time-of-flight mass spectrometer.



Orthogonal TOF<sup>32</sup> analyzers are employed in conjunction with continuous ion sources, especially ESI<sup>33</sup>, and in hybrid instruments. The continuous ion beam is subjected to a pulsed electric field gradient at right angles (orthogonal) to the direction of the ion beam. A section of the ion beam is thus pulsed away instantaneously and can be measured using a TOF analyzer (fig. 1.2.8).

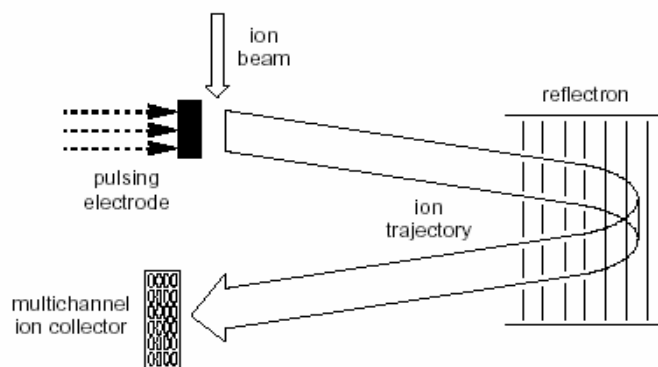


**Figure 1.2.8.** Orthogonal TOF.

Orthogonal TOF analyzers can accumulate tens of thousands of spectra per second and these are summed to provide spectra with high signal-to-noise ratios.

### 1.2.3 Hybrid mass analyzers: triple quadrupole and QqTOF

In a triple quadrupole, two mass analyzers are separated by an rf-only quadrupole used as a collision cell (fig. 1.2.9). MS/MS<sup>34</sup> experiments are easy to set up on triple quadrupoles, and are especially valuable when examining complex mixtures of ions. Each ion may be selected and individually fragmented to provide structural information exclusively on that ion, without any need for consideration of interference from other ions in the mixture.

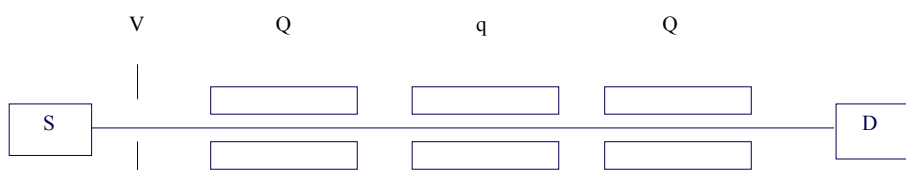


**Figure 1.2.9.** Scheme of triple quadrupole.

With this analyzer is possible to carry out different processes in tandem mass spectrometry.

The processes are:

- **Product ion scan;** the first quadrupole is set so that it passes only ions of a certain  $m/z$  value, the rf-only quadrupole contains an inert collision gas (typically argon) to assist in the creation of fragment ions and the third quadrupole scan the mass range of interest and generates a daughter ion spectrum.
- **Precursor ion scan;** MS1 scan through all ions, which are fragmented in the collision cell, and MS2 is set to detect only product ions of a certain mass.
- **Neutral loss scan;** this involves setting up MS1 and MS2 to scan in parallel but offset by a set mass difference,  $\Delta m$ .
- **Select reaction monitoring;** both MS1 and MS2 are settled on only one ion, father and daughter respectively.

The most popular Hybrid of TOF analyzer is certainly the quadrupole/oa-TOF<sup>35</sup>. In these instruments (fig. 1.2.10), the first mass analyzer (MS1) is a quadrupole, which acts simply as an rf-only ion guide in MS mode.

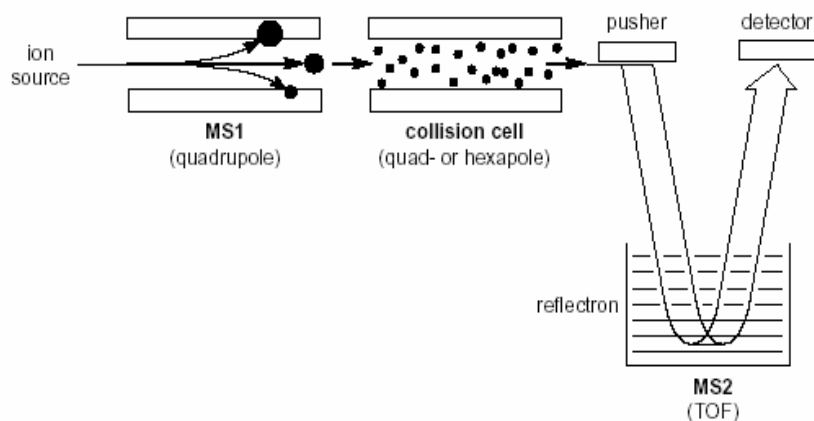


**Figure 1.2.10.** Quadrupole/oa TOF.

Next is a collision cell, followed by the oa-TOF (MS2). To collect MS/MS data, MS1 is used to select a single ion, which is then fragmented in the collision cell, and MS2 is

used to collect the daughter ion spectrum. Fast, highly efficient, sensitive and capable of high resolution, the Q/TOF provides higher quality data than the popular triple quadrupole, though it is less suitable for quantitative work.

### 1.3 Liquid chromatography-Mass spectrometry

The development of new ionization methods as ESI and APCI, has been fundamental for coupling liquid chromatography to mass spectrometry.<sup>1</sup> They represent perfect LC-MS interfacing technologies. Even LC-nano ESI is feasible.<sup>36</sup> With these interfaces it is possible to remove the incompatibility between HPLC, utilizing flow rates of ml/min of a liquid, and the mass spectrometer, which operates under conditions of high vacuum. It's due to the fact which ionization occurs directly from solution and consequently allows ionic and thermally labile compounds to be studied.

This combination allows more definitive identification and the quantitative determination of compounds that are not fully resolved chromatographically.

The major advantage of this coupling is the possibility to study a range of analyte, from low molecular-weight drugs and metabolites (<1000 Da) to high-molecular-weight biopolymers (>100 000 Da). Method development requires the analyst to identify the variables (factors) that are likely to affect the result of the analysis and to carry out experiments that allow those that have an effect on the final outcome to be identified. Having identified the factors of importance, experimental design finally allows the precise experimental conditions that give the 'best' result to be determined. This 'factors' could include for HPLC, the composition of the mobile phase, its pH and flow rate<sup>37</sup>, the nature and concentration of any mobile-phase additive, buffer or ion-pair reagent, the make-up of the solution in which the sample is injected for the ionization technique<sup>38</sup>, spray parameters for electrospray source, nebulizer temperature for APCI, nature and pressure of gas in the collision cell if MS-MS experiment is performed.<sup>22</sup>

#### *1.3.1 LC-MS for low molecular weight compounds.*

When 'low'-molecular-weight compounds are involved, both APCI and electrospray ionization are potentially of value and the first task is to decide which of these will give

the more useful data. The choice of interface is relative to polarity of sample: APCI for low- to medium-polarity and electrospray for medium- to high-polarity.

In general terms, electrospray ionization is considered to be concentration sensitive at 'low' flow rates and mass-flow-sensitive at 'high' flow rates, while APCI is considered to be mass-flow-sensitive. Some compounds may be ionized very effectively under positive-ionization conditions, while others may require the formation of negative ions to allow analysis. Structural studies of low molecular weight compounds may require the extent of fragmentation to be maximized, but in this way is important to have an high resolution analyzer for calculate an exact mass so father as daughters ions. This factor is fundamental for reveal compounds which differ few mDa one another.

Quantification may require the opposite, the efficient production of a small number of ions of different  $m/z$  ratios, in order to maximize sensitivity.

Quantification involves the comparison of the intensity of response from an analyte ('peak' height or area) in the sample under investigation with the intensity of response from known amounts of the analyte in standards measured under identical experimental conditions.

The attributes required of a method usually include good sensitivity, low limits of detection, and selectivity. Good selectivity allows the measured signal to be assigned, with certainty, to the analyte of interest rather than any interfering compounds which may be present. Low limits of detection allows to reveal very few quantities of compounds. There are three methods for quantification utilizing the standard solution: external standard, standard additions and internal standard. The former is the main method used when the detector is a mass spectrometer. Quantitative methodology employing mass spectrometry usually involves selected-ion monitoring or multiple reaction monitoring, sometimes using a labelled internal standard for accurate quantification.<sup>39</sup>

It is the role of the analyst to choose these ions/decompositions, in association with chromatographic performance, to provide sensitivity and selectivity such that when incorporated into a method the required analyses may be carried out with adequate precision and accuracy.

**References**

1. K. B. Tomer. *Chem. Rev.* **2001**, *101*, 297-328.
2. M. Careri; F. Bianchi; C. Corradini. *Journal of Chromatography A* **2002**, *970*, 3-64.
3. L. Di Donna; G. Grassi; F. Mazzotti; E. Perri; G. Sindona. *J. Mass Spectrom.* **2004**, *39*, 1437-1440.
4. A. De Nino; N. Lombardo; E Perri; A Procopio; A. Raffaelli; G. Sindona. *J. Mass Spectrom.* **1997**, *32*, 533-541.
5. V.R.Meyer. *Practical High Performance Liquid Chromatography* Wiley, Chichester, UK, **1994**.
6. H M. Merken; G. R. Beecher. *J. Agr Food Chem.* **2000**, *48,3*, 577-599.
7. R.W. Owen; A. Giacosa; W.E. Hull; R. Haubner; B. Spiegelhalder; H. Bartscha. *European Journal of Cancer* **2000**, *36*, 1235-1247.
8. J.S. Andersen; C.J. Wilkinson; T. Mayor; P. Mortensen; E.A. Nigg; M. Mann. *Science* **2005**, *308*,1472-1477.
9. Y. Takenaka.; T. Tanahashi; M. Shintaku; T. Sakai; N. Nagakura; Parida. *Phytochemistry* **2000**, *55* 275-284.
10. L.R. Snyder. *Anal. Chem.* **1967**, *39*, 698.
11. W. Beck; I. Halasz. *Anal. Chem.* **1978**, *291*,340.
12. T. Roumeliotis; K.K. Unger. *J. Chromatogr.* **1979**, *185*,445.
13. K.P. Hupe; H.H. Lauer. *J. Chromatogr.* **1981**, *203*, 41.
14. M. Dole; L. Mach; L.R. Hines; R.C. Mobley; L.P. Ferguson; M.B.Alice. *J. Chem. Phys.* **1968**, *49*, 2240-2249.
15. M. Yamashita; J.B. Fenn. *J.Phys. Chem.* **1984**, *88*, 4451-4459.
16. M. Karas; F. Hillenkamp. *Anal. Chem.* **1988**, *60*, 2299-2301.
17. M. Wells, S.A. McLuckey. *Chem. Rev.* **2001**, *101*, 571-606.
18. S.A. McLuckey. *Adv. Mass Spectrom.* **1998**, *14*, 153-196.
19. E.R. Badman; R.G. Cooks. *J. Mass Spectrom.* **2000**, *35*, 659-671.
20. S.J. Gaskell. *J. Mass Spectrom.* **1997**, *32*, 677-688.
21. P. Kebarle. *J. Mass Spectrom.* **2000**, *35*, 804-817.
22. V. Gabelica; E. De Pauw. *Mass Spectrometry Reviews* **2005**, *24*, 566-587.

23. H.M. Amad; N.B. Cech; G.S. Jackson; C.G. Enke. *J. Mass Spectrom.* **2000**, 35, 784-789.
24. R.B. Cole. **2000**, 35, 763-772.
25. F. Hillenkamp. *Advance in Mass Spectrom.* **1989**, 11, 354.
26. M. Karas; F. Hillenkamp. *Methods in Enzimology.* **1990**, 193, 280.
27. J.F.J. Todd. *International Journal of Mass Spectrometry and Ion Processes.* **1984**, 60, 3.
28. P.H. Dawson. *Mass Spectrometry Reviews.* **1986**, 5, 1.
29. M. Guilhaus; V. Mlynski; D. Selby. *Rapid Commun. Mass Spectrom.* **1997**, 11, 951.
30. K.G. Standing. *Int. J. Mass Spectrom.* **2000**, 200, 597.
31. B.A. Mamyrin; V.I. Karataev; D.V. Shmikk; V.A. Zagulin. *Sov. Phys. JETP* **1973**, 37,45.
32. J.H.J. Dawson; M. Guilhaus. *Rapid Commun. Mass Spectrom.* **1989**, 3, 155.
33. I.V. Chernushevich; W. Ens; K. G. Standing. *Anal. Chem.* **1999**, 71, 452A.
34. A. Benninghoven; D.Jasper; W. Sichtermann. *Appl. Phys.* **1976**, 11, 36.
35. I.V. Chernushevich; A.V. Loboda; B.A. Thomson. *J. Mass Spectrom.* **2001**, 36, 849.
36. F. Hsieh; E. Baronas; C. Muir; S.A. Martin. *Rapid Commun. Mass Spectrom.* **1999**, 13,67-72.
37. A. Asperger; J. Efer; T. Koal; W. Engewald; *J. Chromatogr. A* **2001**, 937, 65-72.
38. W.Naidong; Y. Chen; W Shou; X. Jiang. *J. Pharm. Biomed. Anal.* **2001**, 26, 753-767.
39. D.C. Harris. *Quantitative Chemical Analysis*, 4th Edn, W. H. Freeman, New York, **1995**.

## **Chapter 2**

*LC/MS applications on food chemistry.*





The development of LC/MS techniques<sup>1-2</sup> has been fundamental for the analysis of mixtures of secondary metabolites from plants and fruits.<sup>3-14</sup> The powerful of this type of analysis is very important in order to improve the research in a life science.

Historically, consumption of particular fruits and vegetables was thought to prevent or cure ailments ranging from headaches to heart disease. In fact, early medicine revolved largely around the prescription of specific food concoctions for certain disorders. Until relatively recently, these attributes of vegetables and fruits were based more on beliefs than on scientific evidence, but during the recent years many studies have examined the relationship between vegetables fruit and health. It has been estimated that up to 70% of all cancer is attributed to diet.<sup>15</sup> Nowadays, the scientific evidence regarding a role for vegetable and fruit consumption in cancer prevention is generally consistent and is supportive of current dietary recommendations. A different type of micro-components called PPT (phenols, polyphenols and tannins) with various mechanisms, may help protect against cancer.<sup>16-17</sup> Continued attention to increasing vegetable and fruit intake is important.

For this reason the structural identification of new compounds derived from these matrixes was becoming an important field of research in which the development of hyphenated methods, like automated semi- or preparative LC-MS, given a very significant contribution.<sup>18</sup> For a more complete structure elucidation, the complementary information derived from NMR is indispensable.

Further developments may be expected with regards to miniaturization, that is, the coupling of micro- and/or nano-LC, to tandem-MS and NMR instruments: this should facilitate the analysis of minute samples, and help to create better operating conditions for NMR detection. However, the progress in this area has been slower than was expected several years ago.<sup>19</sup> In the near future, both, LC with tandem MS detection and preparative LC/MS, will continue to play a dominant role in this analysis.

On other hand, quantitative LC-MS/MS methodology is utilized in food safety, agricultural and forensic chemistry.<sup>20-22</sup> In food safety, there are different problems related to chemicals in foodstuffs. The production and consumption of food is central to any society, and has economic, social and, in many cases, environmental consequences. Although health protection must always take priority, these issues must also be taken into account in the development of food policy.

Certain food have the potential of containing chemicals which, if eaten in sufficient quantities, are harmful to human health. Other food can be contaminated by illegal dyes. The White Paper on Food Safety outlines a comprehensive range of actions needed to complement and modernise existing EU food legislation. Moreover, the Food Standards Agency aims to protect the consumer from these chemicals, and for this reason must maintain the best knowledge base possible on the subject to provide the necessary tools to ensure that consumer exposure to these chemicals is kept as low as reasonably practicable. Mycotoxine, nitrate and Sudan I-IV are the chemicals found in a wide range of foods which needs of research and surveillance projects because are dangerous to human health.

## 2.1 Flavonoids

Flavonoids constitute a large group of naturally occurring plant phenols that cannot be synthesized by humans. They are characterised by the carbon skeleton C6-C3-C6 derived from shikimic pathway. The basic structure of these compounds consists of two aromatic rings linked by a three-carbon aliphatic chain which normally has been condensed to form a pyran or, less commonly, a furan ring.

The main classes of flavonoids, including flavones, flavonols, isoflavones, flavonones (fig. 2.1.1) occur in all types of higher plant tissues.<sup>23-24</sup> Approximately 90 % of the flavonoids in plants occur as glycosides.<sup>25</sup> Usually the aglicones are more active in bulk phase,<sup>26,27</sup> as well as in phospholipid bilayers oxidation.<sup>28</sup> Many studies have suggested that flavonoids exhibit biological activities, including antiallergenic, antiviral, anti-inflammatory, and vasodilating actions. However, most interest has been devoted to the antioxidant activity of flavonoids, which is due to their ability to reduce free radical formation and to scavenge free radicals.<sup>29-32</sup> Other mechanisms of action of selected flavonoids include singlet oxygen quenching,<sup>33-34</sup> metal chelation,<sup>35-36</sup> as well as lipoxygenases inhibition.<sup>37-40</sup> The glycosides are less effective as antioxidants than are the aglycones.<sup>41</sup>

Flavonoids with free hydroxyl groups act as free-radical scavengers, and multiple hydroxyl groups, especially in the B-ring, enhance their antioxidant activity.<sup>42</sup> There is no evidence that flavonoid intake is protective against some types of cancer,<sup>43</sup> but they

have a possible role again coronary heart disease as some epidemiological studies reported.<sup>44</sup>

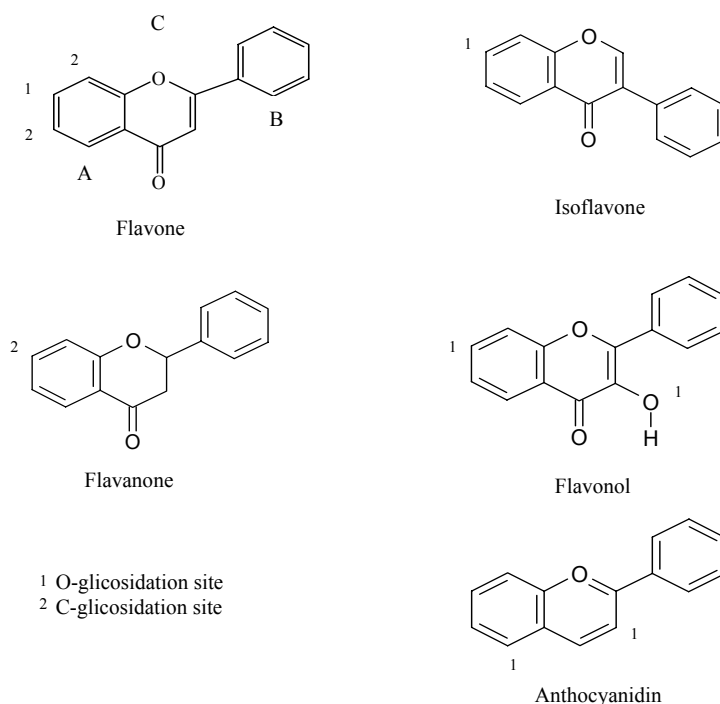


**Figure 2.1.1.** The main classes of flavonoids.

The antioxidant efficacy of flavonoids *in vivo* is less documented, presumably because of the limited knowledge on their uptake in humans. For example only a weak but insignificant inverse correlation was observed for flavonoid consumption and coronary mortality.<sup>45</sup> They are generally poorly absorbed from food, and extensively degraded to various phenolic acids, some of which still possess a radical scavenging ability. Finally, accordingly, the present epidemiological data, far from conclusive, evidence a possible protective role of dietary flavonoids, thus making desirable a regular consumption of foods and beverages rich in flavonoids but is also important to change their role as health-promoting dietary antioxidants and place these observations in a broader context embracing other dietary phenols, and mechanisms other than simple radical scavenging and radical suppression.<sup>46</sup>

### 2.1.1 *Flavonoids in food*

All foods of plant origin potentially contain flavonoids<sup>47,48</sup> and over 4000 individual compounds have previously been identified.<sup>49</sup>

Catechins, flavonols, and proanthocyanidins are abundant in fruits. In contrast, flavanones and flavones are restricted to citrus varieties such as oranges and lemons; in some fruits (e.g., apples), flavonols are principally present in the skin and hence peeling significantly reduces levels unlike catechins which are found in the flesh of fruits.

Quercetin is the most common flavonol in fruits; although kaempferol and myricetin have also been identified in fruits such as peaches and pears, concentrations are generally too low to be readily quantified in the whole fruit. Often termed the citrus flavonoids, flavanones are only found in citrus fruits such as oranges, grapefruit, and lemons.

Allium, Brassica, and Lactuca varieties of vegetables are abundant sources of flavonols, primarily quercetin and kaempferol while catechins are often the most common flavonoids in beverages such as fruit juice, tea, and wine. Wine also contains a complex mix of catechins, flavonols, procyanidins, and flavanones. Procyanidins usually represent 50% of the flavonoids found in red wine, followed by catechins (37%). A similar profile is observed with beer where again procyanidins dominate accounting for 42% of total flavonoid content. Concentrations of flavonoids in foods can vary by many orders of magnitude due to the influence of numerous factors such as species, variety, climate, degree of ripeness, and post harvest storage.<sup>48</sup> The flavonoid content of plant foods may be affected by growing conditions. Flavonoid profiles are also influenced by irrigation, which, for example, modifies concentrations and types of anthocyanins and catechins in berries.<sup>50</sup>

Effects of varietal differences as flavonoid subclasses can vary widely between different cultivars of fruits and vegetables.<sup>51</sup> In general, industrially produced products such as tea, red wine, and fruit juice have significantly different flavonoid levels and profiles than the original fresh product.<sup>52,53</sup> Processing and preservation can expose fresh products to increased risk of oxidative damage and the activation of oxidative enzymes such as polyphenol oxidase.<sup>54</sup> Domestic preparation procedures may also affect flavonoid content.<sup>55</sup> Initial estimate of flavonoid intake of 1000 mg/day<sup>48</sup>, has been

increased including the aglycon form<sup>51</sup> and the different source related to different countries.<sup>56</sup>

### 2.1.2 *Citrus and leek flavonoids*

Flavonoids identified in Citrus fruits cover over 60 types, according to the classes mentioned before<sup>57</sup> (fig. 2.1.1): flavones, flavanones, flavonols, flavans and anthocyanins (the last only in blood oranges).

In particular, this genus is characterized by accumulation of the large quantities of glycosylated flavanones, which are the first intermediaries in the flavonoid biosynthetic pathway<sup>58</sup>. The levels of the flavanones, found in the immature and mature fruits of Citrus, are mainly synthesized during the early stages of fruit growth<sup>59</sup>.

In fact, radiolabel experiment indicates that immature citrus are capable to biosynthesizing flavonoids from simple precursor and suggest that multiple-glycosylation of flavanones may occur by the addition of discrete single sugar units<sup>60</sup>.

Moreover, they have a possible role again coronary heart disease as some epidemiological studies reported.<sup>61</sup>

Citrus flavanones are present in the glycoside or aglycone forms. Among the aglycone forms, naringenin and hesperetin are the most important flavanones. Among the glycoside forms, two types are classified: neohesperidosides and rutinoides.<sup>62</sup> Neohesperidosides, flavanones, naringin, neohesperidin and neoeriocitrin consist of a flavanone with neohesperidose (rhamnosyl- $\alpha$ -1,2 glucose) and they have a bitter taste while rutinoides (flavanones, hesperidin, narirutin and didymin) have a flavanone and a disaccharide residue e.g. rutinose (ramnosyl- $\alpha$ -1,6 glucose) and they are without taste. Flavanones are usually present in diglycoside form, conferring the typical taste to Citrus fruits (fig. 2.1.2).<sup>63</sup>

The Citrus peel and seeds are very rich in phenolic compounds, such as phenolic acids and flavonoids. The peels are richer in flavonoids than are the seeds.<sup>64</sup> Since a Citrus fruit is peeled, peel and seeds are not used. The 7-O-glycosyl flavanones are the most abundant flavonoids in all Citrus fruits;<sup>65</sup> for example, lemon peel is rich in glycosidic flavonoids.<sup>66</sup> The neohesperidoside flavanones, naringin, neohesperidin and neoeriocitrin, are mainly present in bergamot, grapefruit and bitter orange juices while

rutinoside flavanones, hesperidin, narirutin and didymin, are present in bergamot, orange, mandarin and lemon juices.<sup>67</sup>

Flavone chemical structures are specific for every species, which renders them markers of adulteration in commercial juices.<sup>68</sup> Although flavones and flavonols have been found in low concentrations in Citrus tissues, these compounds are studied to evaluate their antioxidant ability.<sup>69</sup> Moreover, the malonate or other ester derivate<sup>70</sup> suggest which the esterification may act to mediate between different metabolic fates for individual flavonoids.

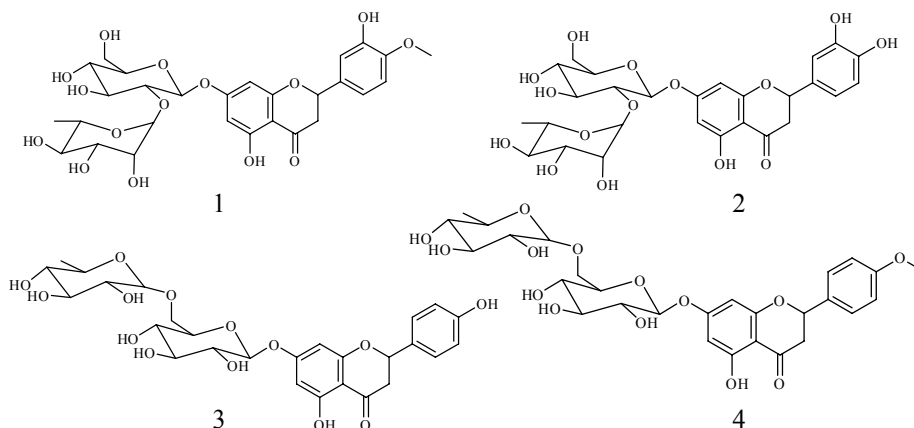


**Figure 2.1.2.** Main flavanone presents in citrus: 1) Neohesperidin; 2) Neoeriocitrin; 3) Narirutin; 4) Dydimin.

Pummelo (*Citrus maxima*) is one of the three progenitor of all citrus and is cropped in Asia, California and Israel where is extensively used in cuisine. There's no paper regard the flavonoids composition of this juice<sup>71</sup> and very few relative its antioxidant proprieties.<sup>72-73</sup> The flavonoids presents in this fruit indicates how the biosynthesis provide an accumulation of naringin flavanone.

Bergamot (*Citrus Bergamia Risso*), indeed is an hybrid between *Citrus aurantium* and *Citrus limon*. Particular, the trees grow extremely well in the narrow strip of land, about a hundred kilometres long which stretches between Villa San Giovanni and Gioiosa Ionica and between the foothills of the Aspromonte and the province of Reggio Calabria. Principally, it's used mostly for the extraction of its essential oil from the peel. Among the *Citrus* peel oils, because of its unique fragrance and freshness, bergamot oil is the most valuable and is therefore widely used in the cosmetic and food industries. The juice

obtained from the endocarp after essential oils extraction is considered just a secondary and discarded product in the working diagram of this *Citrus* fruit.<sup>74</sup>

The consumption of bergamot juice, very rich in flavonoids, can be an important component in human diet becoming a plus value of bergamot industries. On other hands, plants belong to *Allium* genus are rich in flavonoids with important biological activities. *Allium* species are a rich source of phytonutrients, useful for the treatment or prevention of a number of diseases, including cancer, coronary heart disease, obesity, hypercholesterolemia, diabetes type 2, hypertension, cataract and disturbances of the gastrointestinal tract (e.g. colic pain, flatulent colic and dyspepsia).<sup>75-79</sup> *Allium* is the largest and most important representative genus of the Alliaceae family and comprises 450 species, widely distributed in the northern hemisphere. Besides the well known garlic and onion, several other species are widely grown for culinary use, such as leek (*Allium porrum* L.), scallion (*Allium fistulosum* L.), shallot (*Allium ascalonicum* Hort.), wild garlic (*Allium ursinum* L.), elephant garlic (*Allium ampeloprasum* L.var. *ampeloprasum*), chive (*Allium schoenoprasum* L.), Chinesechive (*Allium tuberosum* L.). Leeks are an essential ingredient of cock-a-leekie and of vichyssoise. They can also be used raw in salads, doing especially well when they are the prime ingredient. The presence of flavonoids in leek is poorly to investigate, than other species of the same family<sup>80-82</sup>, and presents different Kaempferol glycosides as a main flavonoid compounds.<sup>83</sup> Moreover, the acylated Kaempferol can be also presents in these vegetable and has been demostred their antimutagen activity<sup>84</sup> to adding at action already evidenced for Kaempferol<sup>85,86</sup>.

### 2.1.3 Liquid chromatography/mass spectrometry for separation and structural determination.

Qualitative and quantitative applications of high performance liquid chromatography (HPLC) for flavonoids analysis are nowadays, very common. These compounds can be separated, quantified, and identified in one operation by coupling HPLC to ultraviolet (UV), mass, or nuclear magnetic resonance (NMR) detectors. This excellent chromophore is, of course, UV active and provides the reason why flavonoids are so easy to detect.

For the analytical HPLC of a given subclass of flavonoids (flavones, flavonols, isoflavones, anthocyanins, etc.), the stationary phase, solvent, and gradient have to be optimized. A very high proportion of separations are run on octadecylsilyl bonded (ODS, RP-18, or C18) phases. As solvents for application, acetonitrile–water or methanol–water mixtures, with or without small amounts of acid, are very common. These are compatible with gradients and MS/UV detection.

API are soft ionization methods and do not typically produce many fragments. This is useful in quantitative analysis or molecular mass determination but is of little use in structure elucidation.<sup>87-89</sup> For flavonoid aglycones and glycosides with a limited number of sugar units LC-MS provide only intense  $[M+H]^+$  ions for the aglycones and weak  $[M+H]^+$  ions of glycosides (mono- or disaccharide), together with intense fragment ions due to the loss of the saccharide units, lead to the aglycone moiety  $[A+H]^+$ .

General type of fragmentations can be showed in fig 2.1.3 were the nomenclature proposed by Domon and Costello<sup>90</sup> is applied. Further structural characterization can be performed by LC-MS/MS and MS/MS analysis in high resolution.<sup>91-94</sup>

It's possible to establish the distribution of substituents between the A- and B-rings and also the determination of the nature and site of attachment of the sugars in O- and C-glycosides.<sup>95-97</sup> Online accurate mass measurements of all MS/MS fragments were obtained on the Q TOF instrument, allowing molecular formulae of compounds to be assessed directly. In order to obtain NMR structural elucidation must be have an adequate quantity of unknown compounds. For this reason is necessary to make a preparative steps for their isolation.

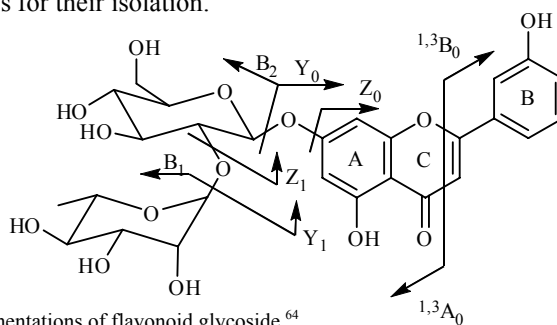


**Figure 2.1.3.** Fragmentations of flavonoid glycoside.<sup>64</sup>

After sample extraction ideal strategy consist in a previous medium-pressure liquid chromatography (MPLC)<sup>98,99</sup> and successive purification by semi-preparative HPLC.



The former covers a wide range of column diameters, different granulometry packing materials, different pressures, and have a high loading capacity (1:25 sample-to-packing-material ratio<sup>100</sup>), the latter use columns of internal diameter 8 to 21 mm, often packed with 10 µm (or smaller) particles and both isocratic and gradient conditions are employed.<sup>101-103</sup>

## 2.2 Secoiridoids

This class of compounds is also included in PPT like mentioned before for the flavonoids. They belong to the family of oleosides and are coumarine-like compounds with a 8,9 or 9,10-olefinic functionality with a phenolic moiety as a result of esterification (fig. 2.2.1). For this reason can be also called as phenolic oleosides and are classified as a secondary metabolites rather than primary that includes proteins lipids etc. (also if the two metabolism are interconnected).<sup>104,105</sup> Moreover are restricted to the Oleaceus plant. The structure of compounds with different oleofinic functionality are structurally similar<sup>106</sup> but derived from two different way.<sup>107</sup>

Secoiridoid constituents are found in all part of the plant but their composition and concentration varies greatly depending on the tissue.<sup>108-110</sup>

An increasing interest for this compounds is due to their antioxidant and health enhancing properties.<sup>111,112</sup> Several species within the family provide commercial products such as food, cosmetics and medicinal. Generally, the leaves are the primary site of plant metabolism; here, are present various secoiridoid glucosides, which have been studied for their therapeutic effects. They are stored almost exclusively as conjugates for several reason.<sup>113</sup>

Each plant of this family have a different secoiridoids which indicates the extensive possibilities of metabolic pathways.

In *Olea Europaea* fruit and oil there are, in different amount, secoiridoids and their derivatives as dialdehydic forms of aglycons, but also simple phenols and hydroxycinnamic derivatives (fig. 2.2.1 A, B), but their quantity depend on cultivars, pedoclimatics and other factors.<sup>114,115</sup> Many of this secoiridoids are known for their antioxidant power, especially those carrying catecholic moieties such as oleuropein, and they are effective against a number of pathologies.<sup>116</sup>

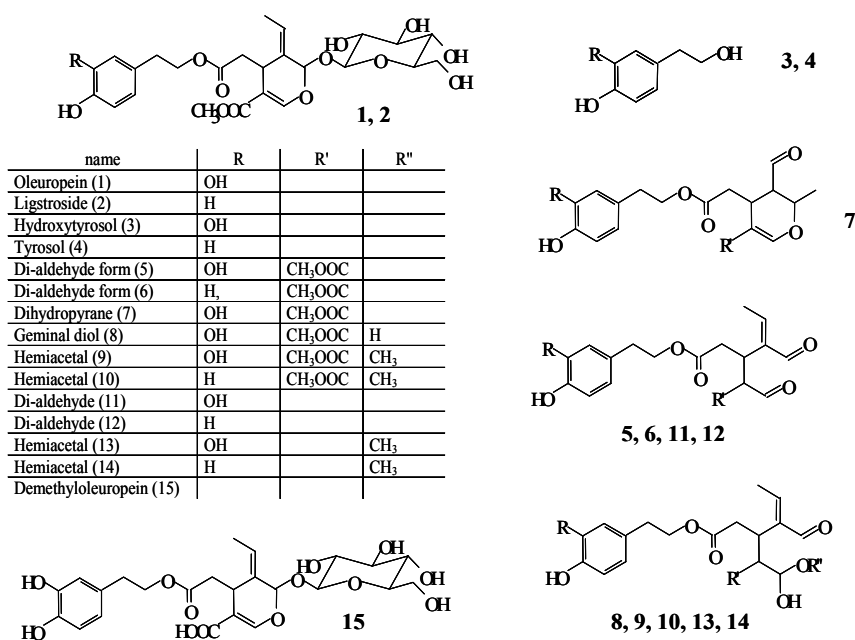
Nevertheless, as verified for other natural anti-oxidants, oleuropein may also act as a pro-oxidant.<sup>117</sup> Very recently, an ibuprofen (anti-inflammatory)-like activity was attributed to the dialdehyde obtained from the aglycone of demethyllygistroside.<sup>118-120</sup> Metabolic pathways have been elucidated for different olive tissues.

However, it is not firmly established whether transport within different parts of the plant involves transfer of precursors or of the final conjugates.

Moreover, because of the number of microcomponents present in different tissues of the olive only the most stable and most abundant species have been identified, as described in many review articles.<sup>121,122</sup>

Oleuropein, is a characteristic but very variable component of leaves, olives and olive oil; in the leaves is the first secoiridoid together a large number of phenolic compounds and several types of flavonoids which are known to have antioxidant and in general therapeutic properties,<sup>123,124</sup>

Their structures have been confirmed by NMR<sup>125</sup> or in alternative by High Resolution Electrospray tandem mass spectrometry<sup>126</sup> after isolation by semi-preparative high-performance liquid chromatography (HPLC).



A

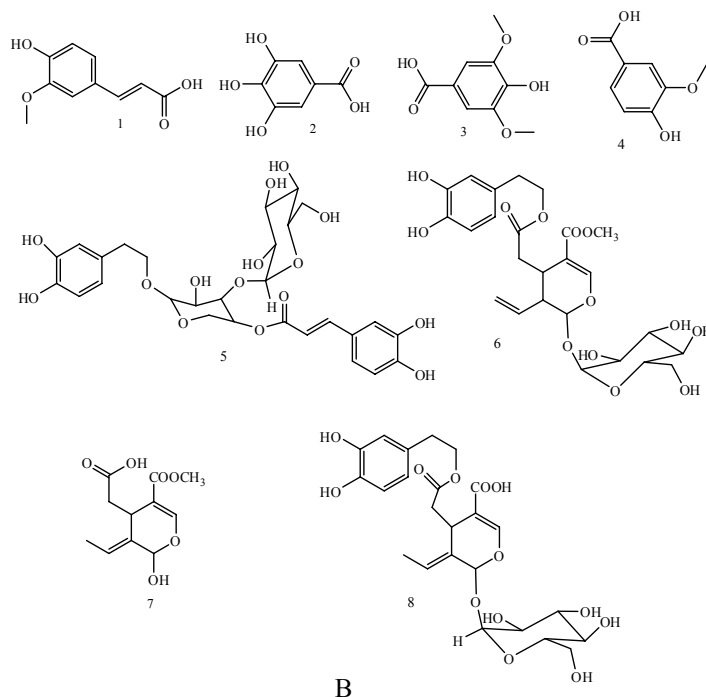


**Figure 2.2.1.** A) main components in drupes and olive oil; B) other important species presents in different tissues: 1-ferulic acid, 2-gallic acid, 3-syringic acid, 4-homovanillic acid, 5-verbascoside, 6-oleuroside, 7-elenolic acid, 8-demetyloleuropein.

After consumption of 25 ml virgin olive oil, hydroxytyrosol, 3-O-methylhydroxytyrosol (homovanillyl alcohol), and homovanillic acid increase in plasma, as conjugates, predominantly glucuronide.<sup>127</sup>

Oleuropein may be deglycosylated by the gut microflora.<sup>128</sup> LC/MS aims to reveal and characterize, together high resolution tandem mass spectrometry, the various metabolites.<sup>129,130</sup> The characteristic pathway of fragmentation of this type of compounds with API methods can be reviewed by historical pattern of oleuropein and relative tandem mass spectrum (fig 2.2.2; fig 2.2.3).<sup>131</sup>

Nevertheless is possible to perform quantitative analysis. Nowadays, are still far from to understand all phenomena related to this species but they passed through identification of unknown compounds and the implementation of metabolic studies. Moreover the statistical approach allows the discrimination of different cultivars.

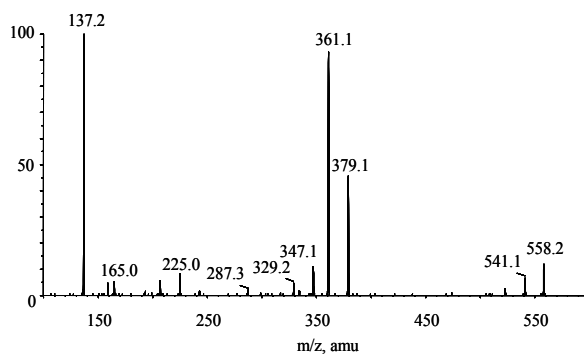


Figure 2.2.2. APCI-MS/MS of Oleuropein.

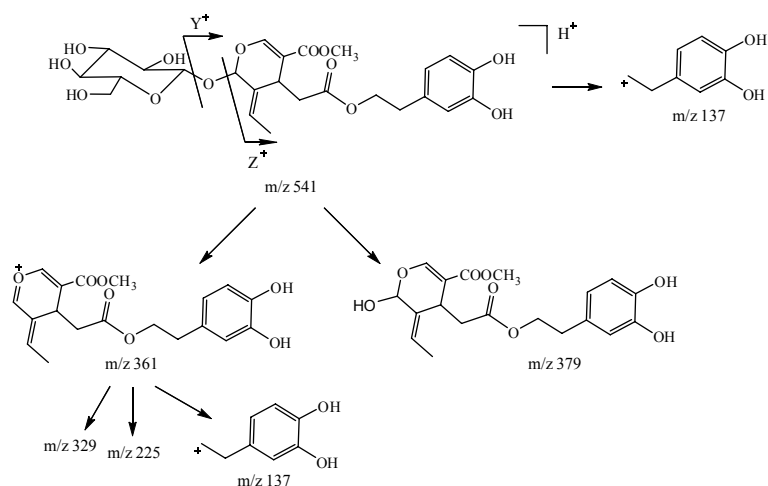


Figure 2.2.3. Mass fragmentation of oleuropein.

### 2.3 Sudan I-IV and Para-red

Azo-dyes, are widely used as colorants in cosmetics,<sup>132</sup> foods,<sup>133</sup> textiles<sup>134</sup> commodities<sup>135</sup> and, incredibly, also in tattooing.<sup>136</sup> Illegal presence of the dye Sudan I in foods in the EU was first reported in May 2003. It was found in chilli powder and in foods containing chilli powder. There have also been occasional notifications of Sudan II and Sudan III in the same range of products. Due to the type of food products concerned, the origin of contaminated raw products has been in imports from outside the EU (India, Turkey, Pakistan, Egypt for raw spices, Ghana, Nigeria and West Africa for palm oil). The presence of industrial dyes in food constitutes an adulteration of food

products, since these substances are not authorised as food colours according to the European Parliament and Council Directive 94/36/EC on colours for use in foodstuffs.

A Community measure was taken in June 2003 to control the unlawful use of Sudan I in chilli powder and chilli products (Commission Decision 2003/460/EC).

These measures were extended to other Sudan dyes in chilli and chilli products (Commission Decision 2004/92/EC) and successively in curcuma and palm oil (Commission Decision 2005/402/EC). Much information is relative at the structural features of dyes that may provide alerts for possible genotoxic and carcinogenic activity due to the fact which can be metabolized to lipid soluble aromatic amines. This mutagenicity, followed by oxidation of the liberated primary aromatic amines can occur in the gastrointestinal tract and in the liver. The structures of Sudan I-IV are shown in fig 2.3.1. Sudan I is genotoxic both *in vitro*, with metabolic activation, and *in vivo*.<sup>137,138</sup>

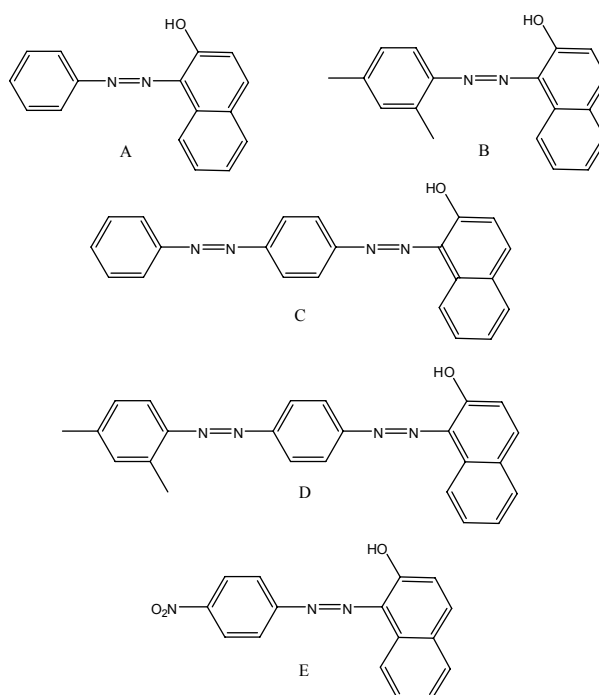


**Figure 2.3.1.** Different structures of Sudan: A) Sudan I, B) Sudan II, C) Sudan III, D) Sudan IV E) Sudan p-Red.

The effects of Sudan I including genotoxicity and carcinogenicity are dependent upon the metabolism to reactive products and *in vitro* studies using rat and human

microsomes showed similar pathways of metabolism and DNA interaction.<sup>139</sup> Sudan II is mutagenic in bacterial tests, after metabolic activation and the high incidence of bladder tumours following implantation of Sudan II impregnated pellets is sufficient to consider this dye possibly carcinogenic until proved otherwise.<sup>140,141</sup>

The structural relationship of Sudan III with Sudan I would suggest that some identical metabolites might be formed but there are no indication of carcinogenic potential. The very limited evidence suggests that metabolism of this dye is much less than that of Sudan I, but in absence of data it may be prudent to assume that it is potentially genotoxic and possibly carcinogenic. Same type of considerations can be done for Sudan IV. Finally, other illegal dye is the Para Red. Data of this are very sparse but structurally it has similarities with other dyes such as Sudan I. There is evidence that the molecule undergoes azo-reduction by microflora in the intestine yielding free amines.<sup>142</sup> Moreover, the effectiveness of human skin bacteria<sup>143</sup> in the formation of carcinogenic amines from the same species has been described more recently. Information on the enzymatic mechanisms have been presented,<sup>144,145</sup> as well as proofs on the dangerous effects on human health caused by ingestion of azo dyes of the sudan families.<sup>146</sup> The development of analytical high-throughput methods in environmental control has become of paramount importance in life sciences.<sup>147</sup>

The LC-MS/MS is a reliable and accurate analytical method for the identification and quantification of Sudan in foodstuffs also by improving the identification of the analytes to perform high throughput safety controls and the set up of sensitive and reliable approaches for their assay, at very low level, in various edible matrices. The fragmentation mechanism of the  $[M+H]^+$  species obtained from commercially available dyes as well as from their deuterated isomers provides the clue for the unambiguous structural assignment to each species. It regards principally the azo-linkage but not exclusively. The MRM (multiple reaction monitoring) provide higher sensitivity and selectivity, very important when our compounds are presents in complex matrices as foodstuffs. In this respect it is important the choice of interface to improve the limit of detection. All the directives do not issue any safety threshold; therefore the use of labelled internal standards coupled with an MS/MS parent ion scan on a common ionic species coming from the fragmentation of each individual analyte could be enough to assess the safety of the analyzed item at the sensitivity of the method.

On the other hand an accurate evaluation of the absolute amount of each analyte, easily achievable by the isotope dilution method<sup>148</sup>, provides clues to assess the risks of human exposure to contaminated foods.

### Scope of the thesis

The scope of this thesis was to apply the LC/MS methods for both separation and identification of microcomponents presents in various natural matrices, as well as to quantify the illegal dyes, Sudan I-IV and Para Red, eventually presents in foodstuffs.

An HPLC and mass spectrometry technology has been introduced in chapter 1 and the LC/MS applications in food in chapter 2. The next chapter will illustrate the powerful of LC/UV/ESI-MS, analytical and semi-preparative, and high resolution ESI-MS/MS in structural elucidation of unknown compounds. Bergamot and Pummelo fruits, leaves and olives of *Olea Europaea*, leek, have been analyzed for their common use in human diet and/or as PPT product sources. The results of these investigations are reported in chapter 3. The chapter 3, paragraph 4, deal the fragment investigation and LC/MS simultaneous analysis of dyes mentioned above. In both cases the labelled deuterium compounds was employed also.

## References

1. P. Arpino. *Mass Spectrom. Rev.* **1989**, 8, 35-55.
2. P. Arpino. *Mass Spectrom. Rev.* **1990**, 9, 631-669.
3. M.P. Maillard; J. Wolfender; K. Hostettmann. *J. Chromatogr.* **1993**, 647, 147-154.
4. J. Wolfender; K. Hostettmann. *Pestic. Sci.* **1997**, 51, 471-482.
5. J. Wolfender; K. Hostettmann. *J. Chromatogr.* **1993**, 647, 191-202.
6. K. Sato; T. Kumazawa; Y. Katsumata. *J. Chromatogr.* **1994**, 674A, 127-145.
7. J. Wolfender; S. Rodriguez; K. Hostettmann; W. Wagner-Redeker. *J. Mass Spectrom.* **1995a**, 35-46.
8. J. Wolfender; S. Rodriguez; K. Hostettmann; W. Hiller. *Phytochem. Anal.* **1997**, 8, 97-104.
9. S. Zhou; M. Hamburger. *J. Chromatogr.* **1996**, 755A, 189-204.
10. J.P.C. Vissero; H.A. Claessens; C.A. Cramers. *J. Chromatogr.* **1997**, 779A, 1-28.
11. M. Careri; A. Mangia; M. Musci. *J. Chromatogr.* **1998**, 794A, 263-297.
12. A.P. Bruins. *J. Chromatogr.* **1998**, 794A, 345-357.
13. W.M.A. Niessen. *J. Chromatogr.* **1998**, 794A, 407-435.
14. W.M.A. Niessen. *Liquid Chromatography-Mass Spectrometry*, 2nd ed. Marcel Dekker, New York, **1999**.
15. R. Doll; R. Peto. *The causes of cancer* New York NY: Oxford University Press; **1981**.
16. K.A. Steinmetz; J.D. Potter. *Cancer Causes Control.* **1991**, 2, 325-357.
17. K.A. Steinmetz; J.D. Potter. *Cancer Causes Control.* **1991**, 2, 427-442.
18. I.D. Wilson; U.A. Th. Brinkman. *J. Chromatogr. A* **2003**, 325.
19. J.-L. Wolfender; K. Ndjoko; K. Hostettmann. *J. Chromatogr. A* **2003**, 437.
20. L. Di Donna; G. Grassi; F. Mazzotti; E. Perri; G. Sindona. *J. Mass Spectrom.* **2004**, 39, 1437-1440.
21. J.F. Van Bocxlaer; K.M. Clauwaert; W.E. Lambert; D.L. Deforme; E.G. Van den Eeckhout; A.P. De Leenheer. *Mass Spectrom. Rev.* **2002**, 19, 165.
22. M.J. Bogusz. *J. Chromatogr. B* **2000**, 748, 3.
23. K. Herrmann. *Gordian* **1993**, 93, 108-11.



24. P.J. White; Y. Xing. *Natural Antioxidants, Chemistry, Health Effects, and Applications* Shahidi F (ed.), Champaign, Illinois, AOCS Press, **1997**, 25-63.
25. J.J. Macheix; A. Fleurit; J. Billot. *Fruit Phenolics* Boca Raton, CRC Press, **1990**.
26. A. Hopia.; M. Heinonen. *J Amer Oil Chem Soc.* **1999**, 76, 139-44.
27. S. S. Pekkarinen; I.M. Heinonen; A.I. Hopia. *J Sci Food Agric.* **1999**, 79 499-506.
28. K. Ioku; T. Tsushida; Y. Takei; N. Nakatani; J. Terao. *Biochim Biophys Acta* **1995**, 1234, 99-104.
29. J. Robak; R.J. Gryglewski. *Biochem Pharmacol.* **1988**, 37, 837-41.
30. J.P. Hu; M. Calomme; A. Lasure; T. De Bruyne; L. Peters; A. Vlietinck; D.A. Van den Berghe. *Biol Trace Element Res.* **1995**, 47, 327-31.
31. U. Takahama. *Phytochemistry* **1985**, 24, 1443-1446.
32. S.R. Husain; J. Cillard; P. Cillard. *Phytochemistry* **1987**, 26, 2489-2491.
33. S. Criado; S.G. Bertolotti; A. T. Soltermann; V. Avila; N.A. Garcia. *Fat Sci Technol.* **1995**, 97, 265-269.
34. U. Takahama. *Plant Physiol.* **1984**, 74, 852-857.
35. S.E.O. Mahgoub; B.J.F. Hudson. *Food Chemistry* **1985**, 16, 97-101.
36. L. Ramanathan; N.P. Das. *Intern J Food Sci Technol.* **1993**, 28, 279-288.
37. T. Dohi; S. Anamura; M. Shikawa; H. Okamoto; A. Tsujimoto. *Japan J Pharmacol.* **1991**, 55, 547-550.
38. J.M. Lyckander; K.E. Malterud. *Acta Pharm Nord.* **1992**, 4, 159-166.
39. F. Richard-Forget; F. Gauillard; M. Hugues; T. Jean-Mark; P. Boivin; J. Nicolas. *J Food Sci.* **1995**, 60, 1325-1329.
40. C. Voss; S. Sepulveda-Boza; F.W. Zilliken. *Biochem Pharmacol.* **1992**, 44, 157-162.
41. G.W. Plumb; K.R. Price; G. Williamson. *Redox Rep.* **1999**, 4, 13-16.
42. S.V. Jovanovic; S. Steenken; M. Tosic; B. Marjanovic; M.G. Simic. *J Amer Chem Soc.* **1994**, 116, 4846-4851.
43. M.G.L. Hertog. *Proc. Nutr. Soc.* **1996**, 55, 385-396.
44. M.G.L. Hertog; M.B. Katan. In *Flavonoids in Health and Disease*; Rice-Evans, C. A., Packer, L., Eds.; Marcel Dekker: New York, **1998**, 447-467.
45. E.B. Rimm; M.B. Katan; A. Ascherio; M. Stampfer; W.C. Willet. *Ann. Int. Med.* **1996**, 125, 384-389.

46. I.C. Arts; P.C. Hollman; *Am. J. Clin. Nutr.* **2005**, 81, 317S.
47. K.J. Herrmann. *Food Technol.* **1976**, 11, 433.
48. J. Kuhnau. *World Rev. Nutr. Diet.* **1976**, 24, 117.
49. J.B. Harborne. *The Flavonoids: Advances in Research Since 1986*; London: Chapman & Hall, **1994**.
50. P. Cuadra; J.B. Harborne. *Z. Naturforsch. C* **1996**, 51, 671.
51. A.G.H. Lea. *Am. J. Enol. Vitic.* **1979**, 30, 289.
52. C.Y. Lee; A.W. Jaworski. *Am. J. Enol. Vitic.* **1990**, 41, 87.
53. Z. Czochanska; L. Foo; L. Porter. *Phytochemistry* **1979**, 18, 1819.
54. H. Fulcrand. In 18<sup>th</sup> International Conference on Polyphenols, Bordeaux, France, **1996**, 203.
55. P. Sarni-Manchado; V. Cheynier; M. Moutounet. *Phytochemistry* **1997**, 45, 1365.
56. S.J. Vidal. *Sci. Food Agric.* **2003**, 83, 564.
57. R. Horowitz & B. Gentili. Flavonoids constituents of citrus. In S.Nagy, P. E. Shaw, & M. K. Vedhuis (Eds.), *Citrus science and technology*. Westport, CT: AVI Publishing. **1977**, 397-426.
58. V.P. Maier; S. Hasegawa; *Phytochemistry* **1970**, 9, 139-144.
59. J.A. Del Rio; M.D. Fuster; F. Sabater; I. Porrai; A. Garcia; L. Ortuno. *Food Chem.* **1997**, 59, 433-437.
60. M.A. Berhow; C.E. Vandercook. *Phytochemistry* **1989**, 28, 1627-1630.
61. M.G.L. Hertog; M.B. Katan. In *Flavonoids in Health and Disease*; C.A. Rice-Evans; L. Packer; Eds.; Marcel Dekker: New York, **1998**, 447-467.
13. M.A. Berhow; R.D. Bennett; K. Kanes; S.M. Poling; C.E. Vandercook. *Phytochemistry* **1991**, 30, 4198-4200.
62. F.Gionfriddo; E. Postorino; F. Bovalò. I Flavanoni glucosidici nel succo di bergamotto. *Essenze-Derivati agrumari*, 66, 404-416.
63. J.J. Macheix; A. Fleuriet; J. Billot. The main phenolics of fruits. In *Fruit phenolics*. Boca Raton, FL: CRC Press 1-103.
64. S. Yusof; H. Mohd Ghazali; G. Swee King; *Food Chemistry* **1990**, 37, 113-121.
65. O. Benavente-García; J. Castello; F. Sabater; J. A. Del Rio. *Plant Physiology and Biochemistry* **1995**, 33, 227-263.

66. G. L. Park; S. M. Avery; J. L. Byers; D. B. Nelson. *Food Technology* **1983**, 37, 98-105.
67. R. M. Horowitz, **1986**, 213, 163-175.
68. W. C. Ooghe; C. M. Detavernier; *Journal of Agricultural and Food Chemistry* **1997**, 45, 1633-1637.
69. O. Benavente-García; J. Castello; FR. Marin; A. Ortunõ; J. A. Del Rý'o. *Journal of Agricultural and Food Chemistry* **1997**, 45, 4505-4515.
70. M.A. Berhow; R.D. Bennett; K. Kanes; S.M. Poling; C.E. Vandercook. *Phytochemistry* **1991**, 30, 4198-4200.
71. S. Hasegawa; M.A. Berhow; C.H. Fong. *Analysis of bitter principles in citrus*. **1996** In H. F. Linskens, & J. F. Jackson (Eds.), *Modern methods of plant analysis*. Berlin, Heidelberg: Springer-Verlag. 18, 59-80.
72. M. Saif Mokbel; T. Suganuma. *Eur Food Res Technol* **2006**, 224, 39-47.
73. H.L. Tsai; S. K. C. Chang; S.J. Chang. *J. Agric. Food Chem.* **2007**, 55, 2867-2872.
74. A. Di Giacomo. *Il Bergamotto di Reggio Calabria*, Baruffa Editore, Reggio Calabria, **1989**, 102-119.
75. W.C. Willet. *J. Clin. Cancer.* **1999**, 49, 331.
76. F. Papasso; T.S. Gaginella; G. Grandolini; A.A. Izzo. *Phytotherapy. A Quick Reference of Herbal Medicine*, Springer-Verlag, Heidelberg, Germany, **2003**.
77. E. Fattorusso; M. Iorizzi; V. Lanzotti; O. Tagliatela-Scafati. *J. Agric. Food Chem.* **2002**, 50, 5686.
78. K.T. Augusti. *Ind. J. Exp. Biol.* **1996**, 34, 634.
79. L.D. Lawson, in: *Phytomedicines of Europe, American Chemical Society Symp. Ser.* **1998**, 691, 176.
80. A. Carotenuto; V. De Feo; E. Fattorusso; V. Lanzotti; S. Magno; C. Cicala. *Phytochemistry* **1996**, 41, 531-536.
81. A. Carotenuto; E. Fattorusso; V. Lanzotti; S. Magno; V. De Feo; C. Cicala. *Phytochemistry* **1997**, 44, 949-957.
82. V. Lanzotti. *Journal of Chromatography A*, **2006**, 1112, 3-22.
83. E. Fattorusso; V. Lanzotti. *Phytochemistry* **2001**, 57, 565.
84. K. Samejima; K. Kanazawa; H. Ashida; G. Danno. *J. Agric. Food Chem.* **1998**, 46, 4864-4868.

85. R. Landolfi; R. Mower; M. Steiner; *Biochemical Pharmacology* **1984**, 33, 1525-1530.
86. S.H. Tzeng; W.C. Ko; F.N. Ko; C.M. Teng. *Thrombosis Research* **1991**, 64, 91-100.
87. U. Vrhovsek et al. *J. Agric. Food Chem.* **2004**, 52, 6532.
88. G.Le Gall et al. *J. Agric. Food Chem.* **2003**, 51, 2438.
89. K. Robards; *J. Sci.Food Agric.* **1997**, 75, 87.
90. B. Domon; C.E. Costello. *Glycoconj. J.* **1988**, 5, 397.
91. M. Stobiecki. *Phytochemistry* **2000**, 54, 237.
92. S. De Pascual-Teresa; J.C. Rivas-Gonzalo. *The Royal Society of Chemistry*; Cambridge, Chap. 3, **2003**.
93. E. De Rijke; P. Out; W.M. Niessen; F. Ariese; C. Gooijer; U.A. Th.Brinkman. *Journal of Chromatography A* **2006**, 1112, 31-63.
94. F. Cuyckens; M. Claeys. *J. Mass Spectrom.* **2004**, 39, 1-15.
95. E. Hvattum; D. Ekeberg *J. Mass Spectrom.* **2003**, 38, 43-49.
96. F. Cuyckens; M. Claeys. *J. Mass Spectrom.* **2005**, 40, 364-372.
97. R. E. Marcha; E.G. Lewars; C.J. Stadey; X.S. Miao. *International Journal of Mass Spectrometry* **2006**, 248, 61-85.
98. Y. Shirataki et al. *Chem. Pharm. Bull.* **1991**, 39, 1568.
99. B. Ducrey. *Phytochemistry* **1995**, 38, 129.
100. T. Leutert; E. Von Arx. *J. Chromatogr.* **1984**, 292, 333.
101. Y.Liu; H. Wagner; R. Bauer. *Phytochemistry* **1996**, 42, 1203.
102. T. Lee et al. *J. Nat. Prod.* **2000**, 63, 710.
103. E.F. Queiroz et al. *J. Nat. Prod.* **2002**, 65, 403.
104. J. Mann. *Secondary Metabolism*; 2<sup>nd</sup> Edition. Clarendon Press, Oxford **1987**.
105. S. Damtof; H. Franzyk; S. R. Jensen. *Phytochemistry* **1995**, 40, 773-784.
106. F. Angerosa; N. D'Alessandro; P. Konstantinou; L. Di Giacinto. *J. Agric. Food Chem.* **1995**, 43, 1802-1807.
107. F. Visioli; C. Galli. *J. Agric. Food Chem.* **1988**, 58, 157-159.
108. A. De Nino; N. Lombardo; E. Perri; A. Procopio; A. Raffaelli; G. Sindona. *J. Mass Spectrom.* **1997**, 32, 533.
109. D. Ryan; K. Robbards. *Analyst* **1998**, 123, 31R.

110. A. De Nino; F. Mazzotti; SP. Morrone; E. Perri; A. Raffaelli; G. Sindona. *J. Mass Spectrom.* **1999**, 34, 10.
111. N. Nenadis; L.F. Wang; M.Z. Tsimidou; H.Y. Zhang. *J. Agric. Food Chem.* **2005**, 53, 295-299.
112. O. Benavente-García; J. Castello; J. Morente; A. Ortun; J.A. Del Rio. *Food Chemistry* **2000**, 68, 457-462.
113. S. Damtoft; H. Franzky; S.R. Jensen. *Phytochemistry* **1993**, 34, 1291-1299.
114. R. Japoa; N-Lujaa; J.R. Jimea; M.D.L. De Castro. *J. Agric. Food Chem.* **2006**.
115. J.A. Pereira; S. Casal; A. Bento; M.B.P. Oliveira. *J. Agric. Food Chem.* **2002**, 50, 6335-6340.
116. D. Ryan; M. Antolovich; P. Prenzler; K. Robards; S. Lavee. *Scientia Horticulture* **2002**, 92, 147.
117. Mazzotti A, Mazzotti F, Pantusa M, Sportelli L, Sindona G. *J. Agric. Food Chem.* 2006; **54**: 7444.
118. GK. Beauchamp; RSJ. Keast; D. Morel; J. Lin; J. Pika; Q. Han; CH. Lee; AB. Smith; PAS Breslin. *Nature* **2005**, 437, 45.
119. G. Montedoro; M. Servili; M. Baldioli; R. Selvaggini; E. Miniati; A. Macchioni. *J. Agric. Food Chem.* **1993**, 41, 2228.
120. A. De Nino; F. Mazzotti; E. Perri; A. Procopio; A. Raffaelli; G. Sindona. *J. Mass Spectrom.* **2000**, 35, 461.
121. C. Soler-Rivas; JC. Espin; HJ. Wichers. *J. Sci. Food Agric.* **2000**, 80, 1013.
122. M. Servili; R. Selvaggini; S. Esposito; A. Taticchi; G. Montedoro; G. Morozzi. *J. Chromatogr. A* **2004**, 1054, 113.
123. F. Visioli; A. Poli; C. Galli. *Med. Res. Rev.* **2002**, 22, 65.
124. A. Petroni; M. Blasevich; M. Salami; N. Papini; G. F. Montedoro; C. Galli. *Thromb. Res.* **1995**, 78, 151.
125. a) G. Montedoro; M. Servili; M. Baldioli; E. Miniati. *J. Agric. Food Chem.* **1992**, 40, 1577; b) G. Montedoro; M. Servili; M. Baldioli; R. Selvaggini; E. Miniati; A. Macchioni. *J. Agric. Food Chem.* **1993**, 41, 2228.
126. L. Di Donna; F. Mazzotti; A. Napoli; A. Sajjad; R. Salerno; G. Sindona. *Rapid Commun. Mass Spectrom.* **2007**, 3, 273.
127. C. Portal; M. Bradley. *Organic and Biomolecular Chemistry* **2007**, 5, 587.

128. D. Caruso; F. Visioli; R. Patelli; C. Galli; G. Galli. *Metabolism* **2001**, 50, 1426.
129. F. Visioli; C. Galli; S. Grande; K. Colonnelli; C. Patelli; G. Galli; D. Caruso. *J. Nutr.* **2003**, 133, 2612-2003.
130. D. Ryan; K. Roboards; S. Lavee. *J. Chromatogr. A* **1999b**, 832, 87-96.
131. A. De Nino; N. Lombardo; E. Perri; A. Procopio; A. Raffaelli; G. Sindona. *J. Mass Spectrom.* **1997**, 32, 533.
132. Chen H. Recent advances in azo dye degrading enzyme research. *Current Protein and Peptide Science* **2006**, 7, 101.
133. L. Di Donna; L. Maiuolo; F. Mazzotti; D. De Luca; G. Sindona. *Analytical Chemistry* **2004**, 76, 5104.
134. B. Mahltig; H. Bottcher; D. Knittel; E. Schollmeyer. *Textile Research Journal* **2004**, 74, 521.
135. *Sudan I – IARC Monographs*, Vol. 8. IARC Lyon: France **1975**, 225.
136. Lundsgaard J. *Investigation of Pigments in Tattoo Colors*, Survey No 2, Danish Environmental Protection Agency.
137. B.M. Elliott; K. Griffiths; J.M. Mackay; J.D. Wade. *Mutagenesis* **1997**, 12, 255-8.
138. A. Wakata; Y. Miyamae; S. Sato; T. Suzuki; T. Morita; N. Asano; T. Awogi; K. Kondo; M. Hayashi. *Environ Mol Mutagen.* **1998**, 32, 84-100.
139. M. Stiborova; V. Martinek; H. Rydlova; P. Hodek; E. Frei. *Cancer Res.* **2002**, 62, 5678-5684.
140. Y. Hayakawa; M. Miyagoshi; T. Nagayama. *Eisei Kagaku* **1984**, 30, 211-215.
141. IARC monograph Vol. 8, **1975**, 217.
142. B.R. Golden; S.L. Gorbach. *JNCI* **1984**, 73, 689-95.
143. T. Platzek; C. Lang; G. Grohmann; U.S. Gi; W. Baltes. *Human and Experimental Toxicology* **1999**, 18, 552.
144. Y. Bin; ZT. Zhou; W. Jing; CH. Du; HM. Hou; ZY, Song; YM. Bao. *FEMS Microbiology Letters* **2004**, 236, 129.
145. S, Zbaida; WG. Levine. *The Journal of Pharmacology and Experimental Therapeutics* **1992**, 260, 554.
146. M. Stiborova; V. Martinek; H. Rydlova; T. Koblas; P. Hodek. *Cancer Letters* **2005**, 220, 145.
147. C. Portal; M. Bradley. *Organic and Biomolecular Chemistry* **2007**, 5, 587.

148. L. Di Donna; L. Mariuolo; F. Mazzotti; D.De Luca; G.Sindona. *Anal. Chem.* **2004**, *76*, 5104-5108.

## Chapter 3

### *Results and discussion*

*New microcomponents detected in drupes and leaves of Olea europaea L. by ESI/high-resolution tandem mass spectrometry and statistical analysis of leaves for cultivar discrimination.*

*Characterization of new flavonoids in bergamot and pummelo juice*

*Determination of new flavonoidic compounds by High-resolution ESI-MS/MS in Allium Porrum.*

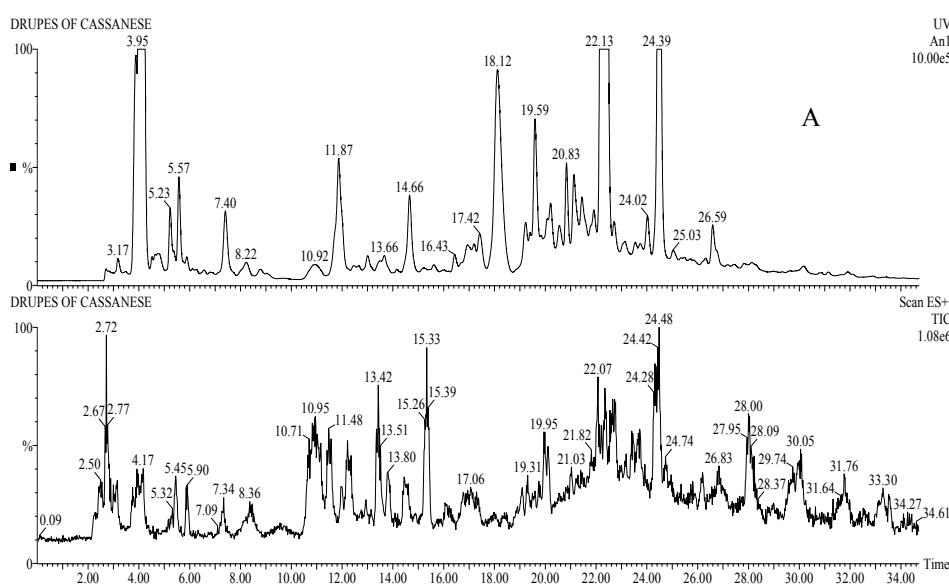
*Gas-phase chemistry of all set of Sudan Azo dyes (I, II, III, IV and Para-red) and relative investigation in foodstuff by LC/MS-MS and Isotope dilution methodology.*





### 3.1 New microcomponents detected in drupes and leaves of *Olea europaea* L. by ESI/high-resolution tandem mass spectrometry and statistical analysis of leaves for cultivar discrimination.

Oleuropein, verbascoside, oleoside and glucosylated hydroxytyrosol are among the most abundant phenolic compounds present in olive pulp. However, there is a large variety of microcomponents structurally correlated to oleuropein and other secoiridoids whose low relative percentage occurrence prevents their detection by conventional HPLC-UV, hence their structural assignment by spectroscopic methods. The approach used in this investigation is based on (a) on-line identification of new compounds by HPLC/ESI-MS (fig. 3.1.1A); (b) their isolation, even if not in a pure state, which means that the collection of fractions at a given  $m/z$  value of a reconstructed chromatogram (fig. 3.1.1B) may contain, besides the species of interest, traces of other compounds; and (c) their structural determination by high-resolution MS/MS in a QqTOF mass spectrometer. Of the microcomponents detectable by the above mentioned procedure, the structural features of those new metabolites, which have been isolated with a sufficient degree of purity, can be suggested with a high degree of confidence. This consideration is based on the spectroscopic evidence that common groups are shared by the newly detected species with those secoiridoids whose structures are firmly established.



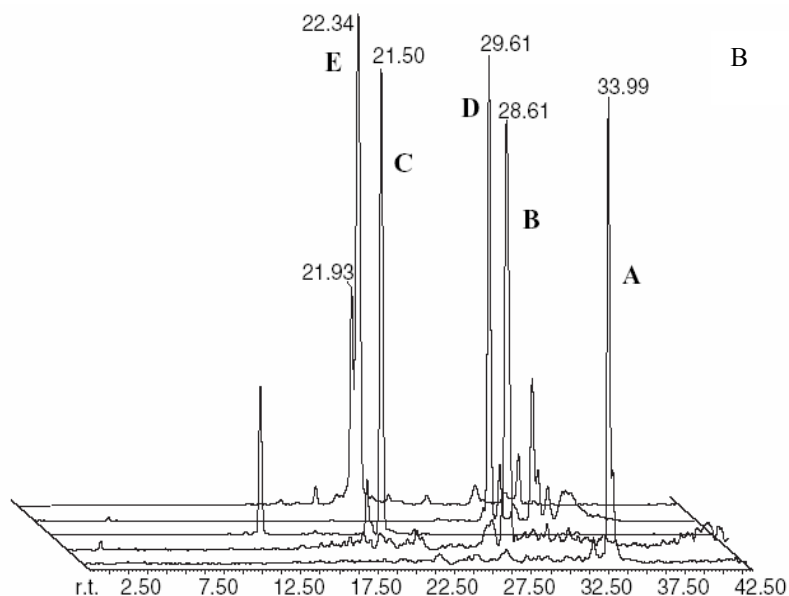


**Figure 3.1.1.** A) LC/UV/ESI-MS of extract of drupes. B) Extracted LC/MS chromatogram of:  $m/z$  944 (A),  $m/z$  882 (B),  $m/z$  562 (C),  $m/z$  720 (D), and  $m/z$  574 (E).

One of the most interesting compounds present in the drupes coming from all the analyzed cultivars is eluted at a retention time of 33.99 min with an ion at  $m/z$  944.

The collected fraction at that retention time was submitted to high-resolution analysis in a QqTOF instrument; the ion showed an experimental mass value of 944.3433 and elemental composition  $C_{42}H_{58}NO_{23}^+$ , corresponding to  $[C_{42}H_{54}O_{23}+NH_4]^+$  determined with 3.5 ppm uncertainty. By matching the two high-resolution MS/MS product ion spectra, performed at different collision energy (figs. 3.1.2A and B), good insights for the identification of the groups present in this new compound can be obtained.

The spectrum at 20 eV showed the typical behaviour of ammoniated precursor species<sup>1,2</sup> which undergo fast ammonia loss giving rise to weak, or absent,  $[M+H]^+$  intermediates that further dissociate. The MS/MS spectrum obtained at 35 eV (fig. 3.1.2B) shares strong similarities, in the low-mass range, with that of oleuropein.<sup>1</sup>

It shows, in fact, the typical fragmentation of this secoiridoid such as the formation of protonated oleuropein aglycone and its dehydrated form ( $Y_1^+$ ,  $Z_1^+$ ), at  $m/z$  379 and 361, respectively, in addition to the formation of the (3,4-dihydroxyphenyl) ethyl cation and the acyl ion of elenoic acid ( $m/z$  137, 225).

Furthermore, the presence of an oleoside moiety gives rise to the formation of the ion at  $m/z$  549 (loss of oleuropein aglycone) together with those at  $m/z$  387 and 369 that represent the protonated oleoside and the dehydrated oleoside acyl cation.

The rest of the molecule includes a hexose unit, whose loss gives rise to  $Y_0^+$  ( $m/z$  747) and  $Z_0^+$  ( $m/z$  729) visible in the low-energy collision-induced dissociation (CID) MS/MS spectrum and to the presence of a formal unit of oleoside which should esterify an oleuropein moiety, as shown by the presence of  $m/z$  541.

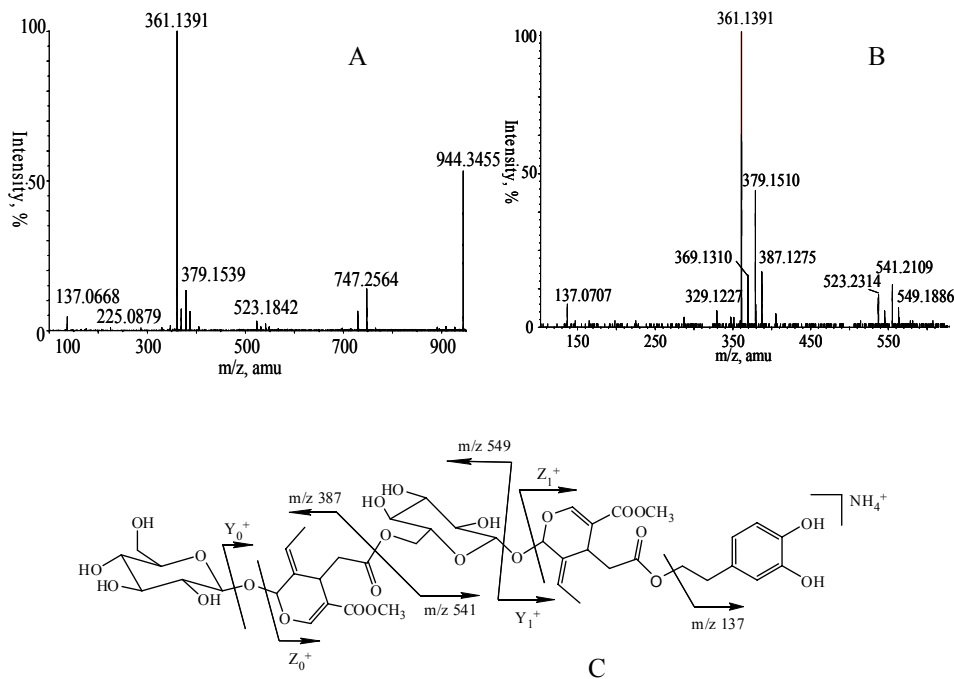


**Figure 3.1.2.** High-resolution MS/MS spectrum at 20 eV (A), at 35 eV (B), and fragmentation pattern (C) of  $m/z$  944.

On the basis of the mass spectral data we propose structure **1** (table 3.1.1) for this unknown species. The assumption is supported by the observation that the oleuropein moiety is clearly detectable in the spectrum ( $m/z$  541) and that the rest of the data agrees with the presence of a oleoside 11-methylester moiety (**2**), which represent one of the steps of the metabolic pathway leading to the biosynthesis of ligstroside, oleuropein and other secoiridoids.<sup>3</sup> It can be reasonably suggested that the conjugation of these two

stable molecules, via an available esterase, leads to the oleoside-oleuropein conjugate (1). The presence of this compound in tiny amounts might be due to its facile degradation to the most stable oleuropein. Carolea is the only cultivar that showed a relevant peak in the extracted ion chromatogram of  $m/z$  882 at the retention time of 28.61 min. The corresponding compound is a homologue of that found in the olive leaves of the Cassanese cultivar<sup>2</sup> (3); the elemental composition of the ion at  $m/z$  882.3277 was, in fact,  $C_{37}H_{53}NO_{23}^+$  corresponding to  $[C_{37}H_{49}O_{23}+NH_4]^+$  with a mass accuracy of 4.5 ppm. Its high-resolution product ion spectrum (fig. 3A) shows series of ions that confirms that two molecules of hexose (probably glucose for genetic reasons) are linked to the hydroxytyrosol moiety (fig. 3.1.3B). The new compound 3 could have the structure of an oleuropein carrying a disaccharide moiety on the catechol ring, as confirmed by the presence of the ions at  $m/z$  163 and 325 corresponding to hexose glycal and disaccharide glycal. Additionally, the ions at  $m/z$  137, 299 and 461, corresponding to the (3,4-dihydroxyphenyl)ethyl cation and its glycosylated linked mono- and disaccharide units, respectively, strongly support the previous assumption.

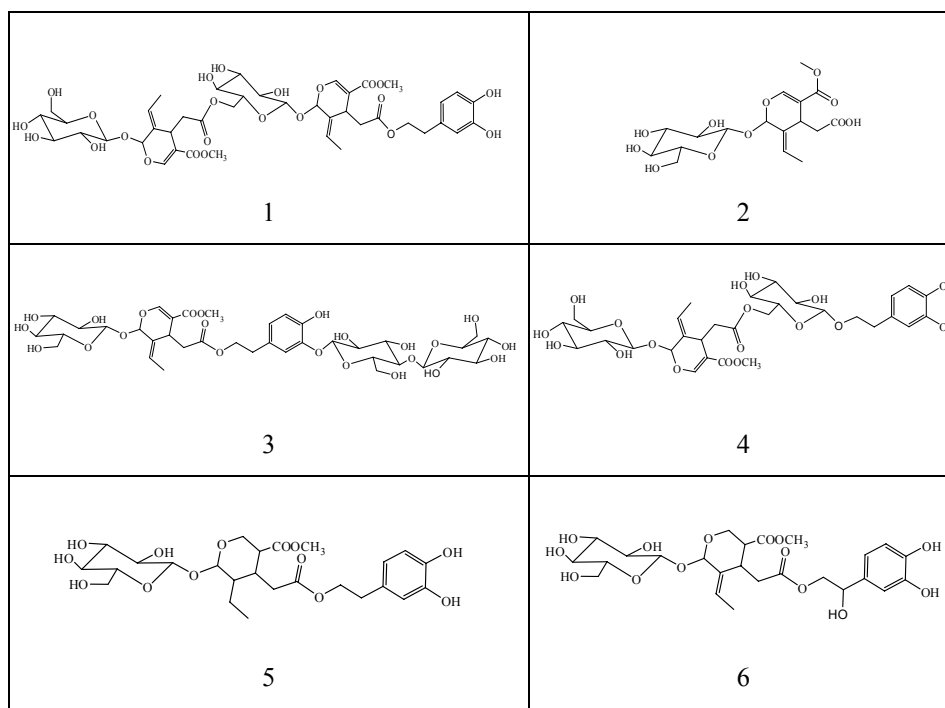


Table 3.1.1. Hypothetical structures of unknown species.

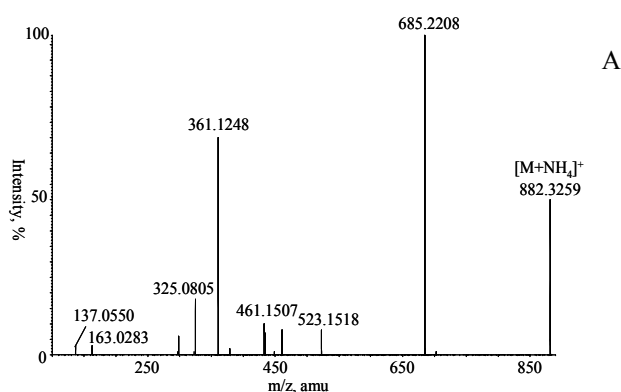
The presence of the oleuropein moiety is further supported by the appearance of the classical protonated aglycone ion and its dehydrated form ( $m/z$  379 and 361) and by the formation of the ions at  $m/z$  685 and 523 ascribed to the loss of one and two hexosemoieties. The latter, in particular, can be easily lost if the deglycosylation occurs at the oleuropein site. The cleavage of the phenolic glucoside corresponds to a high-energy process, as already verified for similar systems.<sup>2</sup>

The existence of glycosylated phenolic sites was reported in earlier investigations of the leaves of *Olea europea*<sup>2</sup> and other species.<sup>4</sup>

Another minor component never previously described is that eluting at 21.50 min, where the ion at  $m/z$  562 could correspond to a  $[M+NH_4]^+$  species. The collected fraction analyzed in the high-resolution mass spectrometer provided an exact mass of 562.2473, which corresponds to an elemental formula of  $C_{25}H_{40}NO_{13}^+$  with an error of 4.7 ppm.

The MS/MS product ion spectrum of  $m/z$  562 (fig. 3.1.4A) is surprisingly similar to that of oleuropein; the only differences being the presence of ions whose  $m/z$  values are increased by 4 mass units. In particular, the spectrum shows the same product ion at  $m/z$  137, characteristic of the hydroxytyrosol moiety, the ions at  $m/z$  365 ( $Z^+$ ) and 383 ( $Y^+$ ), 4  $m/z$  units higher than those at  $m/z$  361 and 379, typical of the oleuropein aglycone, and the ion at  $m/z$  229 characteristic of a saturated acyl ion of elenoic acid.

The fragmentation pattern fits well with that of a saturated oleuropein, ionized by ammonium ion attachment (**4**). This assumption is supported by the fact that another species co-elutes in the same fraction with a  $[M+NH_4]^+$  ion at  $m/z$  560. In this case too, the fragmentation pattern is similar to that of oleuropein (chapter 2).



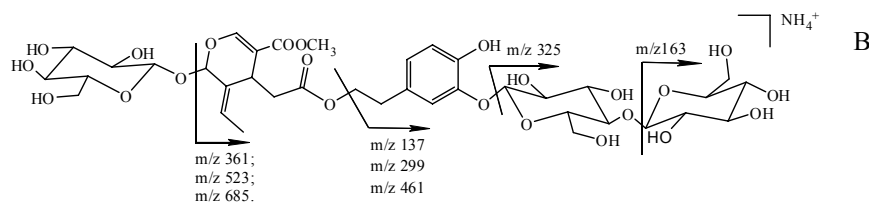


**Figure 3.1.3.** High-resolution MS/MS spectrum at 22 eV (A) and fragmentation pattern (B) of  $m/z$  882.

The latter compound, which has been already found in *Ligustrum lucidum*, is known as lucidumoside B with a structure corresponding to that of oleuropein lacking a double bond at the oleoside moiety.<sup>4</sup>

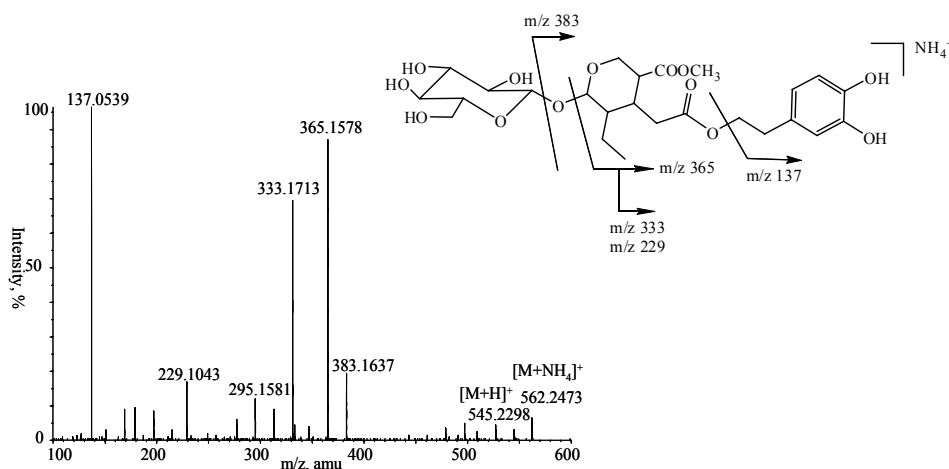


**Figure 3.1.4.** High-resolution MS/MS spectrum at 20 eV (A) and fragmentation pattern (B) of  $m/z$  562.

It was interesting to discover that the olive pulp contains a compound structurally similar to nuzhenide present in large amounts in the stones of drupes.<sup>5</sup>

This micro component, named neo-nuzhenide (**5**), previously found in the *ligustrum*<sup>6</sup> only, is 16 mass units heavier ( $m/z$  720,  $[M+NH_4]^+$ ) than nuzhenide, with which it shares a similar fragmentation pattern. Fig. 3.1.5 shows the spectrum of nuzhenide obtained by a methanol extraction of the stones and the related compound **5** found in the drupes (fig. 3.1.5B). The increase of 16 mass units in the molecular weight is due to the replacement of tyrosol with hydroxytyrosol. The major differences, in fact, between the spectra are due to the formation of the expected  $Y^+$  and  $Z^+$  ions due to the loss of the

external glucose at  $m/z$  525 ( $Y^+$ ) and 507 ( $Z^+$ ) for the nuzhenide, and at  $m/z$  541 ( $Y^+$ ) and 523 ( $Z^+$ ) for **5**.

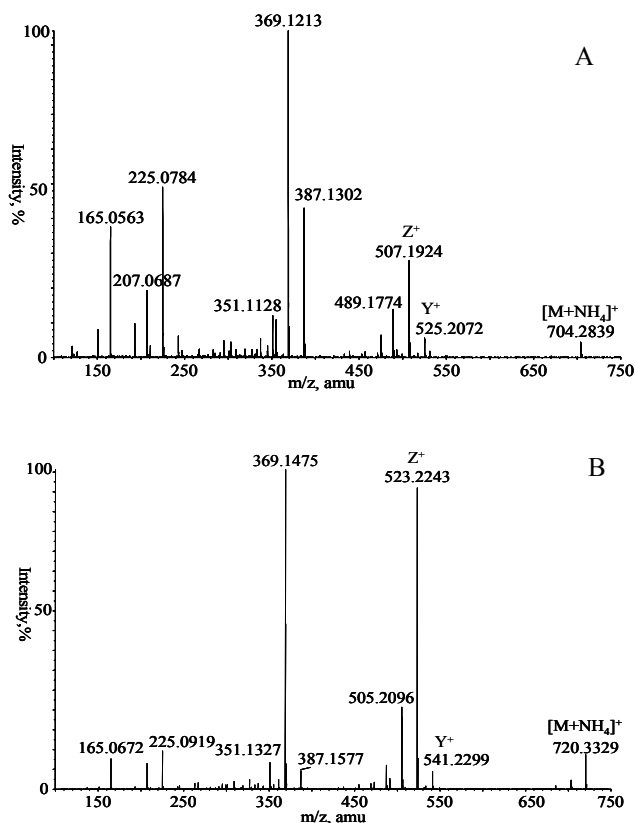


**Figure 3.1.5.** High-resolution MS/MS spectrum of nuzhenide (A) and neo-nuzhenide (B) acquired at 20 eV.

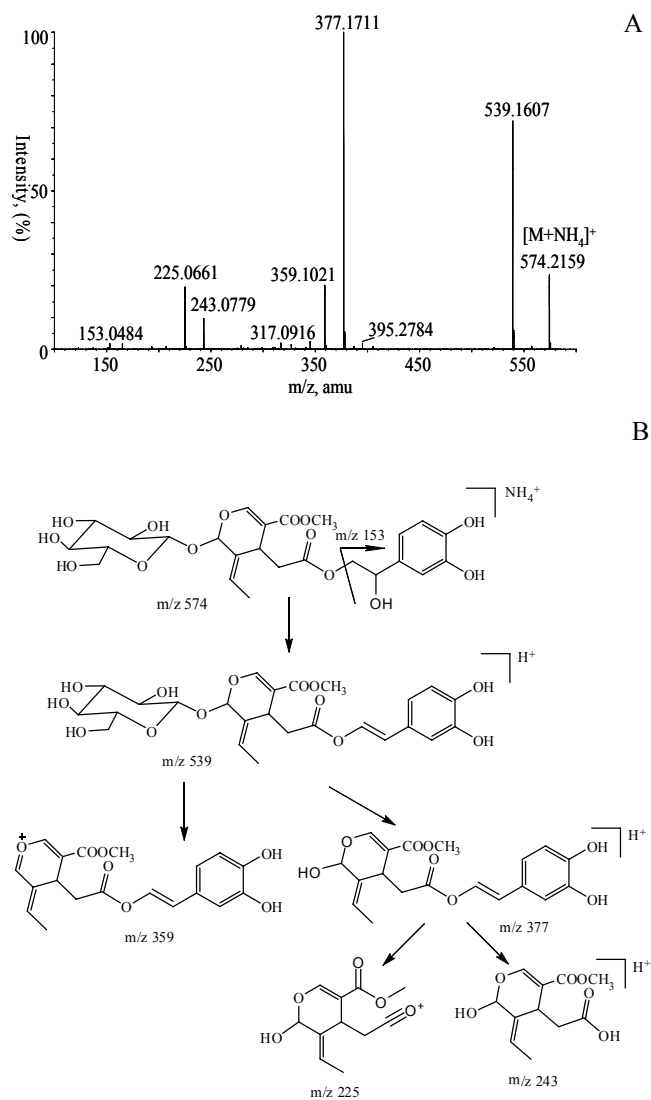
The common ions at  $m/z$  387 and 369 originate by the consecutive loss of tyrosol and hydroxytyrosol from the  $Z^+$  and  $Y^+$  ions, respectively (fig. 3.1.5).

It is known<sup>7</sup> that drupes contain a hydroxylated oleuropein at the elenoic moiety known as 10-hydroxyoleuropein. I provide mass spectrometric evidence for the presence of 2''-hydroxyoleuropein (**6**), where the hydroxyl group is located at the phenylethanolic moiety.

The MS/MS product ion spectrum of the  $[M+NH_4]^+$  ion at  $m/z$  574 (fig. 3.1.6) showed, in fact, (i) the absence of  $m/z$  137 typical of secoiridoids with hydroxytyrosol, and the presence, in contrast, of the ion at  $m/z$  153 that suggests the existence of an OH group on this portion of the molecule; (ii) the presence of the ions at  $m/z$  359 and 377 (fig.

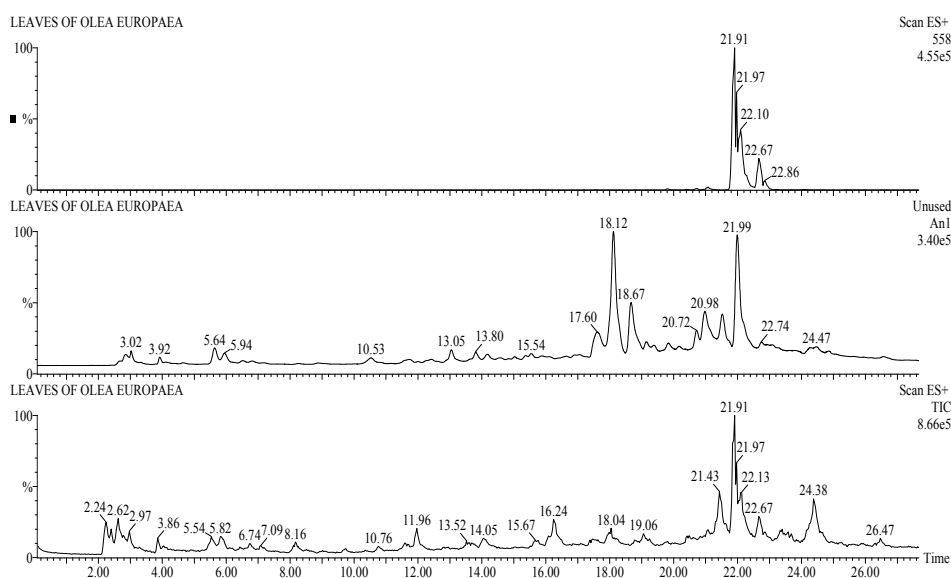


3.1.6 B) formed probably by the loss of a water molecule and thus having an additional double bond with respect to the structure of oleuropein aglycone; and finally (iii) the presence of the ions at  $m/z$  225 and 243 attributed to the elenoic acid and dehydrated elenoic acid<sup>1</sup> that have no traces of the double bond mentioned above, suggesting that this double bond must be on the catechol moiety.



**Figure 3.1.6.** (A) High-resolution MS/MS spectrum at 20 eV and (B) fragmentation scheme of  $m/z$  574.

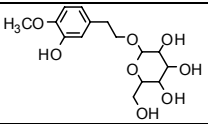
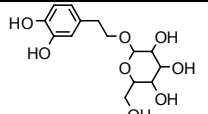
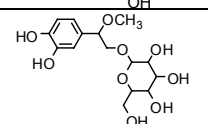
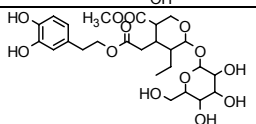
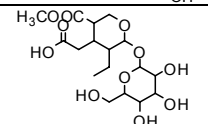
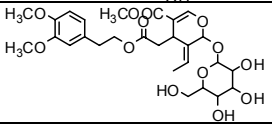
This molecule never found in *Olea Europea* is present in the secondary metabolism of other oleaceae families, such as *fraxinus* and *ligustrum*.<sup>8</sup> On other hands, the HPLC ESI-MS chromatogram as well as the UV chromatogram of the methanolic olive leaf extract is characterized by a predominant peak attributed to the presence of oleuropein, the main components of olive leaves (fig. 3.1.7). The occurrence of the other compounds may be highlighted by means of the extract ion chromatograms (XIC) that can easily display, with different relative abundances, species such as hydroxytyrosol glucoside, oleoside, oleoside 11-methyl ester, ligstroside, verbascoside and others minor compounds (see chapter 2).



**Figure 3.1.7.** LC/UV/ESI-MS of extract of leaves.

The mass chromatogram, in addition, shows the presence of molecules whose molecular weight does not match those of the microcomponents already described in literature. These species (table 3.1.2) have been submitted to the high resolution mass spectrometry analysis in order to, preliminarily, obtain the exact formula, and than to infer the possible structure, by means of the tandem mass spectrometry. Compound **1** (table 3.1.2) elutes, in the chromatographic run at a retention time of 7.09 min; the fraction collected is then submitted to high-resolution mass-spectrometry analysis. The MS spectrum after instrument calibration displays a peak mass value of 348.1672

corresponding to the elemental composition  $C_{15}H_{26}NO_8^+$  with a mass error of 3.9 ppm; considering the presence in the collected fraction of the ammonium salt, the correct ion formula should be  $[C_{15}H_{22}O_8+NH_4]^+$ , as proved by the fast loss, in MS/MS conditions, of neutral ammonia from the ammoniated molecular ions.<sup>9</sup> The MS/MS spectrum (fig. 3.1.8B) of the species at  $m/z$  348 resembles that of hydroxytyrosol glucoside (**2**, table 3.1.2), a known phenolic compound present in olive and oil (figure 3.1.8A),<sup>10</sup> whose ammoniated molecular peak is  $m/z$  334.

Ion $[M+NH_4]^+$	compound	Retention Time (min)	Structures
$m/z$ 348	<b>1</b>	7.09	
$m/z$ 334	<b>2</b>	5.41	
$m/z$ 364	<b>3</b>	5.57	
$m/z$ 562	<b>4</b>	19.12	
$m/z$ 426	<b>5</b>	6.68	
$m/z$ 586	<b>6</b>	21.50	

**Table 3.1.2.**  $m/z$  values, retention times and structures of compounds **1-6**

The tandem mass spectrum of **1** is characterized by the formal loss of neutral ammonia giving rise to the transient  $[M+H]^+$  species at  $m/z$  331; other species come from the losses of a series of water molecules, producing the peaks at  $m/z$  313,  $m/z$  295 and  $m/z$

277. The formation of the ions at  $m/z$  169 and  $m/z$  151, differing 14 units from the possible lower homologues (**2**) in figure 3.1.8; could indicate the presence of a methylated hydroxytyrosol (fig. 3.1.8B). The species at  $m/z$  180 likely corresponds to the hexose moiety in which the hemiacetalic hydroxyl function has been replaced, in the gas-phase, by an ammonia molecule. A similar process has been previously described in literature.<sup>11</sup> The isolated compound **1** should correspond, therefore, to a glycosylated hydroxytyrosol methylated at the phenolic function (figure 3.1.8B). The latter has been previously identified in Laurum.<sup>12</sup> The decisive proof was achieved isolating compound **1** from Laurum extracts at the same retention time previously observed for olive leaves and in the same chromatographic conditions. The molecular weight of **1** thus obtained and the fragmentation pattern of its MS/MS spectrum were identical with those obtained from the equivalent compound isolated from olive leaves.

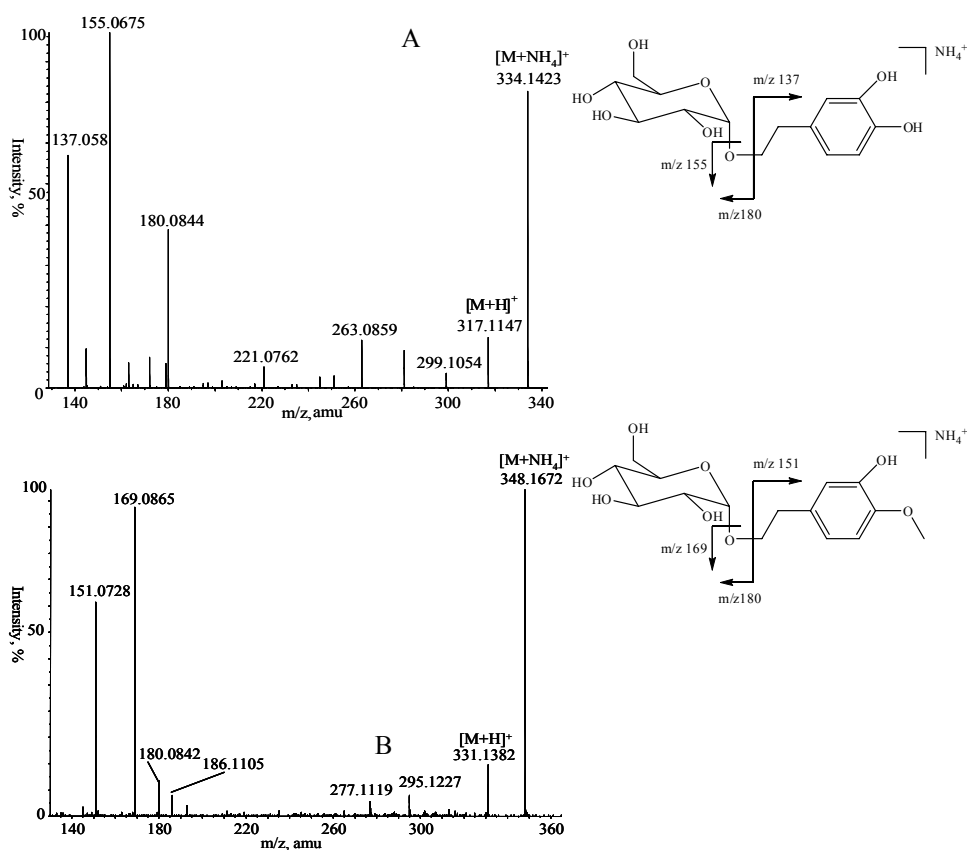


Figure 3.1.8. MS/MS spectrum of compound **2** (A) and **1** (B) with relative structures and main fragments.

A similar molecule (**3**, table 3.1.2) has been found at retention time 5.57 min., whose gas phase chemistry resembles that of compounds **2** and **1**.

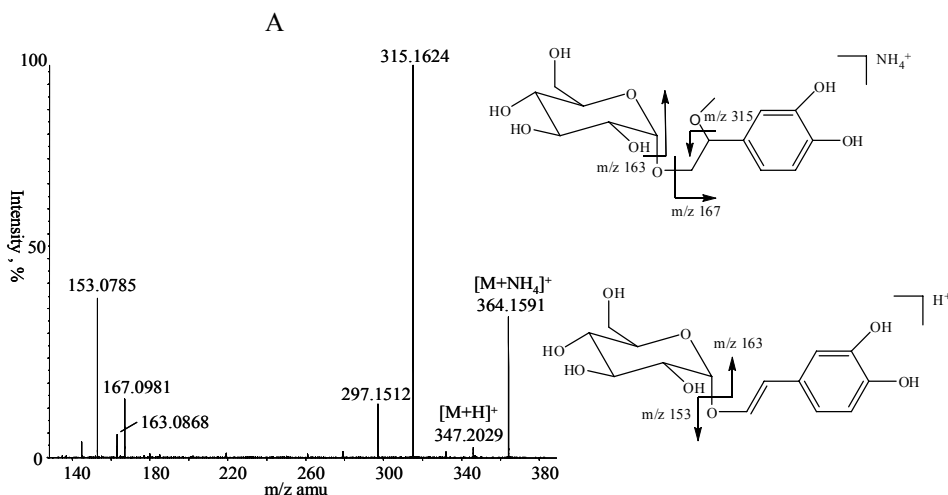
HRMS measurements displayed a peak at 364.1591, corresponding to the formula  $[\text{C}_{15}\text{H}_{22}\text{O}_9+\text{NH}_4]^+$  with a mass error of 4.5 ppm., which takes two competing reaction pathways leading to the abundant product ions at  $m/z$  315, likely originating by consecutive ammonia and methanol losses, and 167, following the releasing of the modified hydroxytyrosol moiety as a neutral (figure 3.1.9B).

The competitive fragmentation of the glycosyl bond afforded the species at  $m/z$  163 and 153, respectively.

Other significant ions are those originated by the loss of water molecules ( $m/z$  297,  $m/z$  279 and  $m/z$  261) and those typical of a hexose moiety ( $m/z$  163 and  $m/z$  145).

As in the case discussed above, the ion at  $m/z$  180 can be formed by gas phase acetal/aminoacetal equilibrium.<sup>11</sup>

The data strongly support the proposed hexose linked to a (2-methoxy)-hydroxytyrosol structure (figure 3.1.9B). Compound **4** (table 3.1.2), eluted after 19.12 min., has been previously found in drupes.<sup>13</sup> Its ammoniated ion peak measures 562.2473 which corresponds to the elemental formula  $[\text{C}_{25}\text{H}_{36}\text{O}_{13}+\text{NH}_4]^+$  with a mass error of 4.7 ppm.



Its gas-phase chemistry is identical to that showed by saturated oleuropein present in drupes.<sup>10</sup> The occurrence of the saturated secoiridoid **4** is supported by the isolation of a compound eluted at 14.70 min, to whom it can be assigned the structure **5** (table 3.1.2).

The MS/MS spectrum of **5** (figure 3.1.10A) displayed, in fact, a fragmentation pattern very similar to that of oleoside 11-methyl ester (figure 3.1.10B)<sup>2</sup>.

The Z and Y<sup>13</sup> glycosidic breakage of the acetal moiety of the ammoniated molecular ion produces, under CID conditions, the species at m/z 247 and m/z 229. The latter can either lose a formal unit of water giving rise to the species at m/z 211, or may release a formal unit of acetic acid to form the species at m/z 169. The elemental composition is confirmed by the HRMS experiments who gave the value of 426.1958 for the ammoniated ion which correspond to the formula [C<sub>17</sub>H<sub>28</sub>O<sub>11</sub>+NH<sub>4</sub>]<sup>+</sup> with 4.1 ppm of uncertainty.

The unknown species **6** elutes at the retention time of 21.50 min. The high resolution spectrum assigns to the pseudomolecular species, the molecular weight of 586.2473 that corresponds to the formula [C<sub>27</sub>H<sub>36</sub>O<sub>13</sub>+NH<sub>4</sub>]<sup>+</sup> with a mass error of 4.5 ppm.

The MS/MS spectrum (figure 3.1.11A) of **6** is quite similar to that of oleuropein with some mass shifts. The ions at m/z 569 [M+H]<sup>+</sup> arises from the loss of ammonia, while the species at m/z 407, m/z 389 could be attributed to the loss of the hexose moiety that produces an aglycon having a shift of 28 mass respect to oleuropein aglycon (figure 3.1.11B); the ion at m/z 225 ion is typical of elenolic acid, while the presence of the species at m/z 165 corresponds to the hydroxytyrosol methylated at the phenolic moieties.

The proposed structure matches that of dimethyl-oleuropein.

To confirm the hypothesis the same compound, present in *ligustrum lucidum*,<sup>14</sup> has been extracted from this plant. The comparison between gas phase fragmentation and retention time on the same chromatographic run for the two species confirmed the structure of **6**.

A further evidence of the structure of **6** has been given by the tandem mass spectrum of the synthesized **6** obtained by a simple methylation of oleuropein.<sup>15</sup> Even in this case the fragmentation patterns are superimposable. Moreover the extract (XIC) of the HPLC chromatogram shows other two species at the same m/z value of 720 (fig. 3.1.12): Angustifolioside A (1° rt 18.63) as confirmed by tandem mass spectrum compared with

that present in literature<sup>9</sup> and probably, the olefinic isomer (2° rt 18.93) as well as oleuropein and oleuroside compounds.<sup>16</sup>

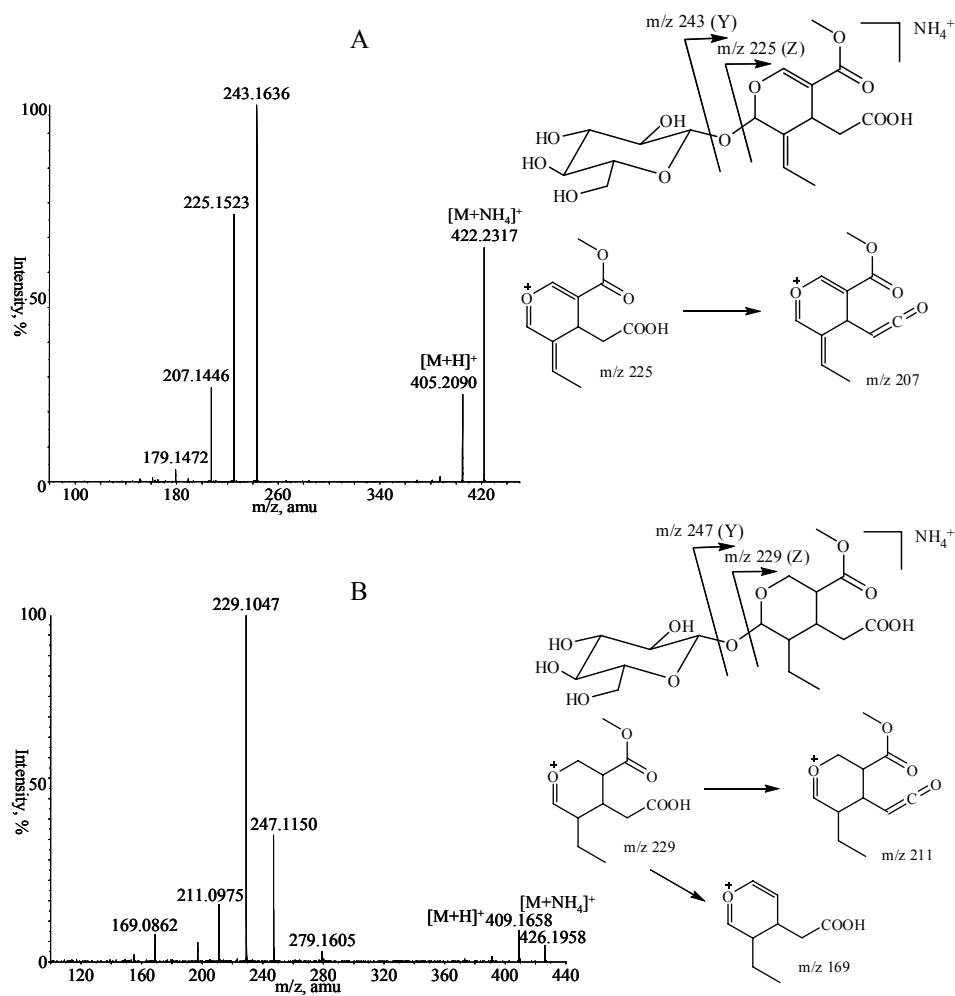
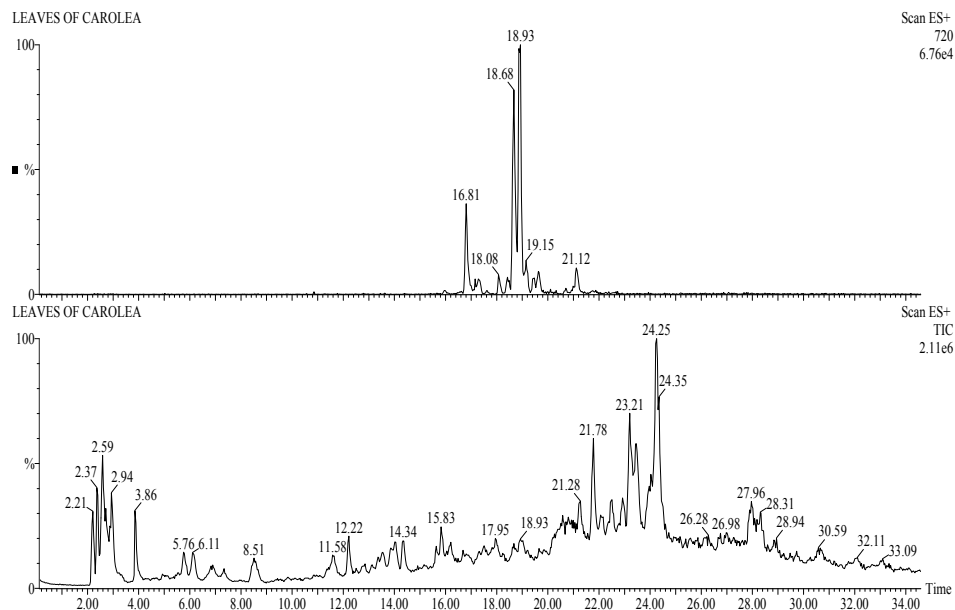
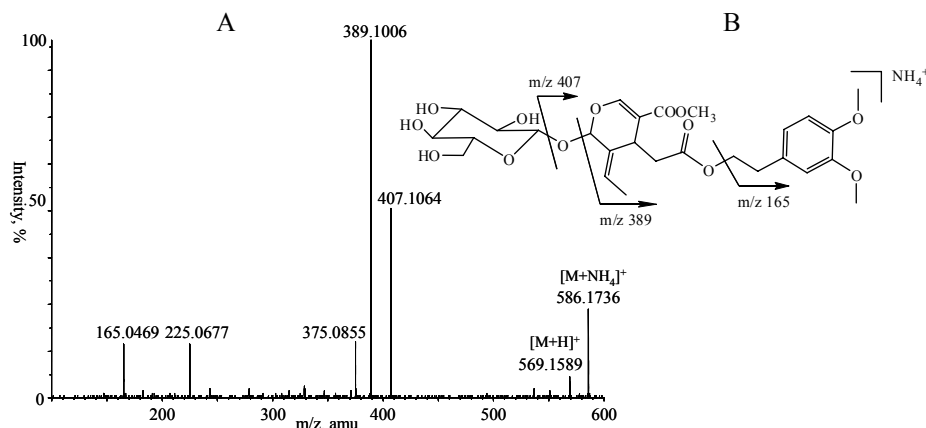


**Figure 3.1.10.** MS/MS spectrum of compound 5 (A) and oleoside 11-methyl ester (B) with relative fragments.

In fact in both cases there are the same fragments at different intensity obtained by the same collision energy (fig. 3.1.13).

In particular, the first fragmentation regards the glucose moiety to give Y and Z protonated ion species at m/z 523 and 541. The latter seems to be the protonated oleuropein since provide the ions of its typical fragmentation (chapter 2). In the second

case, there are the same fragmentations but the intensity of the peaks is different, presumably due to the position of olefin function.



The statistical analysis (LDA) performed on the leaves of five italian cultivars (Carolea, Cassanese, Leccino, Coratina, Nocellara del Belice), in collaboration with CRA [Centro



ricerche agroalimentari; Rende (CS)], collected in the months of March and April in the same ground, therefore under the same pedoclimatic condition, indicates how many of these compounds differ one another in base to the period of growth of the Olive cultivars.

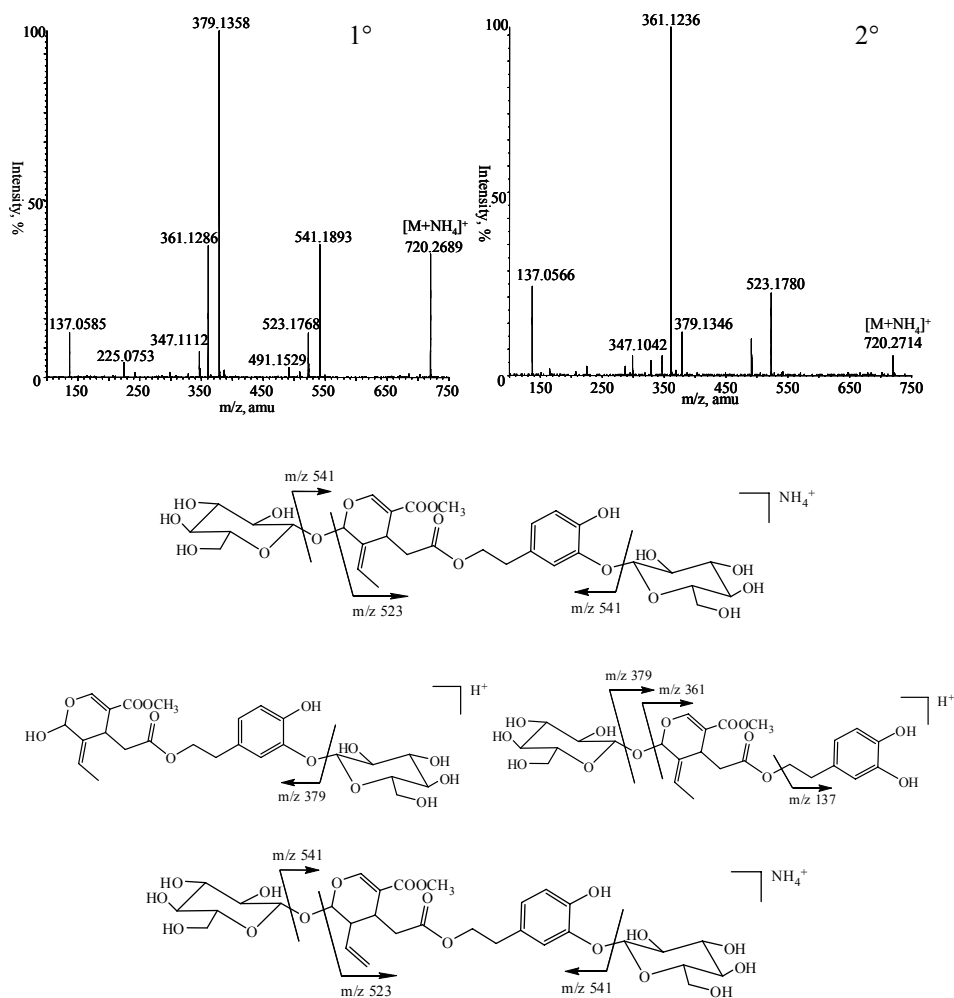


**Figure 3.1.13.** Tandem mass spectra (25 eV) and fragmentation of species at  $m/z$  720.

This is a new statistical approach for cultivar discrimination since regards the leaves and more specifically the microcomponents; in fact, the reports existing in the literature the same discrimination was obtained by DNA analysis.<sup>17-19</sup>

Samples of the same cultivar were analyzed five times using salicin as internal standard. Statistical evaluation of the data could provide tools for interpreting the meaning of the results and clues to identify the cultivar. LDA statistical approach allows the classification of unknown samples after having verified the possible differences among samples of known origin.

Data treatment has been applied to the analyte/I.S. (25ppm) area ratio (XIC on the TIC) of the fourteen compounds ( $m/z$   $[M+NH_4]^+$ , table 3.1.3), using five groups, corresponding to the five selected cultivar as input a priori.

$(M+NH_4)^+$	
$m/z$ 334	Hydroxytyrosol glucosilated
$m/z$ 348	2'Methoxy Hydroxytyrosol glucosilated
$m/z$ 364	2-methoxy 4-glucosil tyrosol
$m/z$ 408	Oleoside
$m/z$ 422	Oleoside-11-methyl ester
$m/z$ 434	Unknown
$m/z$ 642	Verbascoside
$m/z$ 720 (1,2)	Angustifolioside A
$m/z$ 558	Oleuropein
$m/z$ 542	Ligstroside
$m/z$ 586	Lucidumoside -D
$m/z$ 530	Unknown
$m/z$ 562	Satured Oleuropein
$m/z$ 304	Salicin (internal standard)

**Table 3.1.3.** Table of the peak used for statistical analysis.

In the first instance the data of olive leaves samples were subjected to the basic tool for data analysis: principal component analysis (PCA).

PCA is very important especially in the preliminary steps of a multivariate analysis, if one wants to perform an exploratory analysis in order to have an overview of data. It is a powerful visualization tool, provides a way to reduce the dimensionality of the data and to eliminate unnecessary information and, finally, finds possible correlation between variables. The scores of the samples and the loadings of the variables on the two first principal components are plotted in figure 3.1.14: the information retained is

52.65% of the total variance. The plot shows differentiation between harvesting period regardless of cultivar. In samples corresponding to the Leccino, Coratina and, to a smaller extent, Cassanese it was observed a shifting along PC1 going from march to april which indicates the decrease of concentration of compounds 720(2), 720(1), 558, 562 and 586 in leaves harvested in april. On the contrary, tendency shown by Carolea variety was totally different from all the others. Actually, for this cultivar a shift along PC2 only is clear that means an increase of concentration of variables 530 and 334 going from march to april. For Nocellara samples it is not observed meaningful variations, even though it can be noted that Cassanese shift slightly to more positive values of PC1. Finally, in the LDA, the differentiation between groups is significant since the low Wilks  $\lambda$  value (0.0011656) shows that the model is discriminating. Moreover, the information from data treatment is characterized by a high degree of reliability since the  $p$  level is extremely low ( $<0.00001$ ). To check the usefulness of the method for prediction purposes cross validation was performed. The sample set divided into training set including 90% of the components of sample set was used for calculating discriminant functions, and then the validation set which include 10% of the

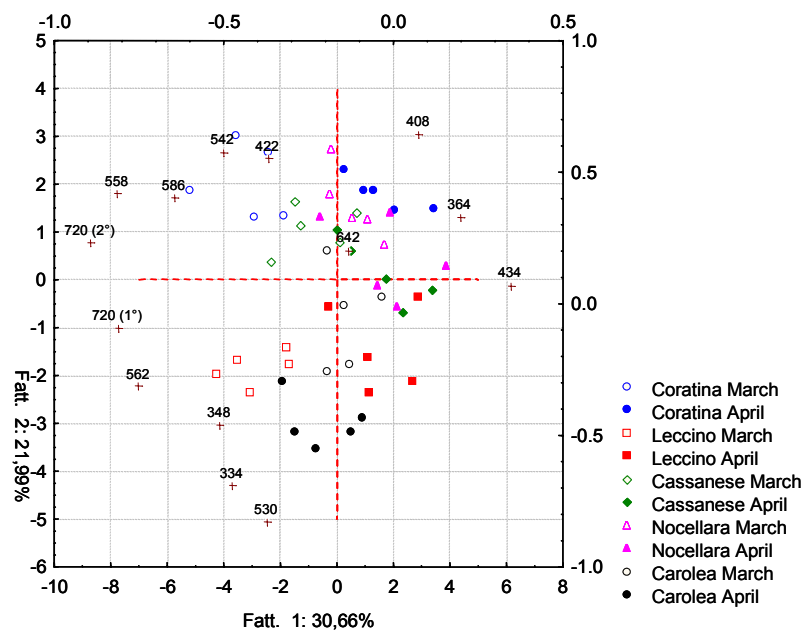


Figure 3.1.14. Principal component analysis.

components of the sampled set, was used as an unknown, and assigned. The training and the validation sets were randomly selected from all samples.

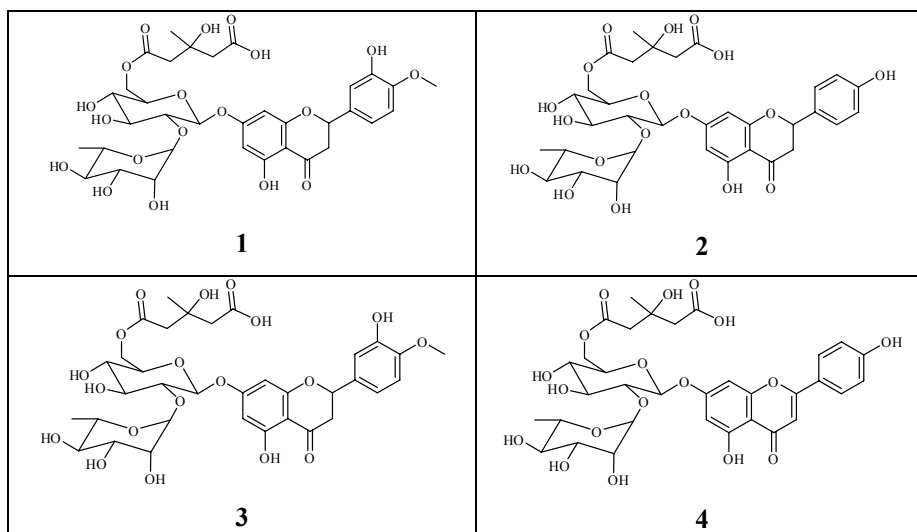
The prediction capacity of the LDA model was determined by analyzing the validation set of samples that had not been used at any to generate the model. The proposed model predicts 82% of correct variety and this suggests that the presented method may be a potential choice for checking cultivar type regardless harvesting period (table 3.1.4).

	<b>Cassanese</b>	<b>Coratina</b>	<b>Carolea</b>	<b>Leccino</b>	<b>Nocellara</b>
<b>Cassanese</b>	9	0	0	0	1
<b>Coratina</b>	0	7	0	0	3
<b>Carolea</b>	1	0	9	0	0
<b>Leccino</b>	1	0	0	9	0
<b>Nocellara</b>	1	2	0	0	7

**Table 3.1.4.** Prediction matrix: rows represent the true class, columns report the assigned class.

### 3.2 Characterization of new flavonoids in bergamot and pummelo juice

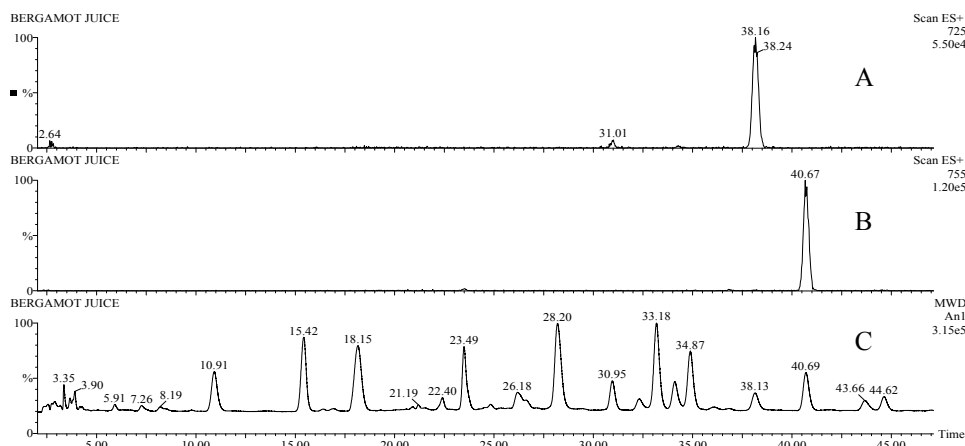
The bergamot juice, was analyzed by HPLC/ESI/UV/MS technique (fig. 3.2.1) and compared with other citrus juice extracts obtained using the same preparation (fig 3.2.2). The profile showed the presence of many flavonoids already identified by HPLC analysis<sup>20,21</sup> together with some unknown components. Fig. 1 shows the UV chromatogram of bergamot juices at 280 nm resulting from a 110 min HPLC run. The extract ion chromatogram (XIC fig. 3.2.1 B, C) reveals the mass value of two unknown flavonoids which has been collected and analyzed by both NMR and high resolution mass spectrometry techniques. The structure of the other two unknown species can be suggested with a high degree of confidence by comparing them with structures firmly established. The LC/MS profile of main citrus juices seems to suggest that the species **1**, (chart) is a marker for bergamot while compound **2** is present in grapefruit also. This fact was confirmed by mixing bergamot juice in a certain percent (15%) with other citrus juice; in this case is possible to reveal traces of bergamot juice in other citrus juices by presence of **1**, absent before (fig. 3.2.2 B,C and fig. 3.2.3 A,B).



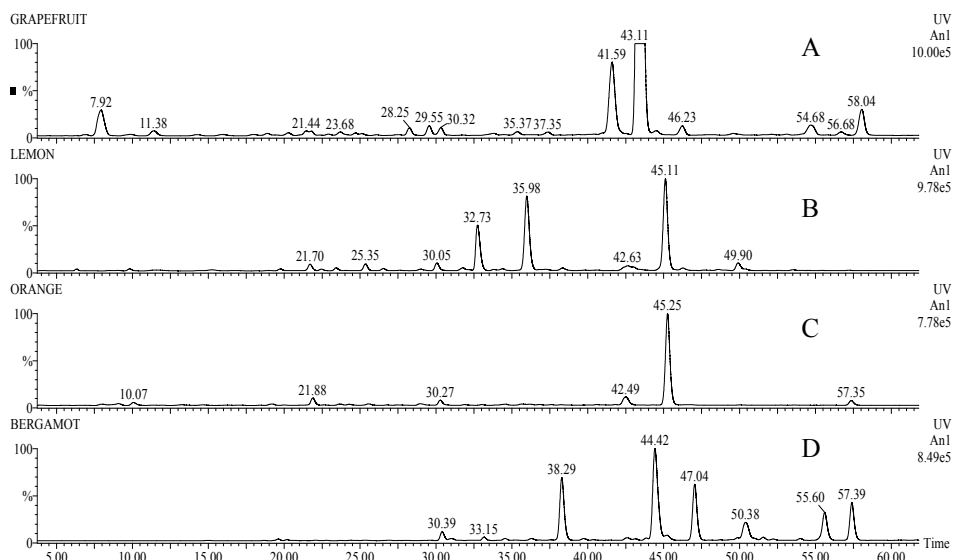
#### Chart

The four collected fractions relative to unknowns were submitted to high-resolution analysis in a QqTOF instrument, already used to study natural product<sup>22,23</sup>; the ion at

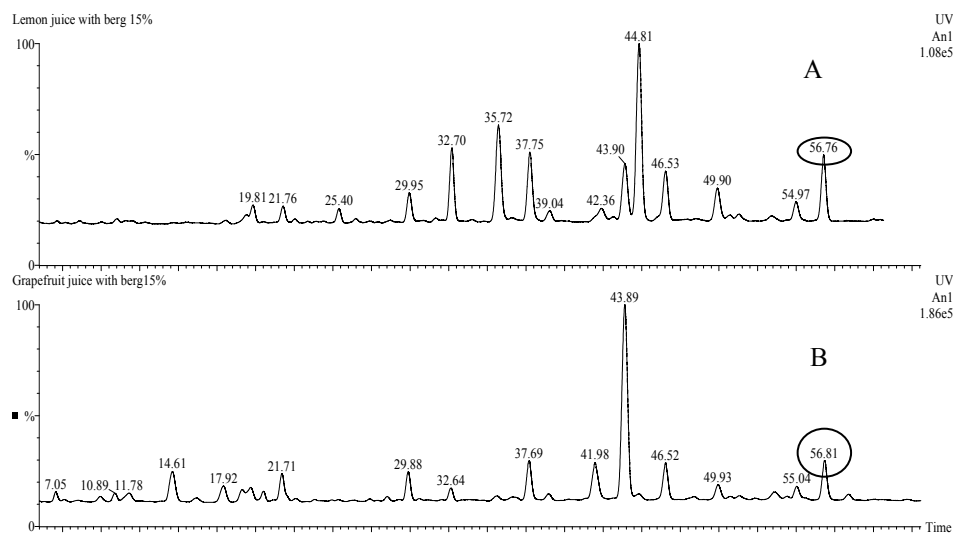
experimental mass value of 755.2387 (XIC 40.67min; fig 3.2.1) which corresponds to the elemental composition  $C_{34}H_{43}O_{19}^+$  (**1**), was determined with 0.80 ppm uncertainty.



**Figure 3.2.1.** LC/UV/ESI-MS of bergamot juice; C: UV at which correspond the  $m/z$  value ( $[M+H]^+$ ; RT): Apigenin 6,8-di-C-glucoside (595; 15.42), Diosmetin 6,8-di-C-glucoside (625; 18.15), Neohesperidin (597; 23.49), Narirutin (581; 26.18), Naringin (581; 28.20), Neohesperidin (611; 30.95), Rhoifolin 4'-glucoside (741; 32.29), 8 Rhoifolin (579; 33.18), Diosmin (609; 34.13), Neodiosmin (609; 34.88), unknown 1 (725; 38.13), unknown 2 (755, 40.69), unknown 3 (723, 43.66), unknown 4 (753, 44.62). B: XIC of unknown 2; A: XIC of unknown 3.

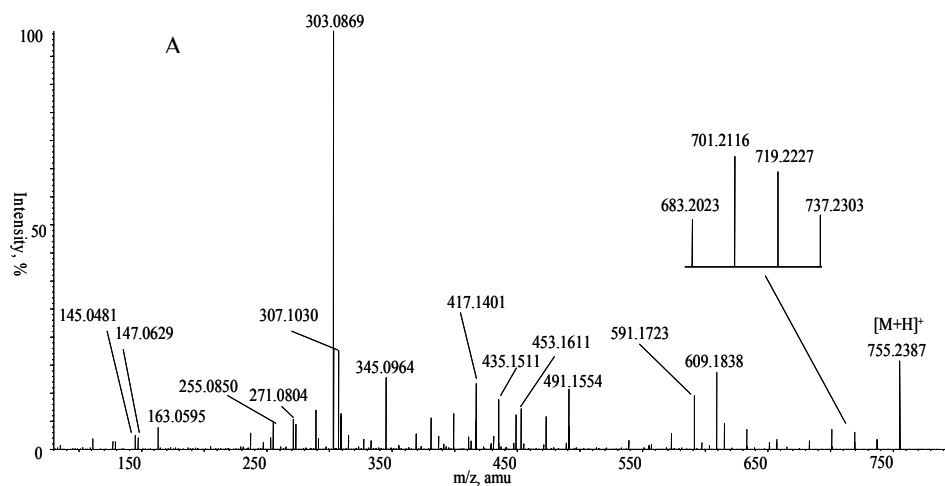


**Figure 3.2.2.** LC/UV/ESI-MS of different citrus juice; the unknown flavonoid at  $m/z$  ( $M+H$ )<sup>+</sup> 755 and rt 57.39 is present only in bergamot (D).



**Figure 3.2.3.** Lemon (A) and orange juice (B) mixed with 15% of bergamot juice. The marker of bergamot is circled.

The high-resolution MS/MS product ion spectrum, performed at 20 eV in positive mode (fig. 3.2.4A), showed a behaviour similar to hesperetin glycoside<sup>24</sup>; this data is supported by the presence of the aglycon moiety ( $C_{16}H_{15}O_6^+$   $m/z$  303.0869) and the loss of external rhamnose moiety that produce the signal at  $m/z$  609.1838 which corresponds to the elemental composition  $C_{28}H_{33}O_{15}^+$  (scheme 3.2.1 B).



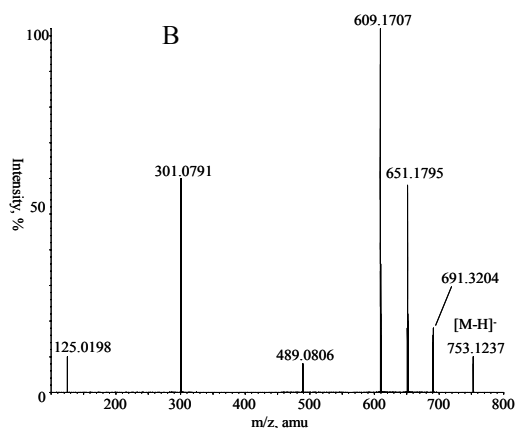


**Figure 3.2.4.** High resolution ESI MS/MS of **1** in positive (A) and negative (B) ion mode at 20 eV and -40eV.

In the same way, the ion at experimental mass value of 725.2298 and elemental composition  $C_{33}H_{41}O_{18}^+$  (**2**) showed in positive MS/MS at 20 eV (fig. 3.2.6), the behaviour of naringenin glycoside; in fact the spectrum shows the naringenin moiety at  $m/z$  273.0719 ( $C_{15}H_{13}O_5^+$ ) but also, as seen before, the ion relative to loss of rhamnose at  $m/z$  value of 579.1563 and  $C_{27}H_{31}O_{14}^+$  elemental composition. Moreover, alkaline hydrolysis performed on **1** and **2** substrates<sup>25,26</sup> gave an other important information in order to identify these compounds. In fact, after 48 hours both species reacted to give the flavonoids neohesperidin and naringin as confirmed by standards (fig. 3.2.7). The hydrolysis confirmed that this two species differs each other only for aglycon part and produced the common unknown moiety, presumably linked through an ester bond to the rest of molecules; the negative high resolution MS/MS of the unknown hydrolyzed moiety (fig. 3.2.5) showed the deprotonated molecular ion at experimental mass value

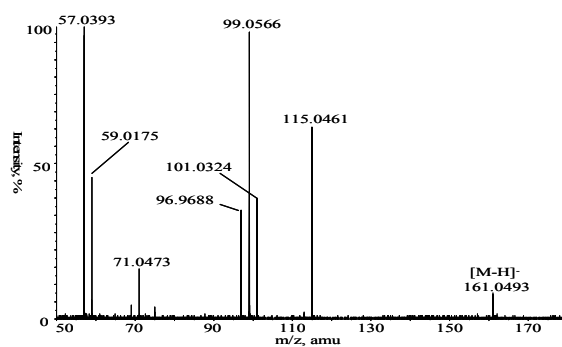


**Figure 3.2.5.** Negative ESI MS/MS of collected fraction obtained after alkaline hydrolysis.



of 161,0493 and elemental composition  $C_6H_9O_5^-$  determined with 3.8 ppm uncertainty. Finally, the characterization of **1** and **2** was obtained by the interpretation of their fragmentations obtained by negative and positive MS/MS spectra (scheme 3.2.1) together NMR analysis.

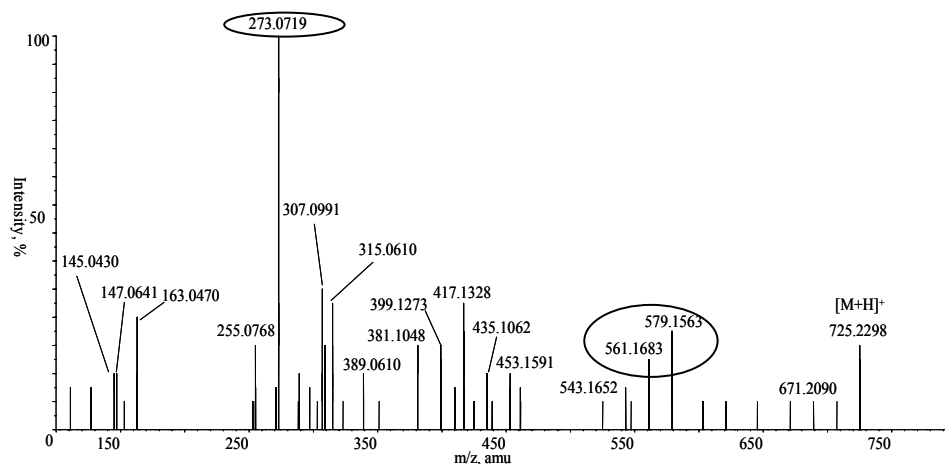


**Figure 3.2.6.** Positive high resolution ESI MS/MS of **2** at 20 eV.

Furthermore, the unknown ester moiety is recognized by the interpretation of negative tandem mass spectrum (scheme 3.2.2) and NMR of the hydrolyzed sample collected by semi preparative HPLC.

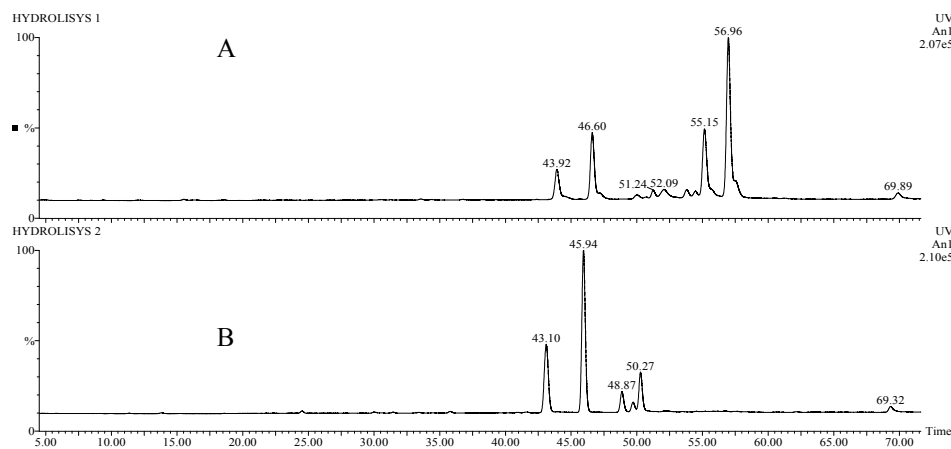
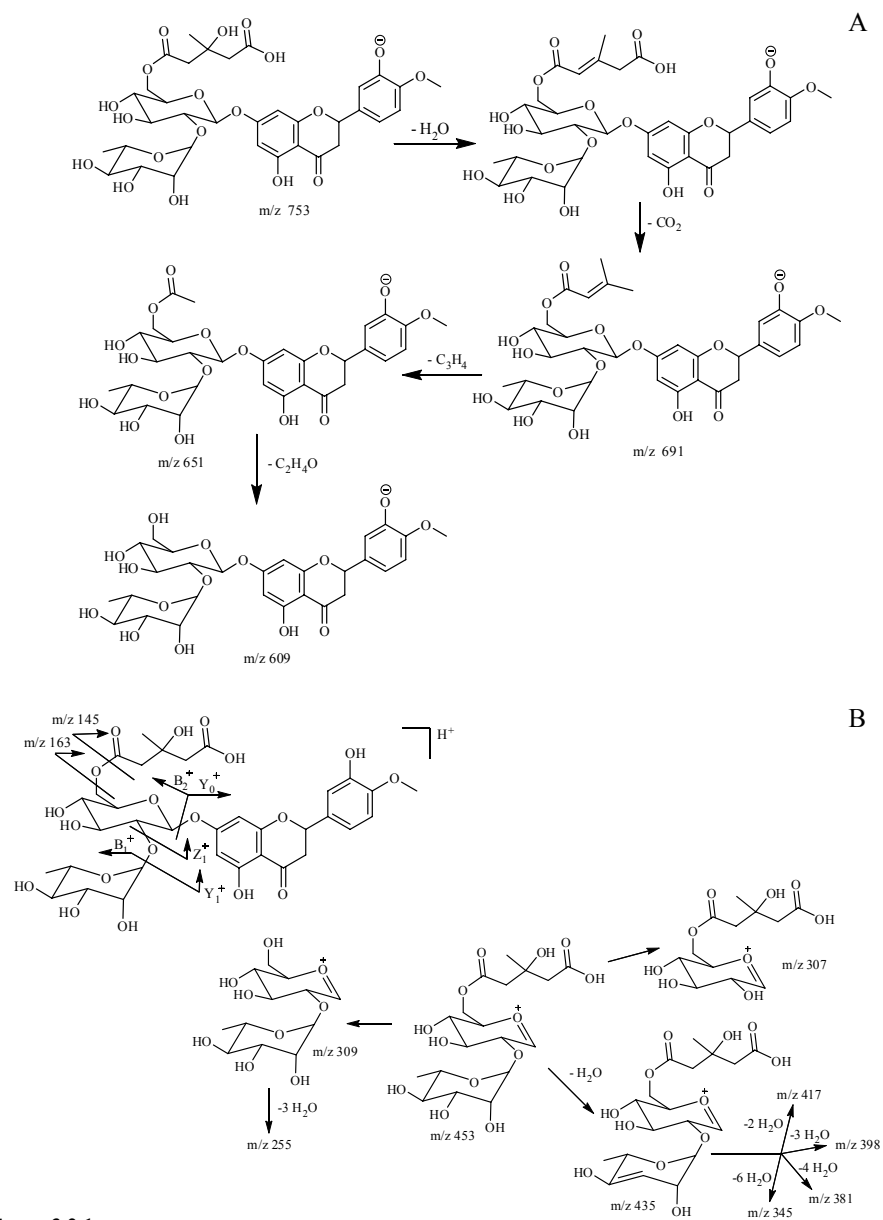
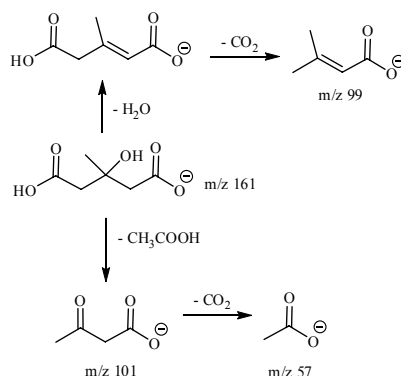


**Figure 3.2.7.** Alkaline Hydrolysis of species at  $m/z$   $(M+H)^+$  755 and 725 (rt 56.96 and 55.15) after 24(A) and 48(B) hours. The complete hydrolysis give the flavonoids neohesperidin and naringin at rt 49.50 and 43.10 respectively.

The negative fragmentation pathway of **1** showed (scheme 3.2.1A) the consecutive losses of  $\text{CO}_2$ ,  $\text{C}_3\text{H}_4$  and  $\text{C}_2\text{H}_4\text{O}$  molecules to give the species at  $m/z$  691.3204, 651.1795 and 609.1707; these ions could be very relevant for the evaluation of the structure; in fact the fragments concerns exclusively the ester function, (scheme 3.2.1B).



The fragmentation of the glutaric function (fig. 3.2.5), in the same way, shows formal losses of water, CO<sub>2</sub> to give the ion at *m/z* 99.0566, and CH<sub>3</sub>COOH, to generate species at *m/z* 101.0324 and 57.0393 (scheme 3.2.2).



**Scheme 3.2.2.**

On the other hand, the positive spectrum (scheme 3.2.1B) showed the fragmentation of the ester moiety (*m/z* 163.0595, 145.0481) and those relative to the glycosidic moiety.

The latter are typically present in the spectra of flavonoids and are extensively reported in literature<sup>27,28</sup>; apart from the protonated aglycon at *m/z* 303.0869 ( $Y_0^+$ ) and that described previously 609.1838 ( $Y_1^+$ ), the MS/MS spectrum shows the species at *m/z* 591.1723 ( $Z_1^+$ ) which corresponds to the loss of rhamnose, while the rhamnose moiety ( $B_1^+$ ) is clearly identified at *m/z* 147.0629. The main important diagnostic peak was the  $B_2^+$  ion; it corresponds to the ion at *m/z* 453, which confirmed the position of glutaric function on the glycosidic part of molecule.

Many fragments regarded the losses of water molecules, from glutaric and glycosidic moieties (scheme 3.2.1B). The flavonoid at *m/z* ( $M+H$ )<sup>+</sup> 725.2298, can be recognized in the same way, as indicated by fragments on tandem mass spectrum reported in figure 3.2.6. The NMR data for compound at *m/z* ( $M+H$ )<sup>+</sup> 755.2387 (**1**) clearly shows the presence of all parts of molecule identified by mass spectrometry; the table 3.2.1 shows the different chemical shift, together with the relative signal multiplicity, of protons (<sup>1</sup>H) and carbons (<sup>13</sup>C) of four spin system: A, M, G, and R, obtained by 1D spectra coupled and decoupled (fig 3.2.8 A,B).

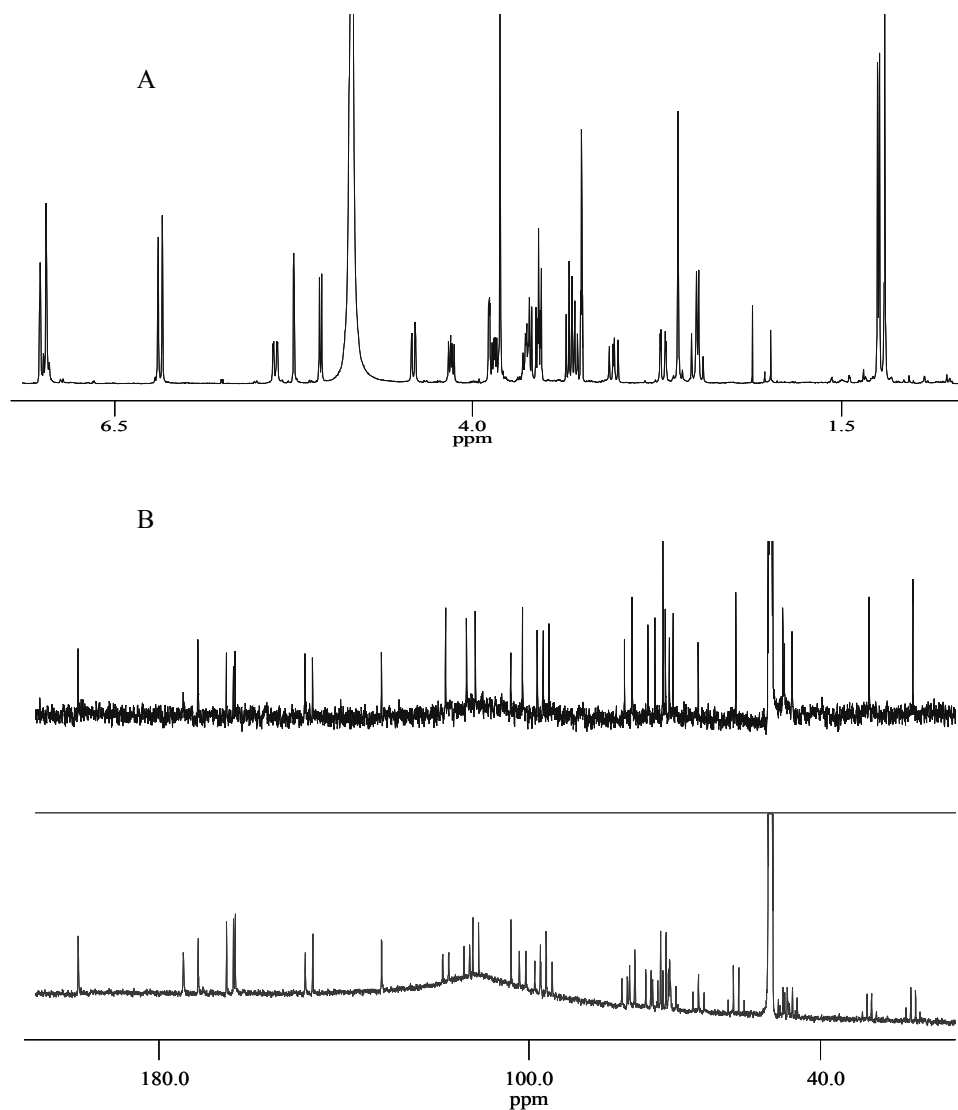


**Figure 3.2.8.**  $^1\text{H}$  (A) and  $^{13}\text{C}$  (B) NMR experiments of **1**.

The characteristic signal of aromatic rings with their chemical shift (ppm) and those of carbonyl functions are present in the M spin system (29, 33); other important signals are those relative to the methyl moieties as well as to the glycosidic systems; the hydroxyl protons are absent because the experiments were carried out in deuterated methanol. The position of the atoms in each spin system was assigned by using correlation

techniques such as  $^1\text{H}$ - $^1\text{H}$  COSY (fig. 3.2.9), COSY LR and TOCSY, and  $^1\text{H}$ - $^{13}\text{C}$  HSQC (fig 3.2.10).

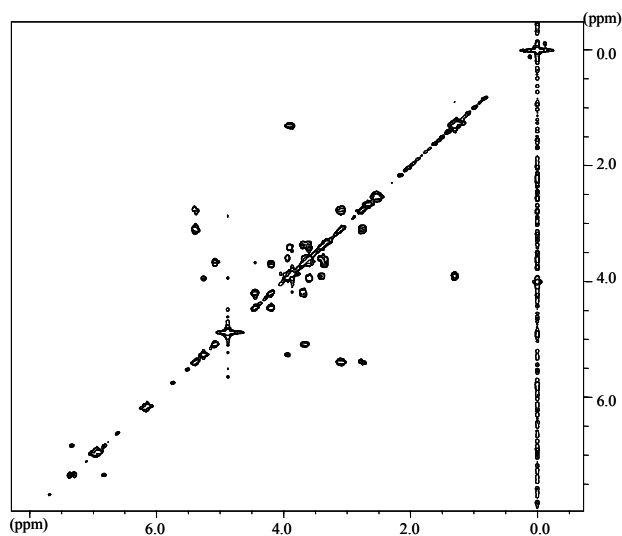


Figure 3.2.9. COSY experiment.

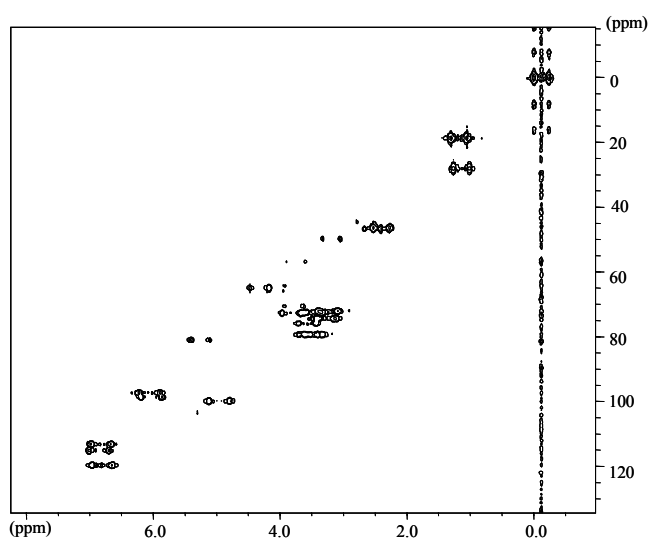
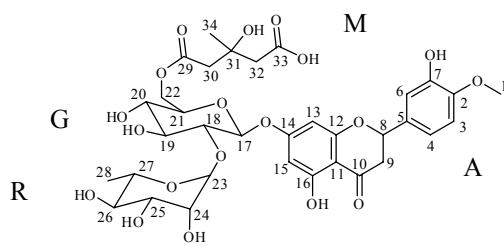


Figure 3.2.10. HSCQ experiment.

The hydrolyzed fraction was, in the same way, submitted to NMR ( $^1\text{H}$ ;  $^{13}\text{C}$ ) experiments. The  $^1\text{H}$  NMR experiment performed on the glutaric moiety showed the methyl signal (singlet) at low chemical shift, while the protons of alkyl chain are presents at ca. 2.5



Position	$^1\text{H } \delta$ ppm	$^{13}\text{C } \delta$ ppm	Correlations
1	3.85 (s)	56.9 (q)	HSQC, COSY LR (3,4,6)
2	-	149.4 (s)	
3	6.9 (ar)	112.6 (d)	HSQC, TOCSY
4	6.92 (ar)	119.1 (d)	HSQC, TOCSY
5	-	132.9 (s)	
6	6.96 (ar)	114.6 (d)	TOCSY
7	-	147.8 (d)	
8	5.38 (dd)	80.5 (d)	COSY (3.09 (9)), HSQC, TOCSY
9	3.09-2.77	44.4 (tr)	COSY (5.38 (8)), HSQC
10	-	198.4 (s)	
11	-	105.0 (s)	
12	-	166.4 (s)	
13	6.14 (ar)	99.3 (d)	COSY (6.17 (15)), HSQC, TOCSY
14	-	164.5 (s)	
15	6.17 (ar)	98.1 (d)	COSY (6.14 (13)), HSQC
16	-	164.5 (s)	
17	5.1 (d)	96.8 (d)	COSY (3.66 (18)), HSQC, TOCSY
18	3.62 (dd)	78.91 (d)	COSY (5.1 (17), 3.39 (19)), HSQC, TOCSY
19	3.39 (dd)		COSY (3.66 (18), 3.37 (20)), TOCSY
20	3.37 (dd)	70.02 (d)	COSY (3.39 (19), 3.69 (21)), TOCSY
21	3.69 (dd)	75.4 (d)	COSY (3.37 (20), 4.20 (22)), TOCSY
22	4.20-4.40 (dd)	64.6 (tr)	COSY (3.69 (21)), TOCSY
23	5.26 (d)	102.5 (d)	COSY (3.94 (24))
24	3.89 (dd)	73.91 (d)	COSY (5.26 (23), 3.59 (25))
25	3.59 (dd)	72	COSY (5.26 (23), 3.59 (25))
26	3.62 (dd)	78.9 (d)	COSY (3.59 (25), 3.90 (27))
27	3.90 (m)	72.8	COSY (3.36 (26), 1.31 (28)), TOCSY
28	1.31 (d)	18.3 (q)	COSY (5.26 (23), 3.59 (25)), HSQC
29	-	172.5 (s)	
30	2.65-2.52	46.0 (tr)	COSY (32), HSQC, TOCSY
31	-	70.8 (s)	
32	2.65-2.52	46.3 (tr)	COSY (30)
33	-	175.7 (s)	
34	1.26 (s)	27.5 (q)	HSQC, COSYLR (30,32)

Table 3.2.1. NMR signals of 1

ppm as multiplet. The presence of the multiplet was due to the fact that the methylenic protons are not magnetically equivalent (fig. 3.2.11). Indeed, coupled  $^{13}\text{C}$  experiment provided two signal (excluding that relative to solvent), a quadruplet and a triplet, due to the methyl and methylenic moiety respectively (fig. 3.2.11).

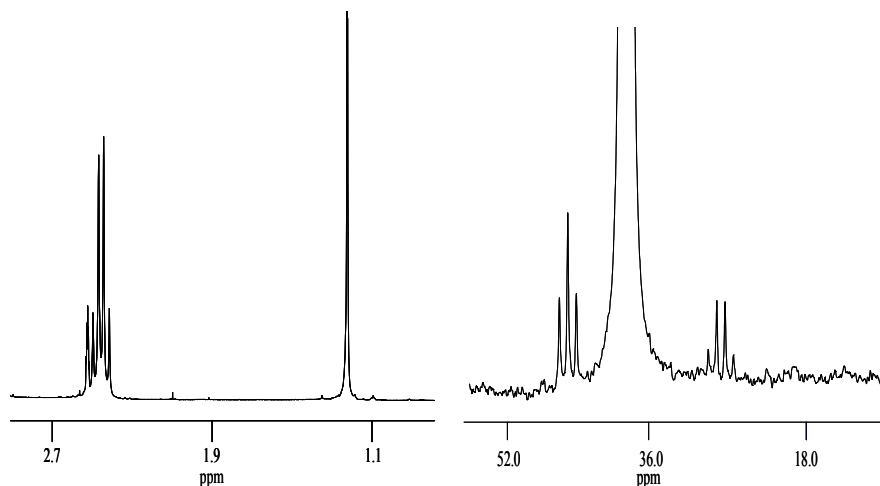


**Figure 3.2.11.**  $^1\text{H}$  and  $^{13}\text{C}$  NMR experiments of hydrolyzed sample.

The NMR data of the other unknown flavonoid at  $m/z$   $(\text{M}+\text{H})^+$  725 (**2**) confirmed the structure of the molecule. In this case the NMR spectra are quite similar to those of compound; the only difference is due to disappearance of the methyl signals.

Finally, the other two compounds, **3** and **4** showed a similar fragmentation pathway of **1** and **2**. The positive high resolution MS spectra shows experimental mass of 753.2250 and 723.2160 respectively, which corresponds to the elemental compositions  $\text{C}_{34}\text{H}_{41}\text{O}_{19}^+$  and  $\text{C}_{33}\text{H}_{39}\text{O}_{18}^+$  with 1.30 and 2.90 ppm uncertainty.

Figure 3.2.12 shows the tandem mass spectra of **3** and **4**; the main fragments, derive from the losses of terminal rhamnose and neohesperidose.

The two fragments presents at 30 eV have  $m/z$  value and elemental composition 607.1690,  $\text{C}_{28}\text{H}_{31}\text{O}_{15}^+$  and 301.0720,  $\text{C}_{16}\text{H}_{13}\text{O}_6^+$  for **3**, and 577.1565,  $\text{C}_{27}\text{H}_{29}\text{O}_{14}^+$  and 271.0630,  $\text{C}_{15}\text{H}_{11}\text{O}_5^+$  for **4**.

It's very relevant, than **1** and **2**, how the spectra were governed from  $\text{Y}_0^+$  and  $\text{Y}_1^+$  fragmentation, presumably due to the effect of double bond in C ring.

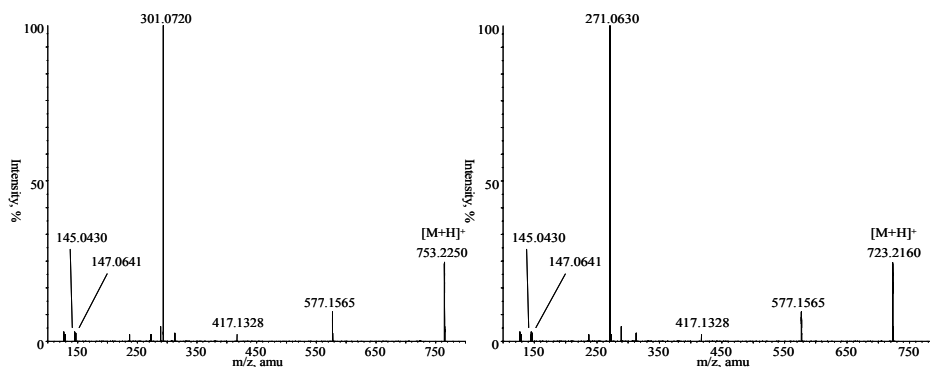


**Figure 3.2.12.** Positive ESI MS/MS spectra of compounds **3** and **4** at 30eV.

The fragmentation of **3** yields the neodiosmin aglycon, while the MS/MS spectrum of **4** gives rhoifolin aglycon. The Pummelo juice, like bergamot, was analyzed by HPLC/ESI/UV/MS technique. The profile showed the presence of few flavonoids in different amounts. In particular, the most abundant is due to naringin and rhoifolin; it is also present malonyl derivative of naringin (fig.3.2.13 and scheme 3.2.3). The first two flavonoids were confirmed by standard.

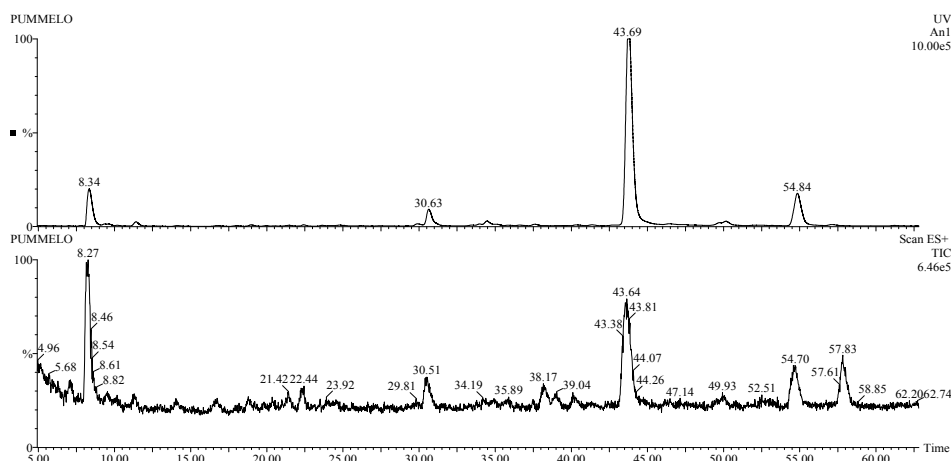


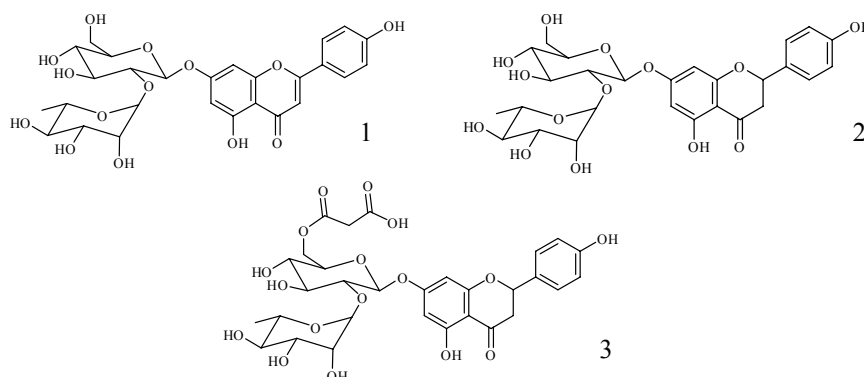
**Figure 3.2.13.** LC/UV/ESI-MS of pummelo (m/z,  $[M+H]^+$ ; rt): naringin, (581; 43.69), rhoifolin (579; 50.00), naringin-6''-O-malonate (667; 54.84).

The collected fraction of preparative HPLC relative to naringin malonate, was submitted to mass spectrometry analysis: the positive high resolution ESI MS spectrum gave the



experimental  $m/z$  value of 667.1872 which corresponds to elemental composition of  $C_{30}H_{35}O_{17}^+$  with 0.3 ppm of uncertainty; the tandem mass spectrum (fig. 3.2.14) provided fragmentation typically present in flavonoid glycosides (scheme 3.2.4).

Product ions from glycoconjugates are denoted according to the nomenclature introduced by Domon and Costello.<sup>29</sup> The base peak on the spectrum obtained at 20 eV of collision energy, was the aglycon moiety ( $Y_0^+$ ) at  $m/z$  value 273.0757; the loss of external rutinose yielded  $Y_1^+$ ,  $Z_1^+$  and  $B_1^+$  fragments at  $m/z$  521.1332, 147.0743, 503.1150 respectively. On other hands from  $B_2^+$  ( $m/z$  395) ion derived the species at  $m/z$  377 and 249 relative to losses of water and rutinose.



**Scheme 3.2.3.** 1. Rhoifolin; 2. naringin; 3. naringin-6''-O-malonate.

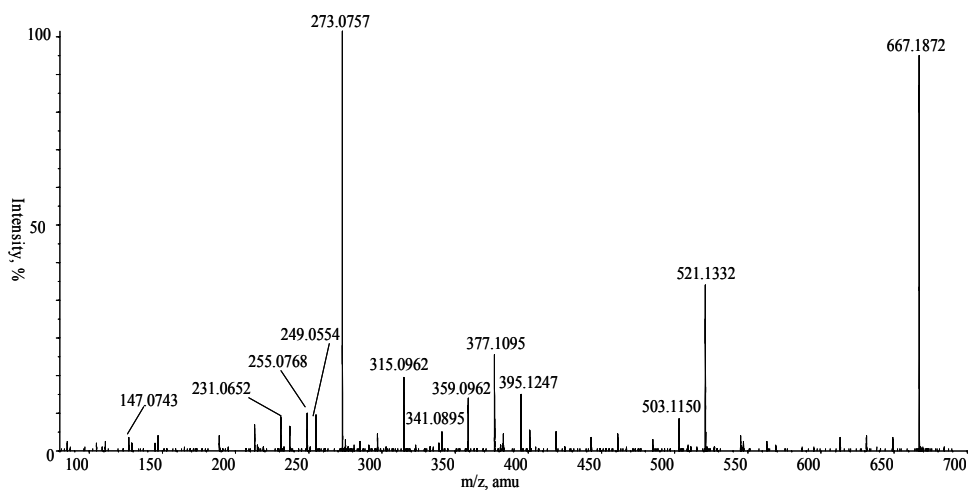
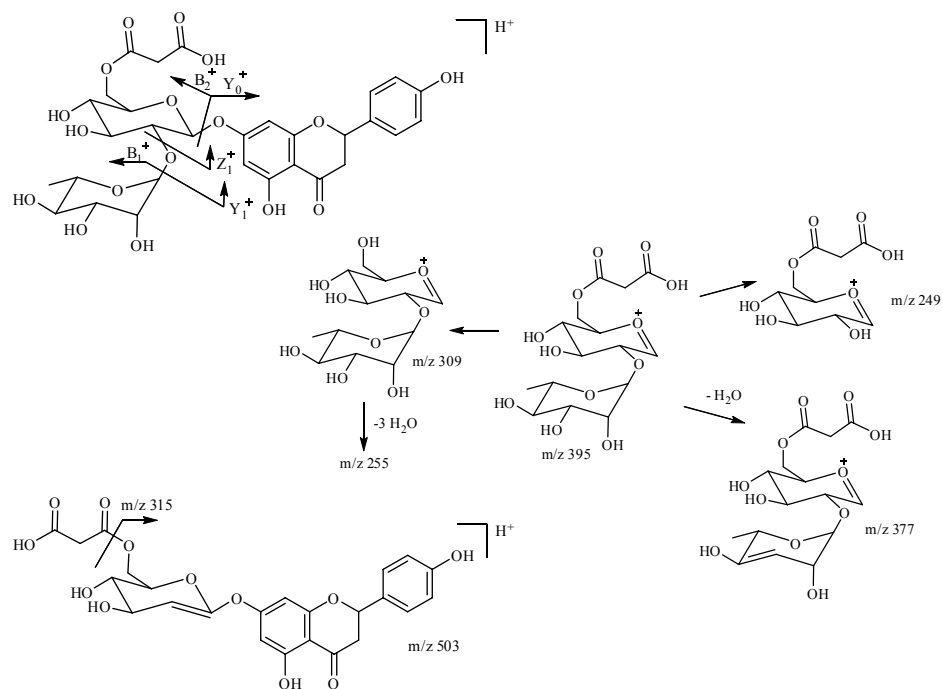


**Figure 3.2.14.** Positive ESI-MS/MS spectrum of naringin-6''-O-malonate.



Scheme 3.2.4.

The consecutive fragmentation of the same ions gave the species at  $m/z$  359.0962, 341.0895 and 231.0652 relative to losses of water molecules. Finally, the fragmentation of neohesperidose ion produced the species at  $m/z$  255.0768.

### 3.3 Determination of new flavonoidic compounds by High-resolution ESI-MS/MS in *Allium Porrum*.

The HPLC ESI-MS chromatogram as well as the UV chromatogram of the methanolic *Allium porrum* leaf extract is characterized, between others, by four unknown species; the figure 3.3.1 shows their XIC (extracted ion chromatogram); each compound was collected at the exhaust of the UV detector and submitted to tandem mass spectrometry experiments. The MS/MS experiments showed that all the unknown species produced the two common ion fragments at  $m/z$  287 and 535, respectively. Moreover, the high resolution mass spectrum of species **1** (table 3.3.1) indicate that its protonated molecular ion have  $m/z$  experimental value of 535.1078 which corresponds to the elemental composition of  $C_{24}H_{23}O_{14}^+$ , with 0.40 ppm uncertainty; the base peak of MS/MS spectrum performed on  $m/z$  535.1078  $[M+H]^+$  has an  $m/z$  value of 287.0565 which correspond to the elemental composition  $C_{15}H_{11}O_6^+$  (fig. 3.3.4A). Reasonably, the latter ion represents the aglycon moiety of **1**; in particular it could correspond to kaempferol.

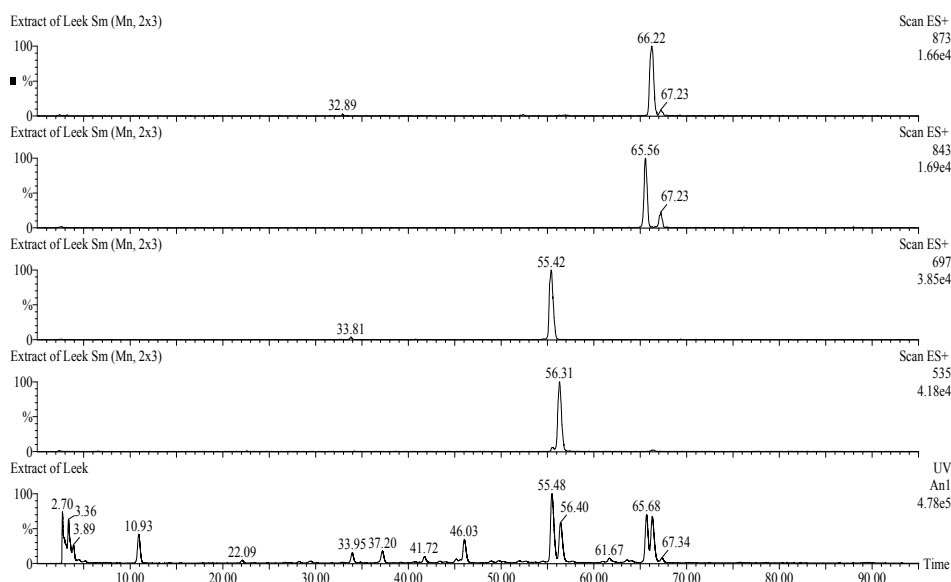


**Figure 3.3.1.** LC/UV/ESI-MS and XIC of methanol extract of leek ( $m/z$ ,  $[M+H]^+$ ; RT): unknown 1 (535; 57.53), unknown 2 (697, 56.61), unknown 3 (843, 66.81), unknown 4 (873, 67.43).

To prove this hypothesis an acid hydrolysis experiment was performed on **1**. The LC/MS of the hydrolyzed showed the presence of only one compound having the same

molecular weight and the same retention time of the Kaempferol standard. The unambiguous confirmation of the structure of **1** was achieved by matching its MS/MS spectrum and LC/MS elution time (fig. 3.3.3A and 3.3.2), with that of the known molecule previously isolated from Endive (coarse frisee)<sup>30</sup>.

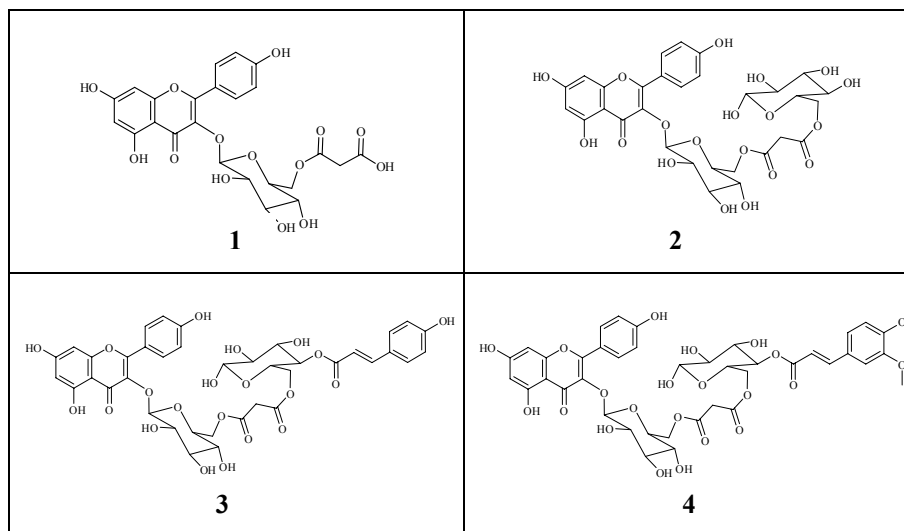


**Table 3.3.1.** Hypothetical structures of unknown species.

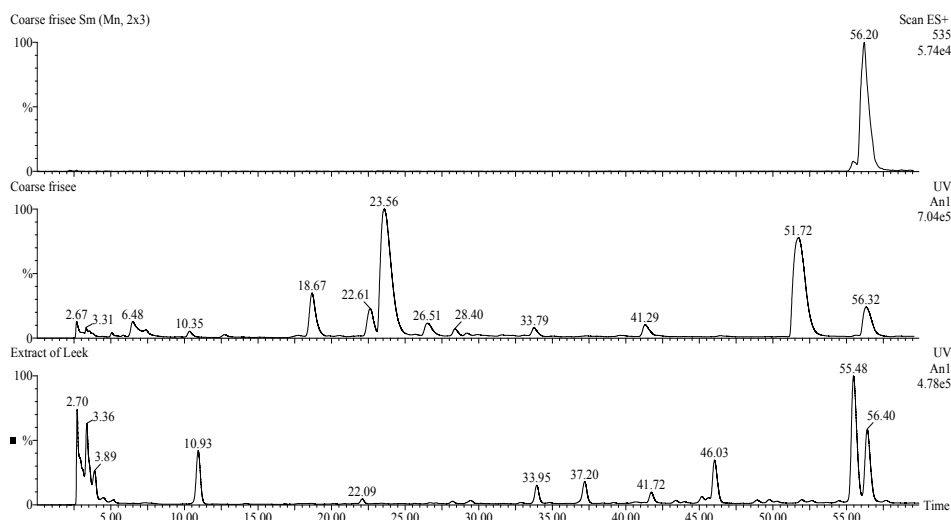


**Figure 3.3.2.** LC/UV/ESI-MS and XIC of methanol extract of coarse frisee and leek( $m/z$ ,  $[M+H]^+$ ;RT): Kaempferol 3-O-(6''-O-malonyl)glucoside (535; 56.32).

The high resolution spectrum for **2** showed the experimental mass of 697.1576 corresponding to the elemental composition  $C_{30}H_{33}O_{19}^+$  with 4.9 ppm uncertainty.

The compound **2** was hydrolyzed in the same manner of **1**; even in this case the reaction product was characterized as kaempferol.

On the other hand, the compound **2** differs from **1** only by 162 amu. The MS/MS spectrum (fig. 3.3.3B) is characterized by the formation of the fragment at  $m/z$  535.1101 ( $C_{24}H_{23}O_{14}^+$ ) that reasonably is produced by the loss of hexose from the parent ion.

Other fragments provides diagnostic peaks at  $m/z$  287.0591 ( $C_{15}H_{11}O_6^+$ ), 249.0642 ( $C_9H_{13}O_8^+$ ), 231.0523 ( $C_9H_{11}O_7^+$ ) (fig. 3.3.3B).

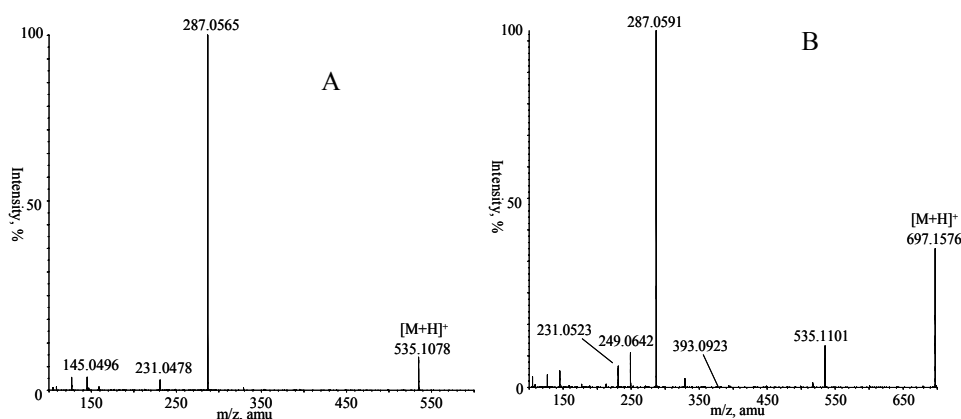


**Figure 3.3.3.** Positive High resolution ESI-MS/MS of species **1** (A) and **2** (B) at 20 eV.

In order to elucidate the position of glycon moiety, the ion at  $m/z$  393.0923 is very important because indicate the loss of kaempferol; the corresponding elemental composition of the latter ion is  $C_{15}H_{21}O_{12}^+$  that could reasonably correspond to the sequence hexose-malonyl-hexose (fig 3.3.4B).

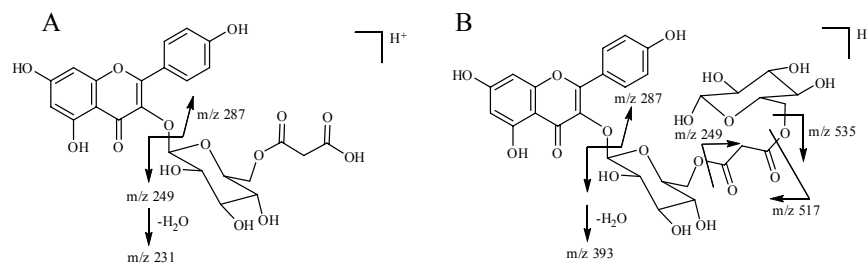


**Figure 3.3.4.** Fragmentation pattern of species **1** and **2**.

The other two flavonoids, **3** and **4** are high molecular weight compounds; they differ each other by 30 amu. The high resolution spectrum of **3** provide the protonated molecular ion at  $m/z$  843.1990 and elemental composition  $C_{39}H_{39}O_{21}^+$  with 1.2 ppm uncertainty; compound **4**, on the other hand, provides the molecular ion at  $m/z$  873.2089 corresponding to the elemental composition  $C_{40}H_{41}O_{22}^+$  with 0.5 ppm uncertainty; thus, **3** and **4** differs formally by a  $CH_2O$  moiety. Nevertheless, the acid hydrolysis obtained in the same conditions used for **1** and **2** gave the same reaction product, kaempferol.

The tandem mass spectrum of species **3**, showed, as seen for **2**, a fragment at  $m/z$  535.1082 ( $C_{24}H_{23}O_{14}^+$ ), due to the loss of 308 amu. On other hands, the base peak of the spectrum provides an  $m/z$  value of 309.0936 amu whose corresponding composition is  $C_{15}H_{17}O_7^+$ . The latter ion, presumably, could correspond at the structure V on the figure 3.3.5. Moreover, a very relevant peak is that at  $m/z$  147.0410 since the accurate measurement indicated for it, the elemental composition of  $C_9H_7O_2^+$ , probably due to the formation of acylium ion of the coumaric acid. (VII fig. 3.3.5).

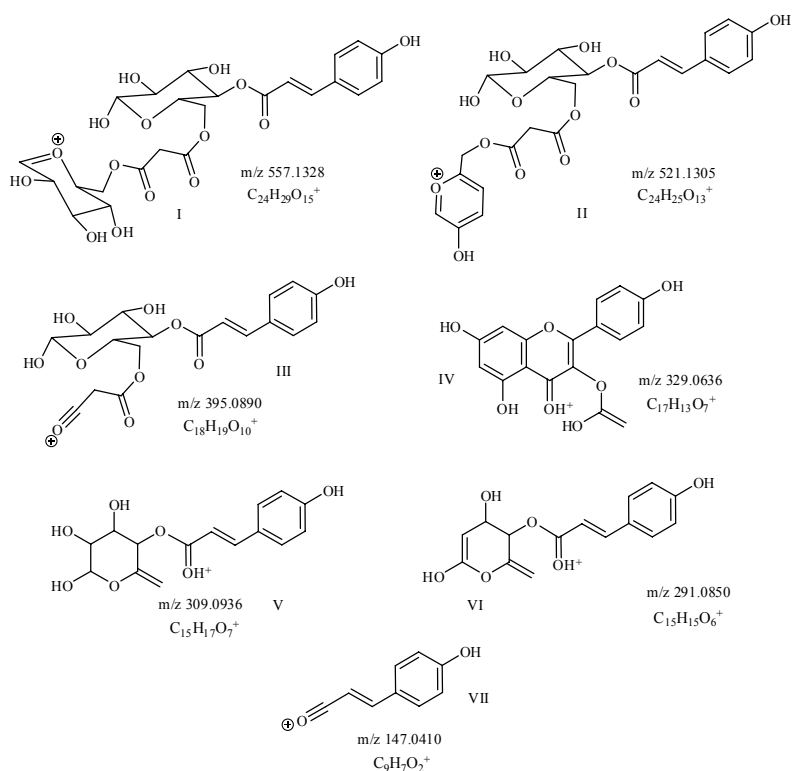


Figure 3.3.5. Hypothetical fragments of **3**.

The ion at  $m/z$  value 287.0550 ( $C_{15}H_{11}O_6^+$ ), corresponds to Kaempferol. To confirm the structural hypothesis showed in fig. 3.3.7A, various fragments structures have been hypothesized and summarized in figure 3.3.5.

The species I, was obtained by the loss of aglycon moiety, while the II and III ion could derived from I, by consecutive fragmentations as well as the species V and VI; therefore, compound **3**, seems to have a Kaempferol 3-O-(6''-O-malonyl) glucoside moiety in common with **1** and **2**. The tandem mass spectrum of **4**, (fig. 3.3.6) showed the same fragmentation pattern of **3**.

They have in common the aglycon moiety, ( $m/z$  287.0540;  $C_{15}H_{11}O_6^+$ ); the peaks at  $m/z$  177.0569, 339.1072, 551.1381, 557.1375, differs from those presents in the MS/MS spectrum of **3** by 30 amu; the former is a diagnostic peak because the relative elemental composition is  $C_{10}H_9O_3^+$ , probably due to the formation of acylium ion of feroulic acid; the presence of feroulic acid moiety, differentiate **4** by **3**; in fact, this acid differs from coumaric by 30 amu, due to the presence of a methoxyl function.

The base peak at  $m/z$  value 339.5553 and elemental composition  $C_{16}H_{19}O_8^+$ , also differs from the base peak of spectrum of **3**, by 30 amu; this means that the difference between the two species is focused only on the fragments in which is presents the feroulic function.

The linkage of the organic acid to the position 4 of the hexose, is inferred from bibliographic data.<sup>31</sup>

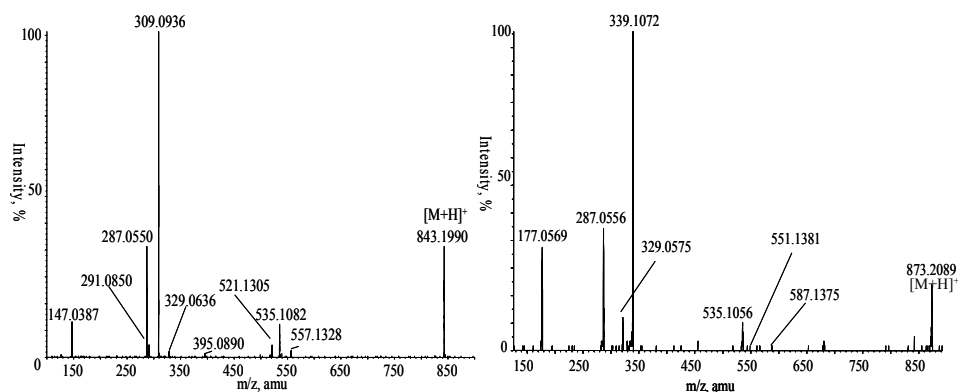
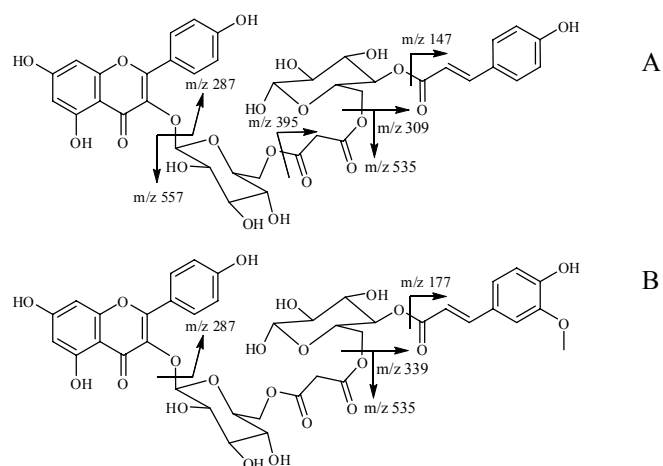


Figure 3.3.6. Positive High resolution ESI-MS/MS of species **3** and **4** at 20 eV.



**Figure 3.3.7.** Main fragmentations of species **3** (A) and **4** (B).

The main ions formed by MS/MS experiment, as seen before for **3**, are shown in figure 3.3.8.

Then, the use of high resolution tandem mass spectrometry allow to investigate the species at very tiny amounts. Therefore, whereas the chemical composition can be

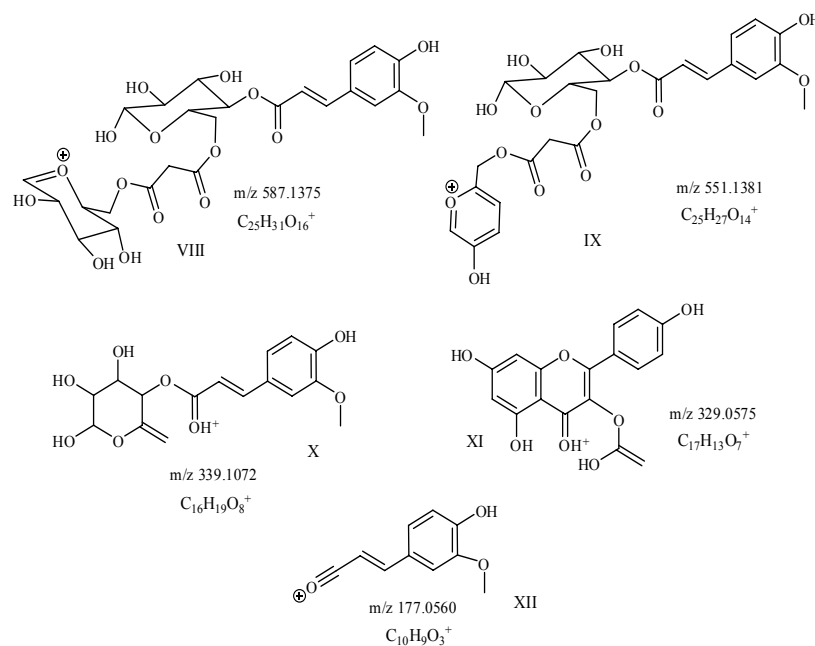


**Figure 3.3.8.** Hypothetical fragments of **4**.



unambiguously assigned, the structure can only be suggested on the grounds of the known gas-phase chemistry of compounds related to them. All compounds seems to belong at the Kaempferol flavonoids family with various organic acid and glucoside functions as results of reactions in a typical biosynthesis of flavonoids<sup>32</sup>.

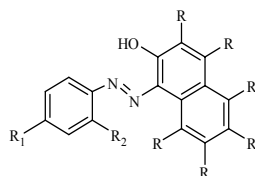
Moreover, these compounds are time dependent because disappears with the plant growth and probably aims as a carrier for antioxidant species like Kaempferol aglycon, coumaric and ferulic acids<sup>33</sup>.

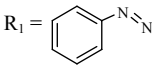
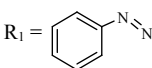
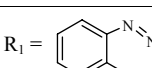
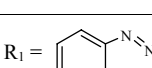
### 3.4. Gas-phase chemistry of all set of Sudan Azo dyes (I, II, III, IV and Para-red) and relative investigation in foodstuff by LC/MS-MS and Isotope dilution methodology.

Different approaches have been exploited to assay sudan dyes in different matrices,<sup>34-36</sup> the more effective one, in terms of specificity and sensitivity, was related to the identification and assay of sudan I in foodstuff by mass spectrometry and isotope dilution methods.<sup>37</sup>

The results presented here shed more light on the gas-phase chemistry of this long-studied<sup>38,39</sup> ‘azo’ functionality and may provide tools for the simultaneous and high-throughput determination of these dangerous species by applying a known method.<sup>37</sup>

Sudan I, II, III, IV and Para-red (P-red, scheme 3.4.1), widely used in many commodities and whose presence in complex mixture can be ascertained by mass spectrometry, are suspected carcinogenic molecules with potential risks to humans.



<b>1</b>	R <sub>1</sub> = H	R <sub>2</sub> = H	R = H	Sudan I
<b>2</b>	R <sub>1</sub> = H	R <sub>2</sub> = H	R = D	d <sub>6</sub> -Sudan I
<b>3</b>	R <sub>1</sub> = CH <sub>3</sub>	R <sub>2</sub> = CH <sub>3</sub>	R = H	Sudan II
<b>4</b>	R <sub>1</sub> = CH <sub>3</sub>	R <sub>2</sub> = CH <sub>3</sub>	R = D	d <sub>6</sub> -Sudan II
<b>5</b>	R <sub>1</sub> = NO <sub>2</sub>	R <sub>2</sub> = H	R = H	Sudan Para-red
<b>6</b>	R <sub>1</sub> = NO <sub>2</sub>	R <sub>2</sub> = H	R = D	d <sub>6</sub> -Sudan Para-red
<b>7</b>	R <sub>1</sub> = 	R <sub>2</sub> = H	R = H	Sudan III
<b>8</b>	R <sub>1</sub> = 	R <sub>2</sub> = H	R = D	d <sub>6</sub> -Sudan III
<b>9</b>	R <sub>1</sub> = 	R <sub>2</sub> = CH <sub>3</sub>	R = H	Sudan IV
<b>10</b>	R <sub>1</sub> = 	R <sub>2</sub> = CH <sub>3</sub>	R = D	d <sub>6</sub> -Sudan IV

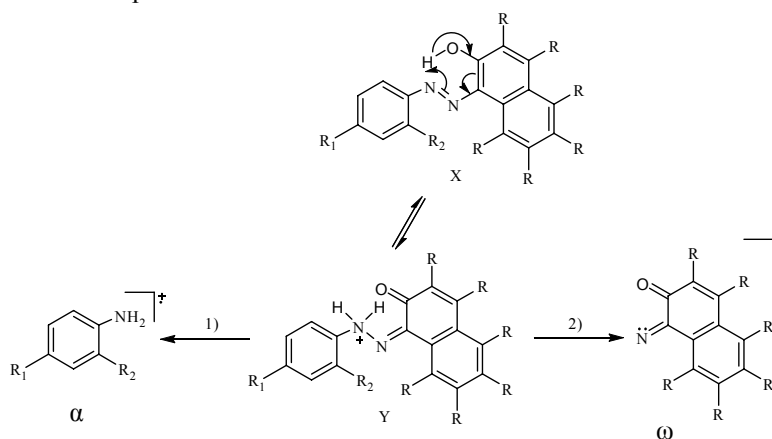
**Scheme 3.4.1.** Structure of the sudan dyes and their analogs.

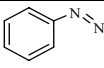
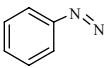
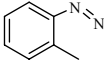
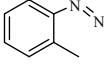
It is important, therefore, to understand the mechanism that governs the chemistry of sudan dyes in the gas phase, particularly in the case of isotopically labelled synthetic homologs which are the compounds of choice in the development of isotope dilution methodologies. The deuterated sudan compounds were synthesized by a modified literature procedure.<sup>40</sup> The distribution of deuterium within each molecule, ascertained by high-resolution ESI-MS on the Q-star instrument, is reported in table 3.4.1.

All the examined sudan azo dyes formally share a common  $\beta$ -naphthol moiety, which is the candidate for convenient labeling when suitable internal standards are needed. A matching of the fragmentation patterns of labeled and unlabeled sudan compounds is crucial in the choice of the best transition to be followed in analytical assays.

The gas-phase fragmentation of protonated sudan molecules (**X**, Scheme 3.4.2)<sup>37</sup> leads, in general, to the breakage of the azo double bond. Their CID spectra are relatively simple, especially for sudan I, II and P-Red, whereas the more complex structure of sudan III and IV induces the formation of additional product ions. Nevertheless, the observed competitive unimolecular reaction pathways lead mainly to two fragment ions, i.e. (1) the radical amine ions ( $\alpha$ ) and (2) the even-electron nitrene ions derived from the naphthol moiety ( $\omega$ ) (scheme 3.4.2). The scission of the aza bond is probably assisted by proton migration from the naphthol to the aza moiety of (**X**), causing the formation of the reactive intermediate (**Y**).

The sudan I (**1**) and  $d_6$ -sudan I (**2**) MS/MS spectra (Table 3.4.2) show a few fragments that are due to the formation of the radical aniline cation at  $m/z$  93 ( $\alpha_{1,2}$ , scheme 3.4.2) and the naphthol nitrene ions ( $\omega$ , scheme 3.4.2) at  $m/z$  156 and 162, the latter arising from the deuterated parent ion.



$R_1 = \text{H}$	$R_2 = \text{H}$	$R = \text{H}$	Sudan I ( $X_1$ )
$R_1 = \text{H}$	$R_2 = \text{H}$	$R = \text{D}$	$d_6$ -Sudan I ( $X_2$ )
$R_1 = \text{CH}_3$	$R_2 = \text{CH}_3$	$R = \text{H}$	Sudan II ( $X_3$ )
$R_1 = \text{CH}_3$	$R_2 = \text{CH}_3$	$R = \text{D}$	$d_6$ -Sudan II ( $X_4$ )
$R_1 = \text{NO}_2$	$R_2 = \text{H}$	$R = \text{H}$	Sudan Para-red ( $X_5$ )
$R_1 = \text{NO}_2$	$R_2 = \text{H}$	$R = \text{D}$	$d_6$ -Sudan Para-red ( $X_6$ )
$R_1 = $ 	$R_2 = \text{H}$	$R = \text{H}$	Sudan III ( $X_7$ )
$R_1 = $ 	$R_2 = \text{H}$	$R = \text{D}$	$d_6$ -Sudan III ( $X_8$ )
$R_1 = $ 	$R_2 = \text{CH}_3$	$R = \text{H}$	Sudan IV ( $X_9$ )
$R_1 = $ 	$R_2 = \text{CH}_3$	$R = \text{D}$	$d_6$ -Sudan IV ( $X_{10}$ )

**Scheme 3.4.2.** Main fragmentation of sudan compounds.

The consecutive fragmentation of the  $\omega$ -ions produces the species at  $m/z$  128 and 134 deriving from the elimination of a formal unit of carbon monoxide. Other ions are present at  $m/z$  231 (237 for **2**) and 232 (238), which originate from the loss of a hydroxyl radical and a water molecule, respectively. The CID spectrum of **2** shows

Sudan	% $d_4$	% $d_5$	% $d_6$
$d_6$ -Sudan I ( <b>2</b> )	-	7.05	92.95
$d_6$ -Sudan II ( <b>4</b> )	-	7.63	92.37
$d_6$ -Sudan Para-red ( <b>6</b> )	-	7.47	92.53
$d_6$ -Sudan III ( <b>8</b> )	-	7.88	92.12
$d_6$ -Sudan IV ( <b>10</b> )	-	6.78	93.22

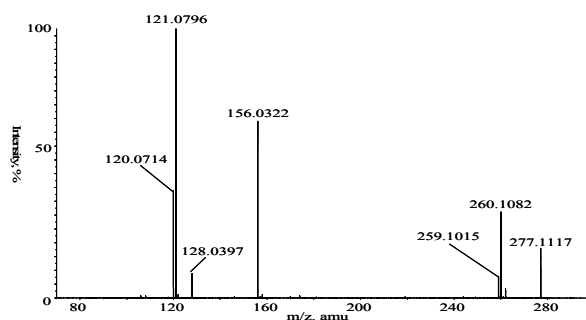
$d_0$ - $d_4$  relative abundances gave insignificant contribution to the  $[M + H]^+$  cluster of each species.

**Table 3.4.1.** Distribution of labeling within the species (**2**–**10**).

some satellite fragments at  $m/z$  161 and 133, accompanying the nitrene ions, which are absent in the spectrum of unlabeled analog.

This behavior could be attributed to some hydrogen/deuterium isomerization, which will be discussed in more detail. The fragmentation of sudan II (**3**) and of its deuterated analog (**4**) resembles that of sudan I. The most important ions of the MS/MS spectra (fig. 3.4.1) are those generated by (1) the loss of a methyl radical giving rise to the species at  $m/z$  262  $[X_3 - \text{CH}_3]^+$  (fig. 3.4.1A) and  $m/z$  268  $[X_4 - \text{CH}_3]^+$  (fig. 3.4.1B)

from the amine moiety of the molecule; (2) the loss of an hydroxyl radical and a formal water unit from both the protonated species originating the ions at  $m/z$  260, 266, 259 and 265 respectively; the ions  $\alpha$  and  $\omega$  (scheme 3.4.2), produced by the cleavage of the aza bond, are present at  $m/z$  121 and 156 ( $m/z$  162 for the deuterated molecule), respectively.  $d_6$ -Sudan II showed the same behavior as the deuterated analog of sudan I concerning the hydrogen/deuterium isomerization in the formation of the species at  $m/z$  161. When **2** and **4** are kept in a water solution for 24 h, no exchange with the deuterium atoms occurs as ascertained by 500 MHz  $^1\text{H}$  NMR. The formation of the species at  $m/z$  161 is, therefore, likely due to the fast H/D isomerization occurring in the gas phase, involving the phenolic moiety of the naphthol ring. Further evidences support that the hydrogen isomerization process depends also on the site of protonation of the aza moiety. The relative ratio 162/161 is strongly correlated with the electronic effect that the groups in *o*-/*p*- position of the amine moiety can exert on the relative basicity of the two nitrogen atoms of the aza group. The more those groups are electron donating, the less is the abundance of the  $m/z$  161 species in the MS/MS spectra of the  $[\text{M}+\text{H}]^+$  precursor (table 3.4.2). In fact, the 162/161 ratio decreases from 0.58 to 0.08 on going from  $d_6$ -sudan P-red (**6**) to  $d_6$ -sudan II (**4**), through the value of 0.12 obtained for  $d_6$ -sudan I (**2**). The rationale for this observation is that electron-withdrawing groups such as *p*-NO<sub>2</sub> affect the basicity of the nitrogen linked to the phenyl ring, thus forcing the competitive protonation of the nitrogen linked to the naphthol moiety (scheme 3.4.2). Accordingly, the electron-donating effect exerted by methyl groups on the *o* and *p*-positions of the aniline moiety prevents the formation of the satellite peak at  $m/z$  161. For a better understanding of the H/D isomerization, the gas-phase chemistry of  $d_5$ -sudan I and  $d_9$ -sudan II, deuterated at the amine moiety and synthesized as previously described, was checked under the same experimental conditions.



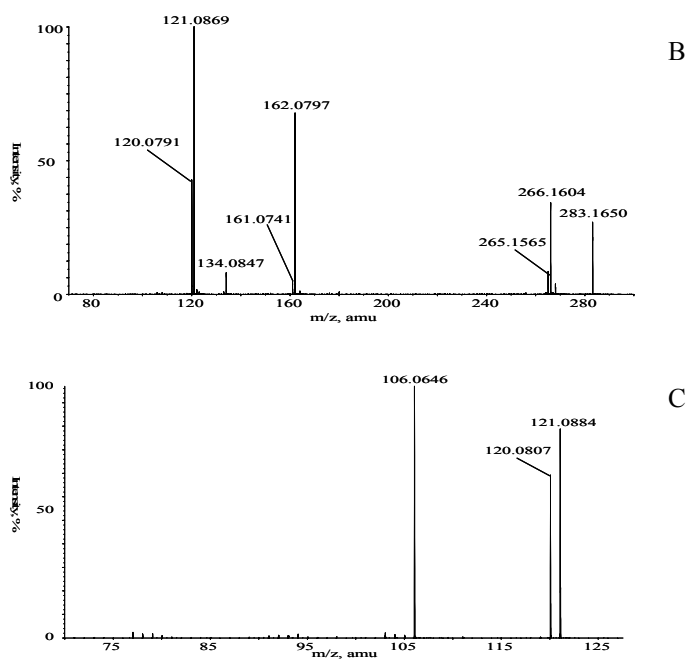
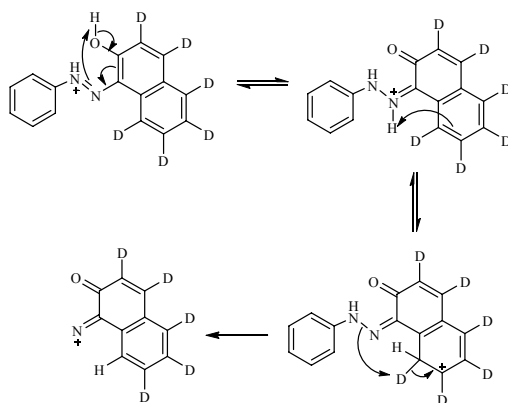


**Figure 3.4.1.** (A) ESI-MS/MS spectrum of sudan II; (B) ESI-MS/MS spectrum of  $d_6$ -sudan II performed at 20 eV. (C) ESI-MS/MS spectrum of the species at m/z 121 ( $\alpha$ ) generated by in-source fragmentation.

The MS/MS spectra of the two species do not show any satellite peaks that could denote H/D isomerization. This evidence strengthens the hypothesis that the competitive protonation of one of the two nitrogen sites drives the formation of satellite peaks when deuterium atoms are on the naphthol moiety (scheme 3.4.3).



**Scheme 3.4.3.** Probable mechanism of H/D isomerization in  $\omega$  ions of deuterated sudan molecules.

Another species of interest in the MS/MS spectra of **3** and **4** (fig. 3.4.1) is that shown at  $m/z$  120. It originates from the loss of a hydrogen atom from the 2-4-dimethyl aniline radical cation ( $\alpha$ ) as demonstrated by quasi-MS<sup>37</sup> measurements on the species  $m/z$  121 produced by setting the DP ion source parameter at 120 V (fig. 3.4.1C).<sup>41</sup>

The sudan P-red (**5** and **6**) are more difficult to be ionized in ESI; nevertheless there are some interesting fragments that differentiate them from the other sudan molecules (table 3.4.2).

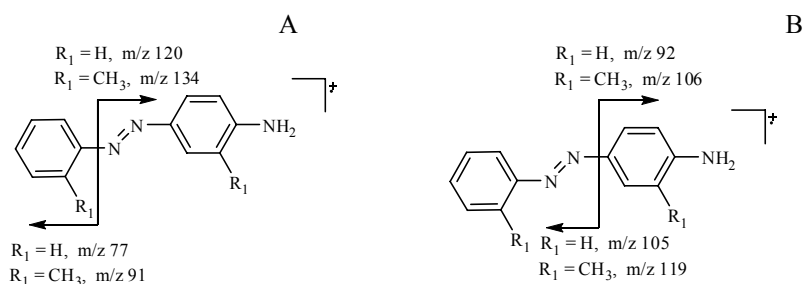
Sudan	[X- OH] <sup>•+</sup>	[X- H <sub>2</sub> O] <sup>+</sup>	$\alpha$	$\omega$	( $\omega$ -1)	( $\omega$ -CO)
Sudan I ( <b>1</b> )	232 (86)	231 (19)	92 (48)	156 (100)	-	128 (24)
d <sub>6</sub> -Sudan I ( <b>2</b> )	238 (99)	237 (28)	93 (56)	162 (100)	161 (13)	134 (24)
Sudan II ( <b>3</b> )	260 (39)	259 (8.1)	121 (100)	156 (66)	-	128 (9.1)
d <sub>6</sub> -Sudan II ( <b>4</b> )	266 (35)	265 (8.7)	121 (100)	162 (68)	161 (5.3)	134 (8.1)
Sudan Para-red ( <b>5</b> )	277 (44)	276 (1.8)	138 (5.3)	156 (41)	-	128 (2.7)
d <sub>6</sub> -Sudan Para-red ( <b>6</b> )	283 (95)	282 (4.8)	138 (3.8)	162 (36)	161 (22)	134 (4.1)
Sudan III ( <b>7</b> )	336 (4.1)	335 (0.7)	197 (86)	156 (67)	-	128 (6.2)
d <sub>6</sub> -Sudan III ( <b>8</b> )	342 (4.4)	341 (0.8)	197 (71)	162 (69)	161 (2.5)	134 (8.7)
Sudan IV ( <b>9</b> )	364 (2.0)	363 (0.7)	225 (69)	156 (28)	-	128 (2.1)
d <sub>6</sub> -Sudan IV ( <b>10</b> )	370 (3.1)	369 (0.7)	225 (61)	162 (27)	161 (2.0)	134 (7.2)

The ionic species derive from common reaction pathways. The collision energy was set at 20 eV for compounds **1–6**, and 30 eV for compounds **7–10**.

**Table 3.4.2.** Main product ions of [M + H]<sup>+</sup> of **1–10** ( $m/z$  (intensity %)).

The loss of a hydroxyl radical from the protonated molecules is evident, which generates the largest fragment peaks at  $m/z$  277 and 283 corresponding to the species [X<sub>5</sub> - OH]<sup>•+</sup> for the sudan P-red and [X<sub>6</sub> - OH]<sup>•+</sup> for the deuterated compounds.

A characteristic fragment is produced at  $m/z$  247 (253 for the labeled species); it originates from the formal loss of a molecule of nitrous acid. The ion at  $m/z$  171 (177 for the d<sub>6</sub>-P-red) is unique in the fragmentation of the azo dye family. It retains, in fact, the aza double bond in the naphthol moiety and loses, afterward, a formal unit of carbon monoxide to give the species at  $m/z$  143 (149). The  $\omega$ -ions at  $m/z$  156 (162) and 128 (134) are common to the other sudan molecules, while the radical ion of the amine moiety ( $\alpha$ ) is quite evident in both P-red and d<sub>6</sub>-P-red at  $m/z$  138. The CID spectra of sudan III (**7**) and d<sub>6</sub>-sudan III (**8**) show a more complicated pattern; the common ion of the two molecules are those related to the loss of the naphthol moiety, giving rise to the ions at  $m/z$  197 ( $\alpha_3$ , scheme 3.4.2) and 196 originating by the loss of a hydrogen atom from  $\alpha$ . Other common ions are those at  $m/z$  120 and 77 (scheme 3.4.4A), and  $m/z$  105 and 92 (scheme 3.4.4B) originating from the fragmentation of the  $\alpha$ -ion.



**Scheme 3.4.4.** Fragmentation of  $\alpha$  ions in sudan III (A) and Sudan IV (B).

The species at  $m/z$  156 and 162 correspond to the  $\omega$ -structures; the MS/MS spectra in both cases reveal the loss of a water molecule and a hydroxyl radical from the parent ion. The CID spectra of sudan IV (**9** and **10**) are almost identical to those of sudan III except for the fact that the observed fragments are shifted by 14 or 28 amu as a consequence of the presence of the methyl groups. The use of stable isotopes, as internal standards, in MS assay of analytes in complex natural and biological matrices represents an extremely accurate method of quantitative chemical analysis. The technique of isotope dilution is being used to improve precision and accuracy by reducing the problems arising from calibration procedure, sample preparation and matrix effects.

A known, exact quantity of labeled internal standard is added to the sample of unknown concentration. When mass spectrometry is used, the choice of the labeled reference compounds should take into account the possibility of gas-phase isotope isomerization, i.e., the possibility that heavy and light atoms might randomize within the framework of the molecule, either before or concomitantly to the breakdown of a specific bond.

The **2**, **4**, **6**, **8**, **10** species, used as reference compounds in the food application, afford by high resolution ESI-MS  $[M+H]^+$  clusters containing 92–93% of  $d_6$  labelled isomers. The gas-phase chemistry, like seen before, allows a reliable use of the selected isotope dilution method. The so-called precursor-ion-scan method was exploited to fulfil one of the goals of this work, i.e., the fast preliminary check on the presence of Sudan dyes in foodstuff. This scanning mode, available in modern tandem mass spectrometers, was initially developed as a tool for identify metastable transitions<sup>42</sup> and is now currently used to multiple screen analytes in complex mixtures.<sup>43</sup> A typical experiment was represented by the identification of Sudan azodyes (**1**, **3**, **5**, **7**, **9**, scheme 3.4.1) spiked,



at 1 ppm level, into commercially available baked products, such as cracker biscuits, by direct flow injection in the APCI-MS/MS mode.

Accordingly, the common ionic species at  $m/z$  156, corresponding to the  $\beta$ -naphthol fragment presents in the tandem mass spectra of all the analyzed dyes, was selected to perform the precursor ion scan measurement. All the spiked analytes were identified as shown in the spectrum reported in figure 3.4.2.

It should be noted that no relationship exists between the relative intensity of the ionic species displayed by the spectra and the actual concentration of each analyte.

The detailed assay of the polluting species is better carried out by the MRM method, coupled with an on-line LC separation of the analytes. The reliability of the selected approach was proved by the specificity, good sensitivity and by the good-to-excellent LOD and LOQ parameters experimentally determined. The specificity of analyte identification was guaranteed by the concomitant determination of two transitions originating from the  $[M+H]^+$  protonated molecular ions by product ion scan mode (table 3.4.3).

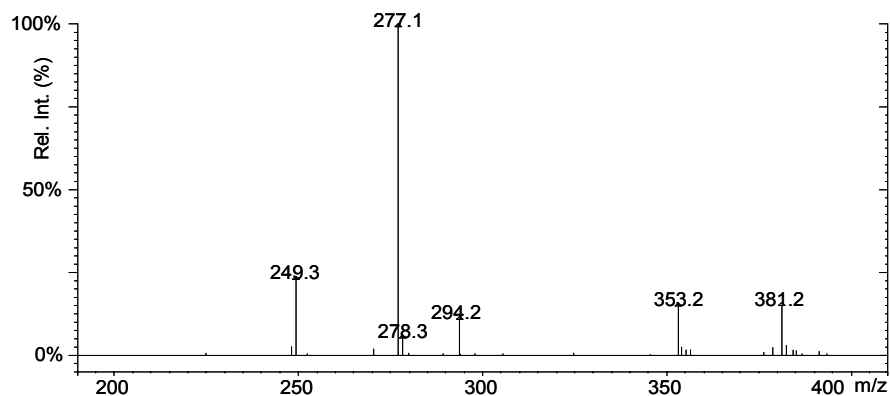


**Figure 3.4.2.** Parent ion scan MS/MS spectrum of the fragment  $m/z$  156 presents in the APCI spectra of azodyes extracted from baked products and sampled by flow injection.

The selection of the species to be used in the quantitative determinations was based both on the relative intensity of the daughter ions and on the specificity of the examined transition. In all cases, but Sudan II (**3**, table 3.4.3), the most abundant transitions was selected, whereas in the case of compound **3** the choice was guided by the need of avoiding possible interferences, hence, the  $m/z$  277  $\rightarrow$   $m/z$  156 transition was considered.

Analyte identification is provided by the two transitions listed in the second column obtained from the product ion scan spectra. Quantitative assay is based on the relative intensity of the transitions indicated in bold. In all cases, except for Sudan II (row 3), the selected process corresponds to the formation of the most abundant daughter ion. In the presence of traces of contaminants, namely in the ppm to ppb range, a crucial step is represented by the clean-up of the analytes after the extraction from the matrixes, since the crude extracts of some foodstuff show several interferences due probably to the presence of fats and other intrinsic components. The procedure can be conveniently carried out by means of commercial SPE silica gel cartridges, using n-hexane/ethyl acetate, 95:5 v/v, as eluant.

Analyte	Monitored Transitions
Sudan I (1)	<b><math>m/z</math> 249</b> → <b><math>m/z</math> 93</b> $m/z$ 249 → $m/z$ 156
$d_6$ -Sudan I (2)	<b><math>m/z</math> 255</b> → <b><math>m/z</math> 93</b> $m/z$ 255 → $m/z$ 162
Sudan II (3)	<b><math>m/z</math> 277</b> → <b><math>m/z</math> 156</b> $m/z$ 277 → $m/z$ 121
$d_6$ -Sudan II (4)	<b><math>m/z</math> 283</b> → <b><math>m/z</math> 162</b> $m/z$ 283 → $m/z$ 121
Sudan Para-Red (5)	<b><math>m/z</math> 294</b> → <b><math>m/z</math> 156</b> $m/z$ 294 → $m/z$ 277
$d_6$ -Sudan Para-Red (6)	<b><math>m/z</math> 300</b> → <b><math>m/z</math> 162</b> $m/z$ 300 → $m/z$ 283
Sudan III (7)	<b><math>m/z</math> 353</b> → <b><math>m/z</math> 77</b> $m/z$ 353 → $m/z$ 120
$d_6$ -Sudan III (8)	<b><math>m/z</math> 359</b> → <b><math>m/z</math> 77</b> $m/z$ 359 → $m/z$ 120
Sudan IV (9)	<b><math>m/z</math> 381</b> → <b><math>m/z</math> 91</b> $m/z$ 381 → $m/z$ 156
$d_6$ -Sudan IV (10)	<b><math>m/z</math> 387</b> → <b><math>m/z</math> 91</b> $m/z$ 387 → $m/z$ 162

**Table 3.4.3.** MRM experiments. List of the transitions monitored.

In this conditions very short-time, i.e. twelve minutes, chromatographic runs can be adopted thus allowing fast investigations of large number of samples (figure 3.4.3). The calibration curve, built by sampling, three times, each of the six solutions at different concentrations, showed a good linearity (table 3.4.4). The concentrations of the analytes

in the standard solutions ranged from 12.5 to 400 ppb (12.5; 25; 50; 100; 200; 400; ppb), while those of the internal standards were fixed at 50 ppb, with the exception of

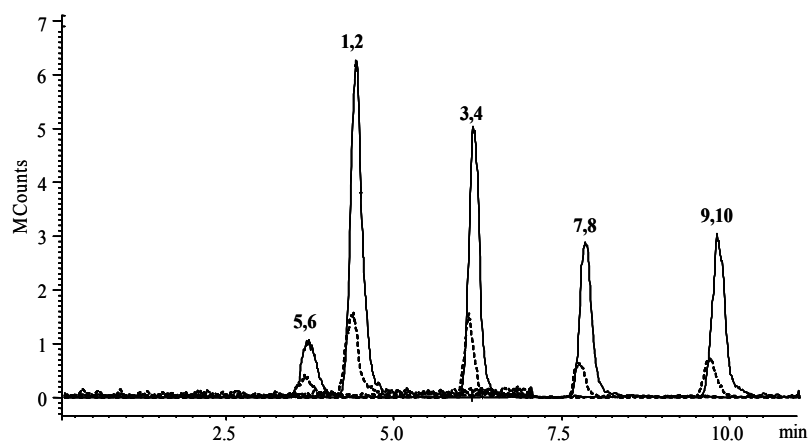


**Figure 3.4.3.** MRM chromatogram of standard solution at 200 ppb of 1, 3, 5, 7, 9 and 50 ppb 2, 4, 6, 8, 10 (dot line).

the Sudan Para-Red whose calibration curve was built using five solution (25; 50; 100; 200; 400; ppb) because of its poor ionization efficiency respect to the other sudan analytes. In any case, the calibration curve gave excellent correlation ( $R^2$ ) coefficients (table 3.4.4). It should be noted that the Sudan Para-Red substrate is characterized by the presence of a powerful electron withdrawing group placed in the *para* position of the benzene ring linked to the azo double bond which is suggested as the protonation site of the analytes, to account for the observed gas-phase chemistry.<sup>44</sup>

Analyte	Equation	Correlation factor
Sudan I (1)	$y = 0.0188x + 0.0805$	$R^2 = 0.9958$
Sudan II (3)	$y = 0.0178x + 0.1172$	$R^2 = 0.9983$
Sudan Para-Red (5)	$y = 0.0255x + 0.0820$	$R^2 = 0.9969$
Sudan III (7)	$y = 0.0209x + 0.1164$	$R^2 = 0.9941$
Sudan IV (9)	$y = 0.0211x + 0.1399$	$R^2 = 0.9966$

**Table 3.4.4.** Calibration curve parameters of the standard solutions of Sudan I-IV and Para-red.

The developed methodology has been applied to different home-made food matrixes free of any possible contaminant. Sausages, powdered chili pepper, baked products and tomato sauces were spiked with azodyes at two different concentrations: 40 and 300 ppb; these values well represent the matrix contaminations in the lower and in the higher part of the calibration curve. It should be noted that all the spiked matrixes have been processed in the same way; thus unifying the methodology when foods of different origin are submitted to a laboratory screening. The precision of the applied methodology is evident from the data reported in tables 3.4.5. The RSD% values are in all cases under 10%. Tables 3.4.5 illustrate also the real amount of dyes found per each spiked matrix: comparing the latter results with the amount spiked in the food, the values of accuracy for the two concentrations was in all cases between the 95% and 110%. The above found percentages for accuracy and precision underline the strength of the isotope dilution procedure, despite the fact that the amounts of contaminants are in the ppb range. The good results obtained are confirmed by the low levels of LOQ; indeed all Sudan dyes may be quantified above the threshold of 10 ppb except for Sudan Para-Red whose LOQ is 20 ppb, probably for the scarce ionization efficiency above mentioned (table 3.4.3). The recovery of the analytes is over 70% for Sudan I-IV in all matrixes except for the tomato sauce whose the recovery is around 50%. The Sudan Para-Red shows recoveries near 60% for all matrixes (table 4.6); this difference could be due to the strong interactions that this molecule could give with the silica gel of the cartridge. The sample preparation conditions have been chosen in order to provide the best instrumental response.

SUDAN I									
<i>Powder chili pepper</i>	ppb	Calculated concentration	RSD % (average)	Accuracy % (average)	<i>Sausage</i>	ppb	Calculated concentration	RSD % (average)	Accuracy % (average)
	40	42.9 ± 1.4	3.3	107.2		40	41.4 ± 1.6	4.1	103.5
300	308.8 ± 9.7	3.1	102.9	300	306.2 ± 7.4	2.4	102.1		
<i>Tomato Sauce</i>	ppb	Calculated concentration	RSD % (average)	Accuracy % (average)	<i>Baked products</i>	ppb	Calculated concentration	RSD % (average)	Accuracy % (average)
	40	42.7 ± 3.5	8.1	107.0		40	39.1 ± 3.0	7.6	97.7
	300	310.8 ± 17.3	5.5	103.6		300	297.9 ± 12.7	4.3	99.3

SUDAN II									
<i>Powder chili pepper</i>	ppb	Calculated concentration	RSD % (average)	Accuracy % (average)	<i>Sausage</i>	ppb	Calculated concentration	RSD % (average)	Accuracy % (average)
	40	37.8 ± 1.7	4.5	94.7		40	41.4 ± 2.7	6.5	103.5
	300	288.8 ± 13.0	4.5	96.2		300	303.7 ± 13.9	4.5	101.2
<i>Tomato Sauce</i>	ppb	Calculated concentration	RSD % (average)	Accuracy % (average)	<i>Baked products</i>	ppb	Calculated concentration	RSD % (average)	Accuracy % (average)
	40	42.5 ± 2.9	6.8	106.2		40	40.2 ± 3.8	9.6	100.5
	300	318.0 ± 13.1	4.1	106.0		300	311.0 ± 13.5	4.3	103.6
SUDAN III									
<i>Powder chili pepper</i>	ppb	Calculated concentration	RSD % (average)	Accuracy % (average)	<i>Sausage</i>	ppb	Calculated concentration	RSD % (average)	Accuracy % (average)
	40	39.60 ± 1.10	2.5	99.1		40	44.6 ± 2.5	5.8	111.6
	300	285.8 ± 6.4	2.2	95.2		300	316.9 ± 26.3	8.3	105.6
<i>Tomato Sauce</i>	ppb	Calculated concentration	RSD % (average)	Accuracy % (average)	<i>Baked products</i>	ppb	Calculated concentration	RSD % (average)	Accuracy % (average)
	40	43.8 ± 3.3	7.5	109.6		40	40.2 ± 3.8	9.6	100.5
	300	293.5 ± 6.4	2.1	97.8		300	311.0 ± 13.5	4.3	103.6
SUDAN IV									
<i>Powder chili pepper</i>	ppb	Calculated concentration	RSD % (average)	Accuracy % (average)	<i>Sausage</i>	ppb	Calculated concentration	RSD % (average)	Accuracy % (average)
	40	40.0 ± 1.6	4.0	100.0		40	41.6 ± 4.3	10.3	104.
	300	307.2 ± 4.2	1.3	102.4		300	305.2 ± 14.4	4.7	101.7
<i>Tomato Sauce</i>	ppb	Calculated concentration	RSD % (average)	Accuracy % (average)	<i>Baked products</i>	ppb	Calculated concentration	RSD % (average)	Accuracy % (average)
	40	39.9 ± 2.6	6.6	99.9		40	44.1 ± 0.8	2.0	110.3
	300	302.8 ± 6.0	1.9	100.9		300	297.9 ± 12.3	4.1	99.3
SUDAN PARA RED									
<i>Powder chili pepper</i>	ppb	Calculated concentration	RSD % (average)	Accuracy % (average)	<i>Sausage</i>	ppb	Calculated concentration	RSD % (average)	Accuracy % (average)

	40	43.69 ± 1.90	4.3	109.2		40	46.40 ± 6.21	13.5	116.1
	300	304.4 ± 20.5	6.7	101.4		300	349.50 ± 13.58	3.9	116.5
<i>Tomato</i>	ppb	Calculated concentration	RSD % (average)	Accuracy % (average)	<i>Baked</i>	ppb	Calculated concentration	RSD % (average)	Accuracy % (average)
<i>Sauce</i>	40	46.7 ± 2.1	4.6	116.9	<i>products</i>	40	45.7 ± 2.9	6.3	114.2
	300	303.6 ± 17.5	5.7	101.2		300	309.1 ± 14.5	4.6	103.0

**Table 3.4.5.** Analytical parameters for assessing the accuracy of the method.

Table 3.4.6 shows in addition the values of the analytical parameters LOD and reproducibility,

Analyte	Food matrix	LOD	LOQ	Recovery	Reproducibility (RSD %)	
					300 ppb	40 ppb
SUDAN I	powder chili pepper	2.8	4.5	93.4	1.3	6.6
	Sausage	3.1	7.3	85.7	2.8	4.1
	Baked product	3.4	7.8	87.7	1.9	6.6
	Tomato sauce	3.8	9.6	50.4	6.0	4.7
SUDAN II	powder chili pepper	3.0	4.1	98.9	4.3	5.8
	Sausage	4.1	6.3	79.9	1.4	4.4
	Baked product	3.9	5.2	88.2	14.8	3.2
	Tomato sauce	4.5	8.6	50.2	4.0	5.3
SUDAN III	powder chili pepper	3.2	6.2	76.6	3.1	6.3
	Sausage	4.1	7.2	73.9	2.2	8.1
	Baked product	4.2	6.1	74.0	2.1	4.9
	Tomato sauce	5.8	9.5	49.2	1.9	7.6
SUDAN IV	powder chili pepper	3.2	5.4	69.7	0.6	3.5
	Sausage	4.3	6.3	68.0	1.9	8.1
	Baked product	4.0	5.6	77.0	17.8	7.1
	Tomato sauce	6.3	8.2	48.5	1.4	6.6
SUDAN PARA RED	powder chili pepper	10.5	16.3	60.6	2.7	5.5
	Sausage	14.2	18.0	65.2	4.4	5.8
	Baked product	12.2	15.6	69.9	4.9	6.8
	Tomato sauce	15.2	19.3	52.0	2.9	5.7

\* The reproducibility of the measurements were obtained by extracting each sample three times over a period of 1 week.

**Table 3.4.6.** Reproducibility\* (RSD %) and analytical parameters of the proposed method.

the latter calculated by extracting three times each foodstuff over a period of one week. The RSD values are in almost all the situations under 10% confirming the goodness of the method; furthermore the values of LOQ and LOD allow a determination of analytes in the lower ppb range. The results presented above show that the determination and quantification of the all set of Sudan azodyes, likely contaminating foodstuff containing hot chili pepper derivatives, and banned by the European Union, can be carried out by means of the classic tools of tandem mass spectrometry, i.e. parent ion scan and multiple reaction monitoring with the isotope dilution method.

The protocols devised for food safety control can be easily extended to other application when the quantification of this type of analyte is required.

---

**References**

1. A. De Nino; N. Lombardo; E. Perri; A. Procopio; A. Raffaelli; G. Sindona. *J. Mass Spectrom.* **1997**, *32*, 533.
2. A. De Nino; F. Mazzotti; SP.Morrone; E. Perri; A. Raffaelli; G. Sindona. *J. Mass Spectrom.* **1999**, *34*, 10.
3. D. Ryan; M. Antolovich; T. Herlt; PD. Prenzler; S. Lavee; K. Robards. *J. Agric. Food Chem.* **2002**, *50*, 6716.
4. SC.Ma; ZD. He; XL. Deng; PPH. But; VEC. Ooi; HX. Xu; SHS. Lee; SF. Lee. *Chem. Pharm. Bull.* **2001**, *49*, 1471.
5. M. Servili; M. Baldioli; R. Selvaggini; A. Macchioni; G. Montedoro. *J. Agric. Food Chem.* **1999**, *47*, 12.
6. ZD. He; H. Dong; HX. Xu; WC. Ye; HD. Sun; PPH. But. *Phytochemistry* **2001**, *56*, 327.
7. D. Caruso; R. Colombo; R. Patelli; F. Giavarini; G. Galli. *J. Agric. Food Chem.* **2000**, *48*, 1182.
8. Y. Takenaka; T. Tanahashi; M. Shintaku; T. Sakai; N. Nagakura. Parida. *Phytochemistry* **2000**, *55*, 275.
9. (a) FW. McLafferty. *Acc. Chem. Res.* **1980**, *13*, 33; (b) KL. Busch; GL. Glish; SA. McLuckey. *Mass Spectrometry/Mass Spectrometry: Techniques and Applications of Tandem Mass Spectrometry*. Wiley, VCH: New York **1988**.
10. HK. Obied; MS. Allen; DR. Bedgood; PD. Prenzler; K. Robards; R. Stockmann. *J. Agric. Food Chem.* **2005**, *53*, 823.
11. V. Kovacic; J. Hirsch; D. Thölmann; HF. Grützmacher. *Org. Mass Spectrom.* **1991**, *26*, 1085.
12. S. De Marino; N. Borbone; F. Zollo; A. Ianaro; P. Di Meglio; M. Iorizzi. *J. Agric. Food Chem.* **2004**, *52*, 7525.
13. L. Di Donna; F. Mazzotti; A. Napoli; A. Sajjad; R. Salerno; G. Sindona. *Rapid Commun. Mass Spectrom.* **2007**, *3*, 273.
14. ZD. He; PPH. But; TWD. Chan ; H. Dong; HX. Xu; CP. Lau; HD. Sun. *Chem. Pharm. Bull.* **2001**, *49*, 780.
15. A. Mazzotti; F. Mazzotti; M. Pantusa; L. Sportelli; G. Sindona. *J. Agric. Food Chem.* **2006**, *54*, 7444.
16. D. Ryan; M. Antolovich; P. Prenzler; K. Robards; S. Lavee. *Scientia Horticulture* **2002**, *92*, 147.
17. P. Bogani; D. Cavaliere; R. Petrucci; L. Polsinelli; G. Roselli. *Acta Hort.* **1994**, *356*, 98-101.
18. V.J. Gemas; M.J. Rijo-Johansen; R. Tenreiro; P. Fevereiro. *J. Hort. Sci. Biotech.* **2000**, *75*, 312-319.
19. K.M. Sefc; M.S. Lopes; D. Mendoca; M.R. Dos Santos; M. Laimer Da Camara Machado. *Mol. Ecol.* **2000**, *9*, 1171-1173.
20. P. Dugo; M. Lo Presti; O. Marcus; A. Fazio; G. Dugo; L. Mondello; *J.Sep.Sci.* **2005**, *28*, 1149-1156.
21. M.L. Calabrò; V. Galtieri; P. Cutroneo; S. Tommasini; P. Ficarra; R. Ficarra. *J. of pharmaceutical and biomedical analysis*, **2004**, *35*, 349-363.
22. L. Di Donna; F. Mazzotti; A. Napoli; R. Salerno; A. Sajjad; G. Sindona. *Rapid Commun. Mass Spectrom.* **2007**, *21*, 273-278.
23. L. Di Donna; F. Mazzotti; R. Salerno; A. Tagarelli; D. Taverna; G. Sindona. *Rapid Commun. Mass Spectrom.* **2007**, *21*, 3653-3657.
24. F. Cuyckens; M. Claeys. *J. Mass Spectrom.* **2004**, *39*, 1-15.



25. H.M. Merken; G.R. Beecher. *J. Agric. Food Chem.*, **2000**, 48, 577.
26. M.A. Berhow; R.D. Bennett; K. Kanes; S.M. Poling; C.E. Vandecook. *Phytochemistry* **1991**, 30, 4198-4200.
27. F. Cuyckens; R. Rozenberg; E. de Hoffmann; M. Claeys. *J. Mass Spectrom.* **2001**, 36, 1203-1210.
28. R.E. Marcha; E.G. Lewars; C.J. Stadey; X.S. Miao; X. Zhao; C.D. Metcalfe. *International Journal of Mass Spectrometry* **2006**, 248, 61-85.
29. B. Domon; C.E. Costello. *Glycoconj. J.* **1988**, 5, 397.
30. S.M. DuPont; Z. Mondin. *J. Agric. Food Chem.* **2000**, 48, 3957.
31. E. De Rijke; F. De Kanter; F. Ariese; C. Gooijer; U.A. Brinkman. *J. Sep. Sci.* **2004**, 27, 1061.
32. J.B. Harborne; T.J. Mabry; H. Mabry; *The Flavonoids*, Chapman & Hall, London, **1975**.
33. I.C. Arts; P.C. Hollman; *Am. J. Clin. Nutr.* **2005**, 81, 317S.
34. YH. Liu; ZH. Song, FX. Dong; L. Zhang. *Journal of Agricultural and Food Chemistry* **2007**, 55, 614.
35. M. Ma; XB. Luo; B. Chen; SP. Sub; SZ. Yao. *Journal of Chromatography A* **2006**, 1103, 170.
36. F. Calbiani; M. Careri; L. Eviri; A. Mangia; L. Pistara; I. Cagnoni. *Journal of Chromatography A* **2004**, 1042, 123.
37. L. Di Donna; L. Maiuolo; F. Mazzotti; D. De Luca; G. Sindona. *Analytical Chemistry* **2004**, 76, 5104.
38. PC. Wszolek; FW. McLafferty; JH. Brewster. *Organic Mass Spectrometry* **1968**, 1, 127.
39. D. Srzc; M. Zinic; Z. Meic; G. Czira; J. Tainas. *Organic Mass Spectrometry* **1992**, 27, 1305.
40. BS. Fukniss; AJ. Hannaford; PWG. Smith; AR. Tatchell. *Vogel's Textbook of Practical Organic Chemistry*, 5th edition. Longman Scientific and Technical: New York **1989**; Chapter 6.
41. S. Hammerum; CB. Nielsen. *The Journal of Physical Chemistry A* **2005**, 109, 12046.
42. M. Barber; W.A. Wolstenholme; K.R. Jennings. *Nature* **1967**, 214, 664-666.
43. R. G. Cooks. *J. Mass Spectrom.* **1995**, 30, 1215-1221.
44. L. Di Donna. A. De Nino; L. Maiuolo; F. Mazzotti; A. Napoli; R. Salerno; G. Sindona. *J. Mass Spectrom.* **2007**, 42, 1057-1061.

# **Chapter 4**

*Experimental*



## 4. Experimental

### 4.1 Materials

HPLC grade solvents were purchased from Carlo Erba (Rodano, Italy).

Naringin, neohesperidin, Rhoifolin, Kaempferol were purchased from Extrasynthese (Genay, France).

Sudan I, II, III, IV and Para-Red were commercially obtained (Sigma-Aldrich, St. Louis, MO). The deuterated Sudan molecules were obtained by modification of existing literature method (Chapter 3). Leaves and drupes of different cultivars of *Olea Europea* L. was collected in CRA [Centro Ricerche Agroalimentari; Rende (Cosenza, Italy)].

Leaves of *laurum* and fruits of *ligustrum lucidum* was collected in Botanical garden (University of Calabria, Rende, Italy). Bergamot, orange and lemon fruits were provided from Azienda agricola Pizzi, Condofuri (Reggio Calabria, Italy). Grapefruits were provided of Fattoria Stocchi Rende (Cosenza, Italy). Pummelo (Origin: Israel), Leek and Endive were bayed at supermarket.

### 4.2 Samples preparation

#### Drupes of *Olea Europaea* L.

Destoned drupes (5 g; Carolea, Coratina, Nocellara del Belice and Leccino cultivars) were crushed in 30 mL of MeOH and sonicated for 15 min. The residual solution was filtered into a Buchner funnel and the filtrate was washed with n-hexane(3 x 20 mL) to remove triglycerides and then evaporated under reduced pressure. The residue was dissolved in 2mL of MeOH and submitted to analysis by high-performance liquid chromatography (HPLC). Fruit stones were extracted using the same methodology.

#### Leaves of *Olea Europaea* L.

A mixture of methanol and water (20 ml 1:1 v/v) was added to 2 g of olive leaf powder. Five cultivars (Carolea, Cassanese, Coratina, Nocellara del Belice and Leccino) were used for the assays. The mixture was homogenized by Vortex for three minutes and

subsequently sonicated for 20 minutes. The residue solution was filtered into a Buchner funnel, and diluted to 25 mL adding salicin as internal standard at 25ppm; 2 mL of the solutions were filtered on a 0.45 micron filter and submitted to HPLC analysis.

The same extraction method was used to obtain the standard molecules from laurum, olive drupes, *ligustrum lucidum*.

#### Fruit of Bergamot juice

A: the juice obtained by squeezing with hand was directly inject (20  $\mu$ l) on HPLC/MS after centrifugation and filtration on HPLC filter (45  $\mu$ m).

B: the peeled fruit (200gr; *Femminello cultivar*) was crushed in 200mL of MeOH/EtOH/CHCl<sub>3</sub> (65:30:5) and sonicated for 15 min. After centrifugation, the residual solution was filtered into a Buchner funnel and then concentrated under reduced pressure. After dissolution in 50mL of water the sample was submitted to RP C18 cartridge separation by washed of water (3 x 10 ml), for remove the polysaccharides, and successive (3 x 10 ml) MeOH. Finally, after elimination of organic solvent, the water solution was utilized for Medium-performance liquid chromatography (MPLC) and semi preparative HPLC.

#### Fruit of Pummelo juice

The peeled fruit (1Kg) was crushed in 500mL of MeOH/EtOH/CHCl<sub>3</sub> (65:30:5) and sonicated for 15 min. After centrifugation, the residual solution was filtered into a Buchner funnel and then concentrated under reduced pressure. After dissolution in 70mL of water the sample was submitted to RP C18 cartridge separation by washed of water (3 x 10 ml), for remove the polysaccharides, and successive (3 x 10 ml) MeOH. After elimination of methanol, 20  $\mu$ l of water solution (4500 ppm) was injected on HPLC/MS previous centrifugation and filtration on HPLC filter (45  $\mu$ m). Finally, the same solution was utilized for Medium-performance liquid chromatography (MPLC) and successively preparative HPLC.

#### Leaves of Allium Porrum (Leek)

The fresh leaves (without bulb; 5 gr.) was powdered, crushed in 50mL of MeOH and sonicated for 15 min. After centrifugation, the residual solution was filtered into a

Buchner funnel, washed with n-hexane (3 x 10 ml) and then concentrated under reduced pressure. Finally, the solution was filtered on a 0.45 micron filter and submitted to HPLC analysis.

#### Sudan I-IV and Para-red

To 1g of milled food (powder chili pepper, tomato sauce, sausage, baked products) a selected amount of **2, 4, 6, 8, 10** and/or 50 ng of **1, 3, 5, 7, 9**, were added and homogenized. 20 mL of acetone were added and mixed for 5 min by vortex apparatus. The solution was filtered and evaporated to dryness under reduced pressure; the residue was dissolved in 5 mL of n-hexane/ethyl acetate, 95:5 v/v, loaded into silica Sep-Pak cartridge Waters (Milford-USA), and eluted with 10 mL of the same n-hexane/ethyl acetate solvent mixture; the eluate, evaporated to dryness, afforded a residue which was dissolved in 1 mL of acetonitrile/acetone, 50:50 v/v and analyzed by LC/MS.

### **4.3 HPLC conditions**

#### Drupes and leaves of *Olea Europea L.*, bergamot, pummelo and leek.

The separation was performed using a 250 x 4.6mm 5  $\mu$ m reversed-phase C18 Luna-Phenomenex column at a flow rate of 1 mL/min.

The collections of unknowns were obtained using the same instrument but working in semi-preparative way.

The column used was AXIA Synergi Fusion C18 Phenomenex 150 x 21.2 mm, particle size 4  $\mu$ m, pore size 80Å. The injection loop was 1 ml and the flow-rate was 21.0 ml/min at room temperature.

#### Drupes of *Olea Europaea L.*

The run time was 45 min and the gradient was performed using 5mM  $\text{NH}_4^+$   $\text{CH}_3\text{COO}^-$  in H<sub>2</sub>O (solvent A) and MeOH (solvent B) as eluting phase.

The solvent run was the following: isocratic 90% A for 1 min; gradient from 90% A to 50% A in 14 min; isocratic 50% A for 8 min; gradient from 50% A to 0% A in 10 min; isocratic 0% A for 5 min; gradient 0% A to 90% A in 5 min; equilibration of the column for 10 min.

Leaves of Olea Europaea L.

The run time was 70 min and the gradient was built using 5 mM  $\text{NH}_4^+\text{CH}_3\text{COO}^-$  in  $\text{H}_2\text{O}$  (solvent A) and ACN (solvent B) as eluting phase. The solvent run was composed by the following steps: isocratic 90% A for 1 min.; gradient from 90% A to 50% A in 14 min.; isocratic 50% A for 8 min.; gradient from 50% A to 0% A in 10 min.; isocratic 0% A for 5 min.; gradient 0% A to 90% A in 5 min.; equilibration of the column for 10 min.

Bergamot, pummelo and leek.

The run time was 110 min and the gradient was performed using 0,1%  $\text{HCOOH}$  in  $\text{H}_2\text{O}$  (solvent A) and  $\text{MeOH}$  (solvent B) as eluting phase. The solvent run was the following: isocratic 80% A for 10 min; gradient from 80% A to 74% A in 2 min; gradient from 74% A to 31% A in 65 min; gradient from 31% A to 80% A in 18 min; equilibration of the column for 10 min.

Sudan I-IV and Para-red

The chromatographic analysis was performed with a C18 column 5.0 cm  $\times$  2.0 mm (Pursuit, Varian Inc.). The flow rate was fixed at 0.25  $\text{mL min}^{-1}$  using the following eluents and linear gradient: solvent A ( $\text{H}_2\text{O}$ , 0.1% formic acid), solvent B ( $\text{CH}_3\text{CN}$ ); from 40% A to 98% B in 10 min; 2 min at 98% B isocratic; from 98% B to 40% A in 3 min.

Preparative LC/MS of bergamot and pummelo samples

The mobile phase for bergamot consisted of 0,1% formic acid in water (55%) and  $\text{MeOH}$  (45%) for 15min. Naringenin-7-O- $\beta$ -neohesperidoside-6"-O-(3"-hidroxy-3"-methyl) glutarate (**1**; paragraph 3.3; chart), was eluted at RT 5 min from *Femminello* MPLC fraction and collected in RT 4.55-5.55 min., while hesperitin-7-O- $\beta$ -neohesperidoside-6"-O-(3"-hidroxy-3"-methyl) glutarate (**2**; paragraph 3.3; chart) was eluted at RT 10 min and collected in RT 9.40-10.40 min. in the same analysis.

The mobile phase for Pummelo consisted of 0,1% formic acid in water (55%) and ACN (45%) for 15min. Naringenin-7-O- $\beta$ -neohesperidoside-6"-O-malonate (**3**; paragraph 3.3 scheme 3.2.3) was eluted at RT x min from Pummelo MPLC fraction and collected in

RT 4.55-5.55 minute. Finally, this collected fractions was concentrated until elimination of organic solvent and lyophilised.

#### 4.4 Chemical hydrolysis

##### Bergamot

Methanol solution (900 µl) of compounds 1 and 2 (1mg) was treated with 100µl of aqueous saturated solution of Na<sub>2</sub>CO<sub>3</sub> at room temperature. The solution was then analyzed by LC/MS after 24 and 48 hours to assess the presence of neohesperidin and naringin (paragraph 3.2).

##### Leek

Methanol solutions (900 µl) of each unknown compounds (1,2,3,4; 0.5 mg) were treated with 100µl of HCl 1M at room temperature. The solution was then analyzed by LC/MS after 3h to asses the presence of kaempferol.

#### 4.5 Mass spectrometry

##### Drupes and leaves of Olea Europea L., bergamot, pummelo and leek.

The profile of flavonoids was obtained using a fractionlynx semi-preparative HPLC/MS system (Waters Corp., Milford, MA, USA) composed of an autosampler/collector Waters 2767 Sample Manager, a 600E pump working in analytical mode, a 486 UV detector and a ZMD quadrupole mass spectrometer equipped with an electrospray ionization (ESI) source. The mass spectrometer conditions were the following: capillary voltage 3.2 kV, cone voltage 10 V, extractor 2V, RF lens 0.2 V, source block and desolvation temperatures 120 and 250°C, respectively, ion energy 0.5 V, LM resolution 14.5, HM resolution 15.0 and multiplier 650 V. The nebulizer gas flow rate was set to 650 L/h. The samples were collected after the UV cell at the same time as the appearance of the mass signal.

High-resolution ESI experiments were carried out in a hybrid Q-Star Pulsar-i (MDS Sciex Applied Biosystems, Toronto, Canada) mass spectrometer equipped with an ionspray ionization source. Samples were introduced by direct infusion (5µL/min) of



the solution coming from the HPLC separation at the optimum ion spray voltage of 4800 V. The nitrogen gas pressure was set at 30 psi and the declustering and the focusing potentials were kept at 70 and 140V relative to ground, respectively. MS<sup>2</sup> experiments were performed in the collision cell *q* on the isotopically pure (<sup>12</sup>C) peak of the selected precursor ions by keeping the first quadrupole analyzer at 20V relative to ground and operating at unit resolution, and scanning the time-of-flight (TOF) analyzer. The collision energy was set from 15 to 40 eV, while the gas pressure of the collision chamber was set at the instrumental parameters CAD 5, which corresponds to a pressure of the chamber of  $6.86 \times 10^{-3}$  Torr and a gas thickness of  $9.55 \times 10^{15}$  mol<sup>15</sup>molecules/cm<sup>2</sup>. All the acquisitions were averaged over 60 scans at a TOF resolving power of 8000. The molecular formulae were evaluated by means of Analyst<sup>TM</sup> QS software (MDS Sciex).

#### Sudan I-IV and Para-red and labelled compounds

A) The high-resolution electrospray experiments were carried out in a hybrid Q-Star Pulsar-i (MDS Sciex Applied Biosystems, Toronto, Canada) mass spectrometer equipped with an ion spray ionization source. Samples were introduced by direct infusion (5  $\mu$ l/min) of the appropriate azo dye dissolved in water/acetonitrile 50/50 at the optimum voltage of 4800 V.

The nitrogen gas pressure was set at 20 psi and the declustering and the focusing potentials were kept at 50 and 220 V relative to ground, respectively. MS<sup>2</sup> experiments were performed in the collision cell *q* on the isotopically pure (<sup>12</sup>C) peak of the selected precursor ions by keeping the first quadrupole analyzer at 20 V relative to ground and operating at unit resolution and scanning the time-of-flight (TOF) analyzer. The collision energy was set at 20 and 30 eV, depending on the compound, while the gas pressure of the collision chamber was maintained at the instrumental parameters CAD 5, which corresponded to a pressure of the chamber of  $6.86 \times 10^{-3}$  Torr and a gas surface density of  $9.55 \times 10^{15}$  molecules/cm<sup>2</sup>. All the acquisitions were averaged over 60 scans at a TOF resolving power of 8000. The deuterated sudan compounds were synthesized by a modified literature procedure. The distribution of deuterium within each molecule, ascertained by high-resolution ESI-MS on the Q-star instrument, is reported in chapter 3 (3.4 table 3.4.1).

B) The LC/MS analysis was carried out with a triple quadrupole mass spectrometer LC 1200 (Varian), equipped with an APCI source interfaced with an HPLC Prostar 210 (Varian Inc. Palo Alto CA). The corona needle current was fixed at 7.5  $\mu$ A, the drying Gas ( $N_2$ ) at 12 psi and 200  $^{\circ}$ C, the nebulizing Gas ( $N_2$ ) at 60 psi and 450  $^{\circ}$ C, the auxiliary Gas ( $N_2$ ) at 17 psi, the housing temperature at 50  $^{\circ}$ C and the electron multiplier was set at 1350 V. The Scan time was 0.25 sec/scan, and the resolution was set using a mass peak width of 0.9. The collision gas pressure (Ar) was fixed at 2 mtorr and the collision energy was -30 V for **1-6** (Chapter 4) and -15 V for **7-10**. The overall MS experiment was composed of two segments: the first from 0 to 7.5 min for the analysis of **1-2, 3-4, 5-6**, and the second from 7.5 to 12.0 min for the analysis of **7-8, 9-10**.

High-resolution electrospray ionization (ESI) experiments were carried out in a hybrid Q-Star Pulsar-i (MSD Sciex Applied Biosystem, Toronto, Canada) mass spectrometer equipped with an ion spray ionization source. Samples were introduced by direct infusion (3  $\mu$ L/min) of the sample containing the analyte (5 ppm), dissolved in a solution of 0.1% acetic acid, acetonitrile/water 50/50 at the optimum ion spray (IS) voltage of 4800 V.

The source nitrogen (GS1) and the curtain gas (CUR) flow were set at a pressure of 20 and 25 psi respectively, while the first declustering potential (DP1), the focusing potential (FP), and the second declustering potential (DP2) were kept at 50, 220, and 10 V relative to ground, respectively.

#### Analytical parameters

The limit of detection (LOD) and the limit of quantitation (LOQ) for each foodstuff were calculated by applying the equations (1) and (2), following the directives of IUPAC and American Chemical Society's Committee on Environmental Analytical Chemistry.

$$S_{LOD} = S_{RB} + 3 \sigma_{RB} \quad \text{eq. 1}$$

$$S_{LOQ} = S_{RB} + 10 \sigma_{RB} \quad \text{eq. 2}$$

Where  $S_{LOD}$  is the signal at the limit of detection,  $S_{LOQ}$  is the signal at the limit of quantitation,  $S_{RB}$  is the signal of the uncontaminated food matrixes and  $\sigma_{RB}$  is the

standard deviation for uncontaminated matrixes. The concentrations were calculated by the standard curve.

The recovery for each foodstuff was calculated from the area of the signal obtained analyzing an uncontaminated product added to a known amount of Sudan standard. The concentration was estimated by using an external calibration curve built from six standard solutions at 12.5, 25, 50, 100, 200 and 400 ppm.